

DEVELOPMENT, CHARACTERIZATION, AND
OPTIMIZATION OF A MULTI-CHAMBER, SINGLE-
USE BIOREACTOR

By

MOMEN AMER

Bachelor of Science in Pharmacy
Ain Shams University
Cairo, Egypt
2006

Master of Science in Biotechnology
The American University in Cairo
Cairo, Egypt
2014

Submitted to the Faculty of the
Graduate College of the
Oklahoma State University
in partial fulfillment of
the requirements for
the Degree of
DOCTOR OF PHILOSOPHY
May, 2019

DEVELOPMENT, CHARACTERIZATION, AND
OPTIMIZATION OF A MULTI-CHAMBER, SINGLE-
USE BIOREACTOR

Dissertation Approved:

Dr. Joshua D. Ramsey

Dissertation Adviser

Dr. Heather Gappa-Fahlenkamp

Dr. Ashlee N. Ford Versypt

Dr. James E. Smay

ACKNOWLEDGEMENTS

I would like to acknowledge everyone who helped me to do this work and turn my ideas into reality. First, I would like to thank my advisor, Dr. Josh Ramsey, for believing in my ideas and for his continuous support along the way. I would like to thank Dr. Fahlenkamp, Dr. Ford Versypt, and Dr. Smay for serving on my committee, and Dr. Feng for the great expertise he provided in the CFD part of this work.

My sincere thanks go to Richard Gajan for all his valuable advice and his huge assistance in developing the business side of this work. I would like to thank Daniel Will and Cowboy Technologies team for financially supporting this work. I would also like to thank everyone at the Technology Development Center: Russell Hopper, Alex Valiaev, and Scott Davis who opened the door to a lot of great learning and funding opportunities that made this work come to reality.

Finally, I would like to thank my wife and my lab mate, Yasmine Gabal, for all her support and sacrifices. I am especially thankful to my parents for their endless support, encouragement, and inspiration. Mom, I know you would have been so proud.

Name: MOMEN AMER

Date of Degree: MAY, 2019

Title of Study: DEVELOPMENT, CHARACTERIZATION, AND OPTIMIZATION OF
A MULTI-CHAMBER, SINGLE-USE BIOREACTOR

Major Field: CHEMICAL ENGINEERING

Abstract: Stirred-tank single-use bioreactors have proven their capability to successfully replace their stainless-steel counterparts in the biopharmaceutical industry. To date, however, only a five-fold volume expansion is achievable in a single-use stirred tank bioreactor, which in turn necessitates intermediate equipment to scale-up the culture to production volume. This work introduces a novel multi-chamber single-use bioreactor design that can help users save costs of purchase and qualification of equipment, reduce factory footprint, and reduce the risk of contamination. A bioreactor prototype is presented in this work that is made of two chambers of different volumes, interconnected as a single, closed system. The design and construction of the prototype is described in detail, and engineering characterization results are reported for both chambers and compared with published data for commercially available bioreactors. The results help identify some areas of potential improvements in the bioreactor design. Optimization of a bioreactor design can be an especially challenging process and can lead to an exceedingly large number of configurations and necessary experiments. Therefore, a computational fluid dynamics model is used in this work to model the multiphase flow in the 50 L chamber of the multi-chamber bioreactor prototype. The model results are validated with oxygen mass transfer coefficient (k_{LA}) measurements within the prototype. The validated model is projected to predict the effect of using different sparger types and sizes and the effect of varying the impeller diameter on k_{LA} . The simulations show that ring spargers result in a superior k_{LA} compared to pipe spargers, with an optimum sparger-to-impeller diameter ratio of 0.8. Also, larger impellers are shown to improve k_{LA} . A correlation of k_{LA} is presented as a function of both the reactor geometry and operating conditions. The resulting correlation can be used to predict k_{LA} in a bioreactor and to optimize its design and operating parameters. Finally, a full commercialization plan for the multi-chamber bioreactor is presented. The plan proves that the proposed design not only offers a solution to a variety of industry problems but also presents an attractive investment opportunity to further develop the technology to a market ready product.

TABLE OF CONTENTS

Chapter	Page
I. INTRODUCTION	1
1.1 Upstream Processing in Biopharmaceutical Manufacturing.....	1
1.1.1 High Density and/or Large Volume Cell Banking	3
1.1.2 Using Perfusion Systems to Seed the Production Bioreactor	3
1.1.3 Increasing the Bioreactor Turndown Ratio.....	5
1.2 Significance of the Research.....	6
II. SINGLE-USE BIOREACTORS AND APPLICATION OF COMPUTATIONAL FLUID DYNAMICS IN BIOPHARMACEUTICAL INDUSTRY	8
2.1 Single-Use Bioreactors in Biopharmaceutical Industry.....	8
2.1.1 Advantages of Single-Use Technology	8
2.1.2 Current Challenges and Limitations for Single-Use Technology.....	10
2.1.2.1 Lack of Universal Regulatory Standards	10
2.1.2.2 Leachables and Extractables	10
2.1.2.3 Limited Scale	11
2.1.2.4 Environmental Impact.....	12
2.1.2.5 Application in Microbial Cultures	13
2.1.2.6 Sensor and Monitoring Technology.....	13
2.2 Computational Fluid Dynamics in Bioreactor Design.....	14
2.2.1 Modelling of Rotating Systems in Agitated Tanks.....	14
2.2.1.1 Multiple Reference Frame Model.....	14
2.2.2 Multiphase Flow Modelling.....	15
2.2.2.1 Euler-Lagrange Approach.....	16
2.2.2.2 Euler-Euler Approach	16
2.2.3 CFD in Modelling Single-Use Bioreactors.....	16
III. DEVELOPMENT AND CHARACTERIZATION OF THE MULTI- CHAMBER SINGLE-USE BIOREACTOR - A PROOF OF CONCEPT PROTOTYPE.....	18
3.1 Introduction.....	18
3.2 Materials and Methods.....	22
3.2.1 Construction of the Prototype	22

Chapter	Page
3.2.2 Engineering Characterization of the Multi-Chamber Single-Use Bioreactor.....	24
3.2.2.1 Mixing Time	24
3.2.2.2 Power Input.....	25
3.2.2.3 Oxygen Mass Transfer.....	25
3.3 Results and Discussion	26
3.3.1 Geometrical Dimensions.....	26
3.3.2 Mixing Time	27
3.3.3 Power Input.....	30
3.3.4 Oxygen Mass Transfer.....	32
3.4 Optimization of the Manufacturing Process for a Second-Generation Prototype.....	35
3.5 Cell Culture Evaluation.....	36
3.6 Conclusions.....	37
3.7 Acknowledgements.....	38
3.8 Notation.....	38
IV. USING CFD SIMULATIONS AND STATISTICAL ANALYSIS TO CORRELATE OXYGEN MASS TRANSFER COEFFICIENT TO BOTH GEOMETRICAL PARAMETERS AND OPERATING CONDITIONS IN A STIRRED-TANK BIOREACTOR.....	40
4.1 Introduction.....	40
4.2 Bioreactor Geometry Reconstruction and Mesh Regeneration	44
4.3 Numerical Setup.....	47
4.4 Governing Equations	48
4.4.1 Eulerian-Eulerian Multiphase Model.....	48
4.4.2 Turbulence Model.....	49
4.4.3 Population Balance Model.....	50
4.4.4 Mass Transfer Coefficients and Bubble Diameter.....	53
4.5 Statistical Analysis and Correlation Equation	53
4.6 Results and Discussion	54
4.6.1 Single-Phase Flow Pattern	54
4.6.2 Multiphase Fluid Simulation and k_{LA} Prediction.....	55
4.6.3 Model Validation and Optimization of Bin Sizes.....	55
4.6.4 Effect of Sparger Shape on k_{LA}	57
4.6.5 Effect of Sparger Size on k_{LA}	59
4.6.6 Effect of Impeller Diameter on k_{LA}	61
4.6.7 Statistical Analysis and Model Equation	63
4.7 Conclusions.....	65
4.8 Notation.....	66

Chapter	Page
V. COMMERCIALIZATION PLAN FOR THE MULTI-CHAMBER SINGLE-USE BIOREACTOR	69
5.1 Summary	69
5.2 Company Overview	71
5.2.1 Business Opportunity.....	71
5.2.2 The Value Proposition	73
5.3 Market Analysis	73
5.3.1 Market Trend	73
5.3.2 Market Size	74
5.3.3 Target Entry Market.....	74
5.3.4 Market Opportunity Validation.....	75
5.4 Competition.....	76
5.4.1 Current Competitors.....	76
5.4.2 Future Competitors	77
5.5 Description of Product	78
5.5.1 Products Offered and State of Development	78
5.5.2 Product Development Milestones	79
5.5.3 Pricing Strategy.....	80
5.6 Operations and Management	81
5.6.1 Operations Model.....	81
5.6.2 Risks and Contingencies	82
5.6.3 Management Team.....	82
5.6.3.1 Chief Officers.....	82
5.6.3.2 Advisory Board.....	83
5.7 Marketing and Sales Strategy	84
5.7.1 Sales Approach	84
5.7.2 Marketing.....	85
5.8 Investment Opportunity	86
5.9 Exit Strategy.....	87
5.10 Financials	87
5.10.1 Research Grants and Awards	87
5.10.2 Income Statement.....	88
5.10.3 Projections and Assumptions.....	91
VI. CONCLUSIONS	93
REFERENCES	96
APPENDICES	108

LIST OF TABLES

Table	Page
Table 2.1. Summary of advantages and disadvantages of single-use technology in biopharmaceutical industry	13
Table 3.1. Torque measurements and calculated Reynolds number (Re), power input per unit volume (P/V), and impeller power number (Ne) in the 50 L chamber at different agitation speeds	31
Table 4.1. Number and size of bins used in the Population Balance Model to simulate the multiphase flow at different impeller tip speeds	57
Table 5.1. Key feedback notes on the value propositions from industry professionals	76
Table 5.2. Milestones for multi-chamber single-use bioreactor product development	80
Table 5.3. Cap table with round 1 of investment	87
Table 5.4. Sources and use of funds received	88
Table 5.5. Projected income statement	89
Table 5.6. Statement of cash flows	90
Table 5.7. Balance sheet	90

LIST OF FIGURES

Figure	Page
Figure 1.1.	Seed-train process of a cell culture production run starting from a few milliliters of frozen cell culture up to thousands of liters.....2
Figure 3.1.	Assembly of the multi-chamber bioreactor prototype.....23
Figure 3.2.	Mixing times in the small 3 L chamber versus the Mobius® CellReady 3 L bioreactor at 1.5 and 2.5 L working volumes and different tip speeds28
Figure 3.3.	Mixing time in the large 50 L chamber versus BIOSTAT® STR, Mobius CellReady, and Hyclone S.U.B. 50 L bioreactors at maximum working volume and different tip speeds30
Figure 3.4.	Calculated P/V at different impeller tip speeds in the large 50 L chamber, HyClone 50 L S.U.B., and BIOSTAT® STR 50 L with 2×3 -blade segment impellers.....32
Figure 3.5.	k_{LA} values in the 3 L chamber at different aeration rates and tip speeds, compared to the experimental results for Mobius® CellReady 3 L.....33
Figure 3.6.	Calculated k_{LA} values at 0.1 VVM aeration rate and different tip speeds in the large 50 L chamber and the BIOSTAT STR 50 L with the 800 μm pore size ring sparger and the 150 μm pore size microsparger34
Figure 3.7.	Sketch for the second-generation prototype fabrication parts and assembly36
Figure 4.1.	Illustration of the bioreactor geometry and mesh.....45
Figure 4.2.	Mesh independence test where k_{LA} is plotted as a function of number of mesh elements. Simulations are carried out at impeller tip speed of 1.8 m/s and aeration rate of 0.1 VVM.....46
Figure 4.3.	Contours and vector plots of fluid velocity in a single-phase flow at different impeller tip speeds. Velocity of liquid (u_L) is shown normalized to the tip speed (u_{tip})54
Figure 4.4.	PBM model validation. (A) validation versus k_{LA} experimental data obtained at different impeller tip speeds and a constant aeration rate of 0.1 VVM, (B) validation versus k_{LA} experimental data obtained at different aeration rates and a constant impeller tip speed of 1.8 m/s56

Figure	Page
Figure 4.5.	Comparison between pipe and ring spargers of same sparging surface area (A) effect of sparger geometry on k_{La} , (B) Effect of sparger geometry on air volume fraction58
Figure 4.6.	Top view of the air volume fraction inside the bioreactor with a pipe sparger (left) and a ring sparger (right)59
Figure 4.7.	Effect of ring sparger diameter on (A) k_{La} and (B) air volume fraction.....60
Figure 4.8.	Contour plots of bubble size distribution at d_{sp}/D ratio of 0.09 (left), 0.8 (middle), and 1.0 (right)61
Figure 4.9.	Effect of impeller diameter to vessel diameter ratio (D/T) on k_{La}62
Figure 4.10.	Contours of air volume fraction (α_G) at the bioreactor midplane with different impeller diameters ($D/T = 0.2, 0.4, \text{ and } 0.6$). In all cases d_{sp}/D is 0.8, the tip speed is 1.2 m/s, and the aeration rate is 0.1 VVM.....63
Figure 4.11.	(A) Linear plot of model predicted versus CFD predicted k_{La} values. (B-G) Contour line maps showing the effect of different variables $d_{sp}/D, D/T, Re,$ and gas flow rate on k_{La}64
Figure 5.1.	A typical seed-train process with multiple vessels of different volumes, multiple support structures, and control units. The mark X indicates intermediate bioreactor steps that could potentially be eliminated by using the multi-chamber bioreactor technology.70
Figure 5.2.	A 3D structure and a side view cartoon for a two-chamber bioreactor.72
Figure 5.3.	Detailed structure of a two-chamber single-use bioreactor78
Figure 5.4.	Products offered and pricing81

CHAPTER I

INTRODUCTION

1.1 Upstream Processing in Biopharmaceutical Manufacturing

The first critical step in biopharmaceutical manufacturing from mammalian cells is the upstream processing. The process is based on seed-train expansion, where the cell culture volume is scaled from a few milliliters up to hundreds or thousands of liters at the production scale. The scale-up process is critical because the quality of the inoculum in the early cultivation stages often determines the quality of the entire production campaign. Therefore, keeping the cells in a good state throughout the whole seed-train process is essential [1, 2].

A cell culture seed-train is time consuming and generates significant corresponding costs. A typical seed-train from a 2 mL scale until inoculation of a 3,000-10,000 L production scale bioreactor lasts in the range of 20-30 days. Deviations from standard growth rates or contamination incidents are common, and if they happen, they will further increase the seed-train time span. Typical seed-train protocols start by thawing a 1-2 mL cryopreserved cell suspension vial, and then the cells are transferred and cultivated in T-flasks. T-flasks are routinely incubated in CO₂ controlled incubators, where cells can grow and multiply. Based on the cell density, which is the number of viable cells per milliliter of cell suspension, the cells undergo successive sub-cultivation (i.e. passaging) into larger vessels. While a T-flask can handle

tens of milliliters of culture volume, roller bottles or shake flasks can handle hundreds of milliliters and bioreactors are subsequently used to handle larger scales up to thousands of liters. On reaching a sufficient viable cell density, the cells are transferred to the production scale bioreactor. In all seed-train vessels, the cell culture typically lasts for 2-3 days before it is transferred to the larger vessel. In the production scale bioreactor, however, cells are cultivated for a longer period, usually more than seven days, where the cell growth, productivity, and metabolic activity are monitored. At the end of the production run, cells are harvested by being separated from the culture media. The culture media then undergoes a whole sequence of events in the downstream processing in order to purify the biopharmaceutical protein of interest.



Figure 1.1. Seed-train process of a cell culture production run starting from a few milliliters of frozen cell culture up to thousands of liters.

The seed-train process, as described, is both time and cost intensive. A lot of manual operations and handling as well as the use of many culture vessels are required [3]. Excessive operator handling increases the risk of microbial contamination, especially during the transfer of the culture from one vessel to another. The use of multiple pieces of equipment also creates its own challenges. In addition to the high cost associated with the purchase, qualification, and maintenance of multiple pieces of equipment, they also occupy much of the production facility floor space and limit the production capacity.

Efforts to offset the limitations of seed-train procedures include high density and/or large volume cell banking, using perfusion systems to seed the production bioreactor, and increasing bioreactor turndown ratio. These approaches aim to streamline the seed-train by reducing the process timeline, factory foot print, and operator's interference.

1.1.1 High Density and/or Large Volume Cell Banking

Generating enough cell mass from a 1-2 mL cryo-vial to initiate the production bioreactor is time consuming. The process can take weeks and is dependent on scale, cell line characteristics, and the process parameters [2]. Previous efforts have shown that high-density cell banking can be an effective means to reduce the number of steps required and improve operational success in seed-train process. Tao et al. [4] reported using a perfusion system to generate high density cell banks for Chinese hamster ovary (CHO) cells. Cell banks were generated at 90-100 million cells/mL and were used to directly inoculate a 20 L Wave bag. This approach eliminated multiple intermediate shake-flask expansion steps and reduced the cell culture process time by up to 9 days at 2,000 L manufacturing scale. In other studies, cryo-bags were used to freeze 50-100 mL of CHO and baby hamster kidney (BHK) cells at a density of 20-40 million cells/mL [2, 5]. Cells were thawed and directly transferred to an inoculation bioreactor at a volume of 2 L. The culture volume in the inoculation bioreactor was stepwise increased to its final working volume and the cells were used to directly inoculate the production bioreactor after a sufficient cell density was reached. This strategy was claimed to reduce seed-train expansion duration by 60–70%.

1.1.2 Using Perfusion Systems to Seed the Production Bioreactor

A perfusion cell culture system involves a continuous supply of fresh media into the bioreactor while the waste byproducts are constantly removed. The advantage of perfusion system is that a much higher cell density can be attained in a relatively small volume bioreactor [6]. Thus, a higher volumetric productivity than conventional batch or fed batch conditions can be achieved.

Perfusion systems are therefore often considered as production bioreactors rather than as elements of seed-train process [7].

Some studies, however, proposed the use of a perfusion $n - 1$ stage bioreactor (the seed-train bioreactor stage immediately prior to the production bioreactor stage) to reduce the seed expansion time by reducing either the number of expansion steps or the growth phase duration in the production bioreactor. Kloth et al. [8] proposed the use of a 5 L perfusion bioreactor to inoculate multiple 35 L production scale bioreactors. After inoculation, the perfusion seed bioreactor was replenished with fresh nutrient medium and continued to operate until other production bioreactors required inoculation. Using this method, the seed-train duration was minimized by inoculating multiple bioreactors in a short period. Pohlscheidt et al. [9] achieved high cell densities up to 15.6 million cells/mL in a 3,000 L $n - 1$ perfusion bioreactor, which was then used to inoculate a 13,500 L fed batch production bioreactor. The inoculation cell densities from the perfusion $n - 1$ were four-fold and an eight-fold higher than those used in a conventional process where the production bioreactor was inoculated from a batch $n - 1$ bioreactor. This process provided a 3 days reduction in the production process and an estimated increase in the facility utilization by 12% - 19%. Padawer et al. [10] also proposed using a perfusion $n - 1$ bioreactor to inoculate the production fed batch bioreactor at a 25-fold higher cell density. A production time reduction from 14 to 8 days was achieved using this approach.

Wright et al. [7] described a seed-train process that combined the use of high density cell banking and a perfusion bioreactor at the $n - 1$ stage. Compared to a conventional process, the use of high cell density cell banking eliminated two intermediate expansion stages in the seed-train process, while the use of a 50 L $n - 1$ perfusion system allowed for a 10-fold increase in the seeding density at the 500 L production bioreactor. The higher seeding density reduced the growth phase duration inside the production bioreactor by 5 days.

1.1.3 Increasing the Bioreactor Turndown Ratio

The turndown ratio for a bioreactor is the ratio between its maximum and minimum operating volumes. For most cell cultures, a 1:5 ratio is used for scaling up the culture volume in each passaging step [11]. A bioreactor that is capable of operating at 20% or less of its maximum capacity can support two expansion stages of the seed-train process. The bioreactor can be initially seeded at 20% of its working volume, and when the cell culture reaches a sufficient cell density, fresh nutrient medium is added to scale the volume up to the full capacity of the bioreactor. Operating bioreactors at a 20% or less of their maximum working volume, however, comes with a challenge. Bioreactors are typically designed with top overlay and bottom spargers. At low culture volumes (i.e. 20% of the total bioreactor volume), the headspace volume is large (i.e. 80% of the total bioreactor volume) and is filled with carbon dioxide and other metabolic gases. The top sparger is not efficient to flush such a large headspace volume. Thus, the heavier CO₂ forms a blanket at the surface of the culture and causes a higher level of dissolved CO₂ in the culture and a lower oxygen transfer, which negatively affects the cell culture performance [11].

In order to tackle this problem, Thermo Fisher Scientific achieved good cell culture performance in their HyPerforma S.U.B. with a 5:1 turndown ratio by introducing an extra crossflow sparger in their bag design. When the bioreactor operated at 20% working volume, the crossflow sparger introduced gas just above the liquid height and produced more efficient oxygen transfer and CO₂ removal from the culture. Best results were achieved when the crossflow sparger was positioned within 12-15 inches above the liquid surface. The efficiency of CO₂ stripping declined when the crossflow sparger was positioned at higher locations, even when the gassing flow rate was increased by fivefold.

A seed-train process based on high turndown bioreactors (i.e. 5:1) is expected to require fewer intermediate bioreactors than a process based on 2:1 turndown bioreactors. For a 2,000 L

production process, the elimination of one intermediate unit is estimated to reduce the operator intervention by 15-25%. The risk of operator error is reduced by decreasing the number of setups and aseptic transfers and by spacing out peak operational labor loads, which results in reduced risk of culture contamination. The benefits of using fewer pieces of equipment in the seed-train process also include increased facility space and reduced fixed costs associated with the purchase and qualification of equipment [12].

1.2 Significance of the Research

The overall aim of this work is to develop one smart solution to various problems in the upstream processing of mammalian cell culture in biopharmaceutical industry. A multi-chamber single-use bioreactor has an innovative, patent-pending design. In addition to all the general benefits of single-use bioreactors discussed in Chapter 2, the new design also offers some extra benefits to the current industry practices. These benefits include the reduction of factory footprint, capital costs, operating costs, and risk of microbial contamination.

Chapter 3 of this work presents the methods of developing an early 50 L prototype of the multi-chamber single-use bioreactor. The chapter also provides a comparative engineering characterization between the prototype and other commercially available single-use bioreactors of similar volumes. A more automation friendly method to produce the second generation 200 L prototype is also presented in Chapter 3.

In Chapter 4, a multiphase CFD model with population balance equations is used to model gas-liquid mixing and gas bubble distribution in the larger chamber of the early prototype. The model is used to predict the effect of using ring or pipe spargers of different sizes and the effect of varying the impeller diameter on the oxygen mass transfer coefficient (k_La). Design of experiment methods are used to develop a correlation of k_La as a function of both the reactor geometry and operating conditions.

Finally, in Chapter 5, a full commercialization plan for the multi-chamber single-use bioreactor is presented with 5-year financial projections. The commercialization plan is based on founding a limited liability company, referred to as Multivate LLC. Foreseeing the design patent is granted, the plan assumes Multivate licensing the intellectual property rights from Oklahoma State University. The financial projections are based on Multivate's success to secure \$600,000 investment. Collectively, the work integrates engineering, computational, biological, and business concepts to develop a novel solution to current problems in biopharmaceutical industry. The work shows that the proposed multi-chamber single-use bioreactor has a potential to succeed on both the technical and business sides.

CHAPTER II

SINGLE-USE BIOREACTORS AND APPLICATION OF COMPUTATIONAL FLUID DYNAMICS IN BIOPHARMACEUTICAL INDUSTRY

2.1 Single-Use Bioreactors in Biopharmaceutical Industry

In addition to the challenges associated with the risky and time-consuming seed-train process, other challenges have developed in the past few years facing the biopharmaceutical industry. The rising biosimilar (i.e. biopharmaceutical generics) competition and the increased quality standards required by regulatory agents put an increasing pressure on the biopharmaceutical manufacturers to drive toward developing more efficient processes at lower costs [13]. Over the past two decades, single-use technologies have shown success in developing efficient, low cost, and flexible manufacturing bioprocesses [14].

2.1.1 Advantages of Single-Use Technology

Single-use bioreactors are pre-sterilized, ready to use vessels that are used once and then disposed of. The first single-use bioreactor was introduced to market in 1996 [15]. Since then, single-use bioreactors have been hugely successful in replacing their stainless-steel counterparts that, for decades, have been considered the standards for upstream processing in the biopharmaceutical industry [16].

Biopharmaceutical manufacturing is tightly controlled by current good manufacturing practice (cGMP) guidelines. In cGMP manufacturing practices, cleaning of all equipment that comes into contact with the product is a crucial procedure that needs to take place in between runs [17]. This cleaning process is laborious, time consuming, and requires a complete shutdown of the production line. The cleaning procedures also need an extensive validation and documentation [18]. Using single-use bioreactors eliminates the need of the cleaning process between runs and thus reduces the validation time and shorten time to market [19].

Single-use bioreactors provide a huge advantage in reducing the production downtime. The time required to prepare a single-use bioreactor for the next batch of the same product is estimated to be 2 hours compared to 6-10 hours for a changeover in a stainless-steel bioreactor. For a full product changeover, the time saving reward of using a single-use bioreactor is more prominent. While a full product changeover in a stainless-steel based process can take up to three weeks, it would not take more than 48 hours with a full disposable manufacturing process [20].

While clean-in-place (CIP) is required for stainless-steel bioreactors to eliminate the risk of cross contamination between multiple products, steam-in-place (SIP) is also required to sterilize the stainless-steel bioreactor before each use to reduce the risk of microbial contamination. Single-use based processes eliminate the need of SIP, which brings an additional environmental benefit in lowering the consumption of highly pure water and heat required to clean and sterilize the stainless-steel systems. The environmental benefit of the reduced energy demand has been reviewed in some studies and was demonstrated to outweigh the negative impact of increased solid waste generated from single-use systems [21, 22].

Economic benefits of single-use equipment also include reduction of initial capital burden and time required to get a facility up and running. The total capital costs for a single-use based facility was reduced by 54% compared to a stainless-steel based facility, as estimated in a study published in

2009 [23]. Operating costs are also reduced by adopting single-use equipment. In 2013, estimates indicated that compared to stainless-steel facilities, single-use operated facilities had annual production rates that were 27% greater and production costs that were 23% lower on a gram of mAb basis [24].

2.1.2 Current Challenges and Limitations for Single-Use Technology

2.1.2.1 Lack of Universal Regulatory Standards

A current challenge that faces the single-use technology is the lack of standardization of components. The manufacturers of single-use technology products need to conduct extensive physical, functional, chemical, biological, and sterilization validation evaluations on their products and to ensure their compliance with multiple qualification specifications [25]. The lack of standard materials of construction, testing, and certifications provided by suppliers limits the ability of the end-users to easily inter-change or inter-connect different process components or to have more flexibility to choose between different suppliers and components [26]. As a part of the process validation, the end-users need to perform risk assessment studies to demonstrate that their selected supplier materials are compatible with their products and processing conditions [27, 28].

2.1.2.2 Leachables and Extractables

The use of single-use technologies raises the concern of organic compounds leaching from the plastic surfaces into the process fluid. Leachables refer to chemicals that migrate into the actual drug product from the product contact surface under normal use conditions, whereas extractables are the chemicals extracted from the product surface materials under extreme conditions of using specific solvents and high temperatures. As a part of process validation, determination of extractables and leachables levels for single-use systems must be done. Studies showed that leachables from commercially available bags can adversely affect cell growth [29]. Leachables also have the potential

to bind to media components, especially the lipid components needed to cultivate NS0 cholesterol dependent cells [30, 31].

Suppliers of single-use systems are required to provide extractable profiles under extreme solvent and temperature conditions. The provided data should include both identification and quantification of extractables [32, 33]. Leachables are usually a subset of extractables. Under normal conditions, leachables are expected to be released in very low levels, if any. A major progression is required to arrive at a common standard set of conditions and analytical techniques to quantify extractables in various single-use products from different suppliers [34].

2.1.2.3 Limited Scale

Scalability is one challenge facing upstream single-use technology. Single-use bioreactors have been limited predominantly to 2,000 L or less for mammalian cell cultures. Leakage and integrity issues have been of big concern when considering the use of disposable bioreactors at large volumes. The plastic materials that are currently used to produce single-use bioreactor films are not capable of sustaining high pressures without compromising their integrity [26, 35]. This volume limitation of single-use bioreactor improved in late 2015, when ABEC, Inc. announced the industry's largest single-use bioreactor so far with a working volume of 3,500 L. Although this is a noticeable increase, the ABEC bioreactor is not yet widely used, and compared to a typical 20,000 L stainless-steel bioreactor, the ABEC bioreactor is still quite limited.

Despite the scale limitation, the 2,000 L maximum scale of single-use bioreactors is becoming more adopted in industry because of many reasons. Some of these reasons are the increased product titers as a result of improvements in cell line development and cell culture processes, increased number of biologics targeting orphan diseases and smaller patient population, and the rapid market growth of biosimilars [35].

2.1.2.4 Environmental Impact

At first glance, single-use products might seem less sustainable than their reusable counterparts. Single-use systems, however, were shown to have less environmental impact than stainless-steel components. The higher environmental impact of using stainless-steel systems is primarily due to the extensive use of highly purified water and heat required for cleaning and sterilization of such systems.

One study that compared the use of disposables to the use of stainless-steel components in a $3 \times 2,000$ L scale facility demonstrated that the most significant savings were derived from reductions in water usage. The study estimated 87% reduction in water usage in the single-use based facility, 38% space reduction, and 30% reduction in energy to operate the facility compared to the stainless-steel based facility. In total, 25.5% reduction in carbon footprint was estimated when using the disposable systems [36]. GE Healthcare Life Sciences performed a lifecycle assessment study that showed that the end-of-life disposal of single-use components has negligible impact when compared to other factors such as energy and water use in stainless-steel based production processes [37].

Waste disposal of single-use systems, however, is still a complex issue that needs to be addressed. Options for disposal include landfill, waste to energy incineration (WtE), and recycling. One challenge that comes with disposing single-use components of bioprocessing is that they are classified as bio-hazardous materials. The end-user needs to autoclave the waste material before sending them to the waste management vendors to be buried in a landfill. Another option is to send the waste to WtE facilities where the plastic is burned to release electric or heat energy. However, the manufacturing facility might not have a WtE facility near its site. Also, not all WtE facilities accept bio-hazardous materials. Recycling also comes with a significant challenge where single-use systems are usually made up of different types of plastic materials that are difficult to separate [21].

2.1.2.5 Application in Microbial Cultures

Single-use bioreactors have not been widely used in microbial cultures. Microbial cultures have very high metabolic rates and oxygen demands, and they typically run under high pressure and high gas flow rate. For a plastic-made single-use bioreactor, it is a big challenge to provide the needed power required for adequate mixing and oxygen mass transfer. The low heat transfer rate of the plastic material of the bags also generates excessive heat and makes it challenging to maintain the temperature of the culture inside the bioreactor. For the above-mentioned reasons, the use of single-use bioreactors in microbial cultures is not common and is limited to a maximum of only 200-500 L [35, 38, 39].

2.1.2.6 Sensor and Monitoring Technology

The concept of process analytical technologies (PAT) was introduced by the FDA to improve process monitoring and to allow online control rather than testing the final product specifications at the end of the process [40, 41]. PAT is associated with the quality by design (QbD) concept, which aims to minimize production error by building quality within the process [42]. A big focus, therefore, has been placed to developing robust single-use sensor technologies. The most commonly used sensors are fluorescent-based pH, dissolved oxygen, and carbon dioxide sensors. Recent technologies include sensors for viable cell mass, glucose, and lactate concentrations [35].

Table 2.1. Summary of advantages and disadvantages of single-use technology in biopharmaceutical industry.

Advantages	Disadvantages
Reduced risk of cross contamination between different products	Limited scale, especially in microbial fermentation
Reduced capital costs	Waste disposal
Reduced need for cleaning validation	Lack of universal standards
Eliminated need for CIP and SIP	Leachables and extractables
Reduced turn down time and accelerated time to market	Limited number of vendors

2.2 Computational Fluid Dynamics in Bioreactor Design

Computational fluid dynamics (CFD) is a computer aided technique that uses numerical methods and algorithms to describe fluid flow patterns. While CFD is a powerful tool to study and improve existing operating systems, CFD can also be used in the design of new systems to implement QbD concepts and shorten the product development cycle. Application of CFD in modeling pharmaceutical processes has gained a big interest in the past few decades [43-45], specially to model the fluid flow in bioreactors.

2.2.1 Modelling of Rotating Systems in Agitated Tanks

Many scientific papers have used CFD to model fluid flow and turbulence inside agitated systems [46-50]. CFD models have been proven to predict with sufficient accuracy the mean flow-field and the power number in various agitated bioreactor systems equipped with different types of impellers [51-56].

Efficient mixing is crucial in cell culture and fermentation processes to ensure even distribution of nutrients, oxygen, and pH. CFD has been frequently employed to study the mixing performance in stirred-tank reactors [57-61], and how mixing is affected by the reactor hardware configuration [52]. The multiple reference frame and the sliding mesh models are often used to model rotating motion in agitated tanks.

2.2.1.1 Multiple Reference Frame Model

In the multiple reference frame model, two distinct fluid domains are created. A rotating reference frame is defined at the impeller region and is set to rotate at a velocity corresponding to the impeller tip speed. The other domain is set as a stationary reference frame in the outer region. At the interfaces between cell zones, a local reference frame transformation is performed to enable flow variables in one zone to be used to calculate fluxes at the boundary of the adjacent zone.

2.2.1.2 Sliding Mesh Model

In the sliding mesh technique, two or more cell zones are used. The interface zones of adjacent cell zones are associated with one another to form a "mesh interface". During the calculation, the cell zones slide relative to one another along the mesh interface in discrete time steps and perform time-dependent calculations using implicit or explicit interpolation of data at successive time steps. The sliding mesh model provides a time-accurate rather than a time-averaged solution. The model is the most accurate method for simulating flows in multiple moving reference frames, but also the most computationally demanding.

2.2.2 Multiphase Flow Modelling

Many studies used CFD to model multiphase flow including gas phase, particle tracking, or reaction processes in stirred-tank reactors [52, 62-67]. In cell culture and aerobic fermentation systems, the rate of oxygen transfer to the cells is critical. The rate of oxygen transfer is dependent on the bubble size distribution, because bubble sizes dictate the available surface area for gas-liquid mass transfer [68]. Modelling multi-phase flow in aerated tanks, requires taking bubble breakage and coalescence into account. Population balance models, therefore, have been used to model the evolution of gas bubbles in bioreactors [69-71]. However, the mechanisms responsible for bubble breakage and coalescence are not yet fully understood and need further exploration [72].

The CFD models can generate high-resolution localized predictions regarding some parameters that are hard or even impossible to measure in situ, such as the shear stress, power consumption, Kolmogorov eddy length scale distribution, and turbulence characteristics including Reynolds stress, kinetic energy, and energy dissipation rate [73-75].

For multiphase flow, two computational approaches for modeling the interaction between phases have been widely used: the Euler-Lagrange approach [56, 76-78] and the Euler-Euler approach [56, 79-82].

2.2.2.1 Euler-Lagrange Approach

In the Euler-Lagrange approach, the primary phase is treated as a continuum by solving the time-averaged Navier-Stokes equations. In the secondary dispersed phase, the motion of large number of individual particles is tracked as the particles move through fluid. The Euler-Lagrange model is typically used when the secondary dispersed phase occupies a low volume fraction. The particle trajectories are computed individually at specified intervals during the fluid phase calculation [83].

2.2.2.2 Euler-Euler Approach

In the Euler-Euler approach, both dispersed and continuous phases are treated as interpenetrating continua. The concept of volume fraction is introduced because the volume of one phase cannot be occupied by another phase. These volume fractions are assumed to be continuous functions of space and time, and their sum is equal to one. The Euler-Euler model is computationally more economical than the Euler-Lagrange model, and it can handle both dilute and dense flows [83].

2.2.3 CFD in Modelling Single-Use Bioreactors

The suitability of CFD models for engineering characterization of single-use bioreactors has been demonstrated. Many case studies have been reviewed by Loffelholz et al. [84], as well as some other recent studies [85, 86]. These studies involved stirred-tank and wave-mixed bioreactors, as well as other bioreactor designs with uncommon mixing mechanisms like the oscillating disk with conical orifice in the Vibromix system and the air wheel in the PBS Biotech bioreactor. The case study of the PBS bioreactor was unique in the sense that the CFD simulations were used to develop the market ready bioreactor based on only a prototype, which relates to one scope of this work regarding the

multi-chamber bioreactor development. Applying CFD in the bioreactor development process led to a significant reduction in time and costs [84]. CFD has been also used to optimize cultivation and scale-up conditions in bioreactors by predicting the critical shear stress and hence proposing optimum impeller speeds for cell cultivation processes [87, 88].

CHAPTER III

DEVELOPMENT AND CHARACTERIZATION OF THE MULTI-CHAMBER SINGLE-USE BIOREACTOR - A PROOF OF CONCEPT PROTOTYPE

This Chapter is published in Biochemical Engineering Journal, 15 February 2018, Volume 130, pages 113-120 [115].

3.1 Introduction

For quite some time, the gold standard for upstream processing in the biopharmaceutical industry has been reusable stainless-steel bioreactors. However, since the first WAVE bioreactor system was introduced in the late 1990s [15], single-use technology has garnered extensive interest and been a tremendous success in the field [16]. Drawbacks associated with the use of stainless-steel bioreactors have helped lead to the quick adoption of single-use technology. The need for continual re-sterilization, reduction of the overall production time due to required cleaning time between batches, and increased risk of cross contamination between different cell lines or proteins produced in the same bioreactor are commonly acknowledged as some of the biggest drawbacks [89]. In contrast, processes based on single-use technology offer many advantages. Disposable systems eliminate the need for cleaning-in-place, sterilization-in-place, and cleaning validation. They also reduce the risks of cross contamination and decrease production turnaround times [90]. Further, reduction in validation time shortens time to

market [19], which is undoubtedly a tremendous value given the extensive development and increased demand of recombinant protein therapeutics. Moreover, compared to a stainless-steel facility, a single-use technology operated facility is estimated to complete 27% more production batches per year to save about 23% of the cost for every gram of mAb produced. The same study also suggests that a modular facility incorporating single-use equipment for manufacturing would save over a year in design and construction compared to a conventional facility, and hence, would generate a faster return on investment [24].

There are still key challenges facing single-use technology developers and end-users. One challenge is the limited bioreactor volume, where single-use bioreactors have been limited predominantly to 2,000 L or less for mammalian and insect cell cultures. This limitation improved slightly in late 2015, when ABEC, Inc. announced the industry's largest single-use bioreactor so far with a working volume of 3,500 L. Although this is a noticeable increase, the ABEC bioreactor is not yet widely used, and compared to a typical 20,000 L stainless-steel bioreactor, the ABEC bioreactor is still quite limited. For microbial fermentations, disposable systems still pose significant engineering challenges. These challenges are attributed to the fact that in aerobic microbial fermentations, oxygen demand and the rate of heat evolution are 25-70 times higher than in mammalian and insect cell cultures. Thus, much faster transfer of oxygen and better removal of heat from the culture are required. These needs are mostly addressed within glass and stainless-steel bioreactors but are not yet fully met within large volume bioreactors built from disposable plastics [38, 39]. Despite regulatory guidelines, leachables and extractables from disposable plastics still impose a risk, especially with existing studies showing that leachables from commercially available bags adversely affect cell growth [29].

A single-use bioreactor system typically consists of a fixed support structure and a control unit. The bioreactor is a disposable bag that is inserted in the support structure and

connected to the control unit which has the process control software installed. The bag is used for only one time and is then disconnected and disposed of when the batch is complete.

A traditional single-use bag is designed as a single compartment bag with a typical turndown ratio (i.e., the ratio of the maximum and minimum capacity of the bag) in the range of 2:1 to 5:1. Although the wave-rocking bioreactor Cell-tainer[®] is currently available in the market with the capability of expanding the cell culture volume by approximately 100-fold in the same bag (i.e., turndown ratio of ~100:1) [91], the unusual mixing principle and restricted scalability of a wave-rocking bioreactor often limits its use to low volume and simple applications such as seed-train expansion. For stirred tank reactors, the turndown ratio is still 5:1 at maximum. This volume limitation for cell cultivation inside a single, disposable bag necessitates the use of multiple bags with different working volumes throughout the seed-train process, which is the process of a stepwise scale-up of cell culture until inoculating the production scale bioreactor. Each of these intermediate bags typically requires its own control unit and support structure. In addition to the high cost, the large amount of equipment requires significant production floor space, as well as a regular qualification and documentation upon operation. Moreover, a stepwise seed-train process requires connecting separate bags each time the cultivated cells and nutrient medium are transferred from the smaller to larger bag, a procedure that requires highly trained personnel working under aseptic conditions.

Here, we introduce a novel design for a single-use, multi-chamber stirred tank bioreactor. The two-chamber bioreactor presented in this study is an early prototype demonstrating the concept of employing multiple chambers. The general design consists of an outer bag, or chamber, enclosing one or more additional smaller chambers. Together, all chambers require only a single control unit and supporting structure that fits the dimensions of the largest chamber. The current prototype has a small chamber with a minimum working volume of 1 L and a maximum working volume of 2.5 L. The large chamber has a working volume range from 12.5 to 50 L.

Thus, our prototype allows for a 50-fold expansion of the cell culture volume. Although this is 10 times higher than the permissible range of any stirred tank single-use bioreactor, it is not the upper limit of the invention. While the two-chamber bioreactor prototype serves as a proof of concept, other volumes (e.g. a two-chambers bioreactor with a minimum working volume of 10 L and a maximum working volume of 1,000 L) and additional chambers (e.g. a three-chambers bioreactor with an operating volume range of 1 L-1,000 L) can be used.

These unique design features enable a user to reduce production costs significantly, as the savings can be quite large when multiple seed-train intermediates are affected. This includes the costs associated with the purchase and qualification of the equipment, as well as the costs of current good manufacturing practice (cGMP) footprint. Freeing upstream production space can be of great value in industry, especially with the growing trend of providing fully equipped, modular flexible facilities, like the KUBio system from GE Healthcare and FlexMoSys™ from Sartorius Stedim Biotech [92]. The freed space can be used either for introducing more production scale bioreactors and multiplying the production capacity, or to include both upstream and downstream processing in the same room. Moreover, all chambers in our design are inter-connected through a closed tubing system. This allows the cell culture transfer from one chamber to another to be done simply using a peristaltic pump without the need of opening the system. This completely closed system reduces the risk of contamination by eliminating the processes of connecting separate bags for the transfer of the cell culture during the seed-train process.

In this study, we describe the construction of the two-chamber bioreactor in detail. We also evaluate the engineering aspects in both chambers. This includes mixing time (θ_m), power input per unit volume (P/V) and oxygen mass transfer coefficient ($k_L a$). Our results are compared to the published data of some commercially available bioreactors, with the same operating volumes.

3.2 Materials and Methods

3.2.1 Construction of the Prototype

A Mobius[®] CellReady 3 L bioreactor from Millipore was used as the smaller chamber of the two-chamber bioreactor, with some modifications. The shaft of the original vessel was replaced by a longer shaft, penetrating through the vessel bottom. The long shaft still carried the 3-blade marine impeller of the Mobius[®] vessel and ended with another larger 3-blade marine impeller to serve for mixing in the large chamber (Figure 3.1A). A Eurostar 100 Control stirrer, from IKA[®] Works, Inc. was connected to the shaft from the top of the small chamber head plate and was used to control agitation. Nice Ports with integrated dissolved oxygen (DO) and pH sensors, from PreSens-Precision Sensing GmbH (Germany), were welded to the wall of the small vessel for DO and pH measurements, with the ultimate aim of DO and pH process control. A dip tube was inserted from the head plate of the small vessel, to allow the fluid transfer across the two chambers via a peristaltic pump. The Mobius[®] 3 L bioreactor base was removed. The probes openings on the head plate were plugged, and all bottom tubing ends were blinded, except for the microsparger, which was connected to the gas sparging port on the top of the larger chamber. An early version of the prototype used a large 50 L chamber constructed from a flexible, polyethylene (PE)-ethylene vinyl alcohol (EVOH) 9101 barrier film from Renolit Corp. (California, USA). The film was heat welded using an impulse hand sealer to shape the 50 L flexible bag. At the top of the bag, a spout with an open top sleeve was made (Figure 3.1B). The bag constructed from this film was used in mixing time measurements because of the superior transparency of the film. A second version of the prototype was constructed by Flex Concepts, Inc. (Utah, USA), according to same specifications used for the first prototype. A double layered bag was used where the inner layer was made of PE and the outer layer was PE/EVOH/nylon/PE.

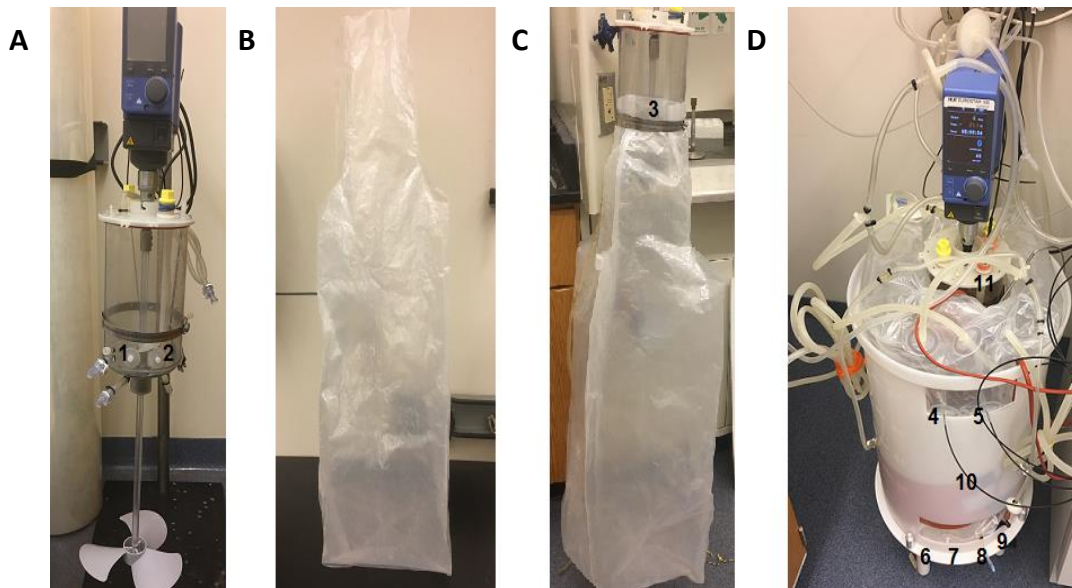


Figure 3.1. Assembly of the multi-chamber bioreactor prototype. (A) 3 L chamber, (B) 50 L chamber, (C) the two chambers connected, and (D) operating two chambers assembly. (1,2) pH and DO sensor ports, (3) clamp wrapping the 50 L bag around the 3 L chamber, (4, 5) ports for optical fibers insertion to connect with pH and DO sensor ports (1, 2) on the 3 L chamber through internal tubing, (6,7) pH and DO sensor ports, (8) sampling port, (9) thermocouple port, (10) optical fibers, (11) heating blanket inserted in the pocket formed by flipping and wrapping the 50 L chamber sleeve around the 3 L chamber.

The smaller chamber was fitted inside the open top sleeve (Figure 3.1C) and secured by a clamp to maintain the inner space of the larger chamber isolated from the outer atmosphere. Nice Ports with integrated DO and pH sensors were welded onto the surface of the larger chamber, and a sampling port and thermocouple port were added. Another two ports were welded on the side of the bag and are connected to the sensor ports of the smaller chamber, internally via silicone tubes. These tubes act as channels to connect optical fibers between the control unit and the sensors of the small chamber, while maintaining the sterile conditions in both chambers. Other ports for sparger, overlay gassing, exhaust and fluid transfer were welded at the top of the bag. Silicone tubes and Y-shaped connectors were used to connect these ports with the head plate ports of the smaller vessel, and clamps were used to control the flow across one or both chambers. A bottom port for harvesting was also welded to the bag. Securing the smaller chamber in the top sleeve of the larger one, creates an outer pocket surrounding the small chamber (Figure 3.1D). This pocket

was used to insert a silicone rubber heating blanket for temperature control of the fluid inside the small chamber. The heating blanket was wrapped around the small chamber and connected to a thermocouple and a digital temperature controller. A similar approach was used to control temperature of the large vessel, with a heating blanket wrapped around its bottom part.

3.2.2 Engineering Characterization of the Multi-Chamber Single-Use Bioreactor

3.2.2.1 Mixing Time

Mixing time was determined in both chambers using the de-colorization method described by Kaiser et al. [93]. Different fluid volumes and agitation speeds were tested under unaerated conditions. For every liter of deionized water, 12 mL of starch solution were added, and the fluid was then colorized by the addition of 0.2 mL/L of Lugol's iodine. Then, 0.2 mL/L of the tracer (1M sodium thiosulfate) was pipetted into the fluid, and time was taken immediately until the blue color disappeared completely. Each measurement was taken three times, by the same person to minimize inter-observer differences.

For the small 3 L chamber, measurements were taken using 1.5 L and 2.5 L volumes, at a tip speed ranging from 0.2 to 1.0 m/s. For the large 50 L chamber, measurements were taken at the maximum working volume at tip speeds of 0.6, 1.2, and 1.8 m/s. For the smaller chamber, results were compared to the published data for the Mobius® CellReady 3 L bioreactor [93]. For the larger 50 L chamber, results were compared to published experimental data for the Mobius® CellReady 50 L bioreactor [94] and the BIOSTAT® STR 50 L bioreactor [19]. While for HyClone 50 L S.U.B., the following regression of both experimental and computational fluid dynamics (CFD) data reported by Löffelholz [95] for mixing time (θ_m) as a function of the power input per unit volume (P/V) was used to generate data points for comparison.

$$\theta_m = 63.5(P/V)^{-0.44} \quad (\text{Equation 3.1})$$

3.2.2.2 Power Input

The Eurostar 100 Control stirrer was used to obtain real-time torque measurements in the large 50 L chamber. These torque measurements were used to calculate (P/V) at different agitation speeds and aeration rates. The impeller power number (N_e) was calculated subsequently using

$$N_e = \frac{V(P/V)}{\rho n^3 D^5} \quad (\text{Equation 3.2})$$

where ρ is the density of water at room temperature, n is the impeller speed, D is the impeller diameter, and V is the fluid volume.

The final reported N_e was the average of 10 different calculations at different agitation speeds and with Reynolds number (Re) $>10,000$, which implies a fully turbulent flow and a constant N_e .

3.2.2.3 Oxygen Mass Transfer

Oxygen mass transfer coefficient ($k_L a$) was determined by the gassing-out method. First, nitrogen gas was sparged into the fluid, and the DO reading was monitored until it reached 0%. Then, air was sparged into the liquid at specific aeration rates and agitation speeds. The DO reading was recorded at regular time intervals using the Fibox 4 fiber optic oxygen transmitter from PreSens- Precision Sensing GmbH (Germany), until the DO level reached saturation. All measurements were taken in a phosphate buffer saline solution for the 50 L chamber and a 0.5 M sodium sulfate solution for the 3 L chamber. Using the following formula, $k_L a$ was obtained:

$$\ln \left(\frac{c_{O_2}^* - c_{O_2}(t)}{c_{O_2}^* - c_{O_2}(0)} \right) = -k_L a t \quad (\text{Equation 3.3})$$

In the small chamber, $k_L a$ was calculated at tip speeds of 0.4, 0.6, and 1.0 m/s and at aeration rates of 0.05, 0.10, and 0.15 VVM (volume of air per volume of liquid per minute). For the large chamber, measurements were taken at tip speeds of 0.6, 1.2, and 1.8 m/s at the aeration rate of 0.1 VVM. Results were compared to published data for the following commercial bioreactors: Mobius® CellReady 3 L [93], BIOSTAT® STR 50 L [19], and HyClone 50 L S.U.B [96].

3.3 Results and Discussion

3.3.1 Geometrical Dimensions

In our first attempt to design and construct a multi-chamber single-use bioreactor, we aim to achieve acceptable and predictable results of the reactor engineering evaluation. Serving that purpose, in all stages of development, our goal is to maintain a standard design of both chambers. This includes, a standard geometry, constructing materials, mixing, heating, and sparging approaches.

The general configuration is a 3 L chamber within a larger 50 L chamber as depicted in Figure 3.1. The inner chamber is a Mobius CellReady 3 L bioreactor, which has been well characterized both experimentally and in terms of CFD simulations [86, 93]. Only minor modifications were implemented to the vessel in order to serve as the smaller chamber in our bioreactor. The most dominant of which is the exclusion and replacement of conventional probes with optical sensors mounted on the vessel wall. It is worth mentioning here that conventional, top mounted probes for the small chamber would be applicable in the two-chamber design presented in this study. However, our design, with the optical sensors mounted to the vessel wall, and an internal tubing serving as a secure channel for the optical fiber to connect the sensor to the control unit, offers an ultimate solution for any inner chamber in a multi-chamber bioreactor. For

instance, in a three-chamber bioreactor, the top mounted probes may still work for the smallest chamber, but our design would be necessary for the middle one.

The 50 L chamber is designed with a minimum working volume of 12.5 L and a maximum of 50 L. The chamber has a diameter of 38.0 cm and an overall height of 67.0 cm. The liquid height at the maximum working volume is 44.0 cm, thus, the aspect ratio of the fluid inside the chamber is 1.2, which lies within the 1-3 range recommended by Barradas et al. [97] for stirred tank reactors. The approach to mixing in the large 50 L chamber is identical to that in the smaller one. A top mounted, centered, 3-blade marine impeller is used. Both chambers are unbaffled. The ratio of the impeller diameter to the vessel diameter (D/T ratio) is 0.55 in the 3 L chamber and 0.59 in the 50 L chamber. A 3-cm long pipe sparger with 10 μm holes is mounted just below the impeller in the large chamber. While for the smaller chamber, the standard Mobius® CellReady bioreactor microsparger with 15-30 μm pore size is used.

3.3.2 Mixing Time

For the 3 L chamber, removal of the conventional probes was expected to have a negative impact on mixing behavior. Whereas the long probes immersed in the liquid would act, somehow, like baffles and improve radial mixing. However, our mixing time measurements showed very consistent results with the original Mobius® CellReady 3 L vessel, with less than 20% deviation observed at any data point, as shown in Figure 3.2.

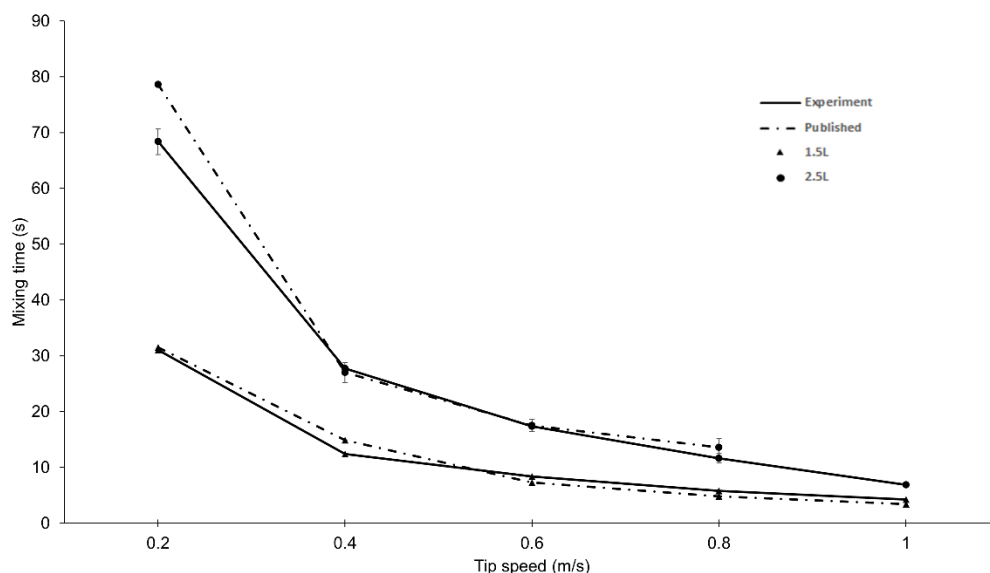


Figure 3.2. Mixing times in the small 3 L chamber versus the Mobius[®] CellReady 3 L bioreactor at 1.5 and 2.5 L working volumes and different tip speeds.

The 50 L chamber has a mixing mechanism similar to the smaller chamber, with a centered, 3-blade marine impeller and no internal baffles within the vessel. The centered impeller and lack of internal baffles could potentially lead to formation of a vortex at high agitation speeds and subsequently poor mixing. The three commercially available 50 L bioreactors used in this study avoid the formation of a vortex and poor mixing through various approaches. The HyClone S.U.B is designed with an angled impeller shaft. The BIOSTAT[®] STR has two impellers on a single shaft with one impeller located above the other, and the Mobius[®] CellReady bag contains baffles. For the simplicity, however, our strategy to enhance mixing is based on selecting a high (D/T) ratio. Nienow [98] showed that for any type of agitator, a larger D/T ratio improves bulk mixing. Other studies quantified the relationship between D/T ratio and mixing time, reporting that mixing time is inversely proportional to the squared D/T ratio [99, 100]. The D/T ratio in our large chamber is 0.59 compared to 0.32, 0.34, 0.38 and for the Mobius[®] CellReady, Hyclone S.U.B, and BIOSTAT[®] STR, bioreactors, respectively. Based on the D/T ratios of the

commercially available bioreactors and the relationship between mixing time and D/T ratio mentioned above, there is at a minimum of a 2.4-fold enhancement in the mixing time of our 50 L chamber compared to the commercially available bioreactors. An additional design approach we use to overcome potentially poor mixing is reduction of the aspect ratio. The liquid height to diameter ratio (H/T) in our large chamber is 1.2, compared to 1.3, 1.5, and 1.6 for the BIOSTAT® STR, Hyclone S.U.B, and Mobius® CellReady bioreactors, respectively. Others have also reported in the literature [101] that mixing time is directly proportional to the aspect ratio raised to the 2.5 power. According to this relationship, a 22% improvement in mixing time is achieved with just the 0.1 difference in aspect ratio between our chamber and the BIOSTAT® STR.

While conditions that favor formation of a vortex tend to lead to poor mixing, our results show that the D/T and H/T ratios can be varied to compensate for these effects. From Figure 3.3, it can be presumed that at higher agitation rates, where the negative effects of vortex formation are likely to be most apparent, both the increase in the D/T ratio and the reduction of the H/T ratio work together to partially compensate for the negative effects of a centered impeller and lack of internal baffles on mixing. At lower agitation rates, where the negative effects of vortex formation are likely to be substantially less, the improvements gained by varying the D/T and H/T ratios are not offset. Consequently, the mixing time of our chamber is similar to those of the commercially available bioreactors at high agitation rates and significantly better than two of the three commercially available bioreactors at low agitation rates.

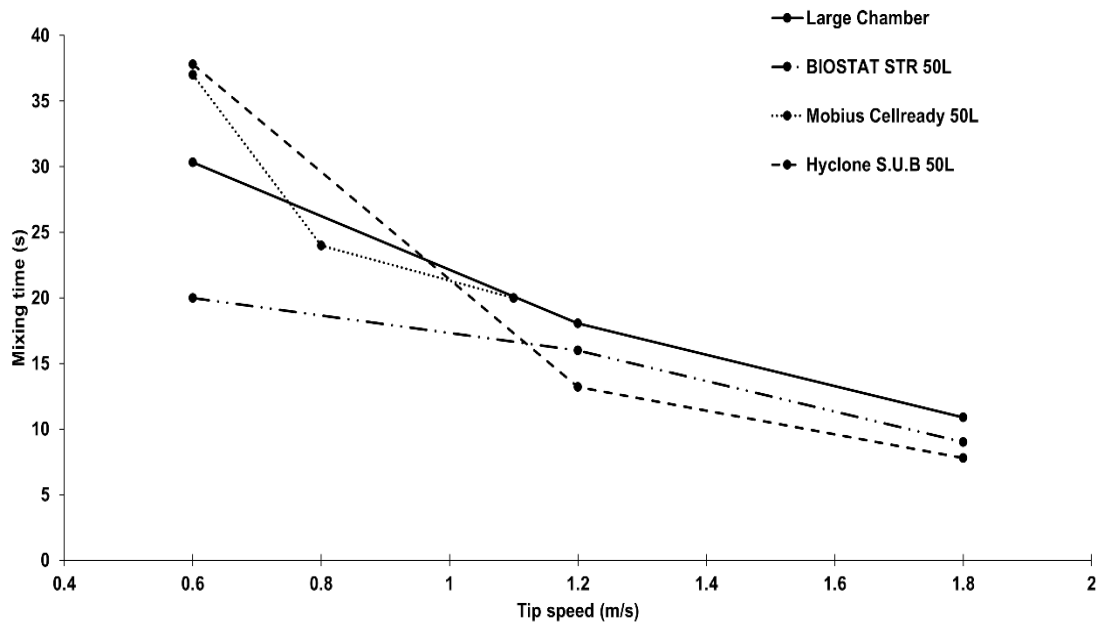


Figure 3.3. Mixing time in the large 50 L chamber versus BIOSTAT® STR [19], Mobius CellReady [94], and Hyclone S.U.B. 50 L bioreactors at maximum working volume and different tip speeds. (Mixing times reported for the Hyclone S.U.B. 50 L were generated from a regression of experimental and CFD data acquired by Löffelholz [95])

3.3.3 Power Input

Maintaining a constant P/V is one of the most commonly used approaches for scaling bioreactors. The impeller power number (N_p) is a dimensionless number that is a characteristic of the impeller geometry and is essential to predicting P/V at any operating condition using Equation 3.2. As shown in Table 3.1, our torque measurements at ten different fully turbulent conditions, give an average power number of 0.32 ± 0.01 . This result is in good agreement with the 0.3 power number for the pitched 3-blade impeller reported by Kaiser et al. [93] and by Couper et al. [102].

Table 3.1. Torque measurements and calculated Reynolds number (Re), power input per unit volume (P/V), and impeller power number (N_e) in the 50 L chamber at different agitation speeds.

RPM	Re	Torque (N.cm)	P/V (W/m ³)	N_e
90	58,834	0.07	13.19	0.31
120	78,445	0.13	32.67	0.33
150	98,056	0.19	59.69	0.30
160	104,593	0.21	70.37	0.30
170	111,131	0.25	89.01	0.31
180	117,668	0.29	109.33	0.32
190	124,205	0.33	131.32	0.33
200	130,742	0.37	154.99	0.33
210	137,279	0.41	180.33	0.33

As shown in Figure 3.4, calculated P/V values for our 50 L chamber are lower than those of the commercially available bioreactors. This can be attributed to the considerably low power number of our impeller, 0.3, compared to the power numbers reported for Hyclone 50 L S.U.B. [95] and BIOSTAT® STR 50 L with two 3-blade segment impellers [19], 2.2 and 1.3, respectively. Thus, for our reactor to operate at the same P/V of these commercially available bioreactors, a higher tip speed is needed. It is generally proposed to keep the tip speed value within the range of 1 and 2 m/s for mammalian cell cultures [103], which in our case, corresponds to a P/V range of 10-80 W/m³. This covers a wide spectrum of the typical 1-50 W/m³ range suggested for mammalian cell culture [104], with an average of 10 W/m³ [105]. Collectively, these results show that prototype can provide good mixing behavior at a relatively low power, without fearing cell damage.

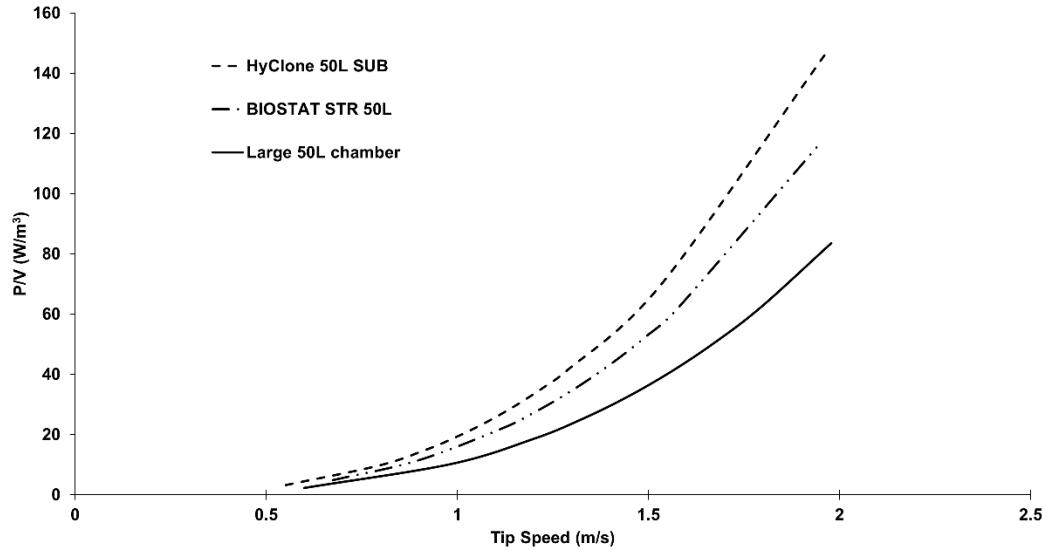


Figure 3.4. Calculated P/V at different impeller tip speeds in the large 50 L chamber, HyClone 50 L S.U.B., and BIOSTAT® STR 50 L with 2×3 -blade segment impellers.

3.3.4 Oxygen Mass Transfer

For aerobic processes like mammalian cell culture, the oxygen transfer rate becomes critical. The DO level should always be kept above a critical limit to maintain cell growth which is achieved by sparging air or pure oxygen into the culture. The mass transfer rate of oxygen to the culture, which is dependent on the oxygen mass transfer coefficient $k_L a$, should be higher than the rate at which growing cells take up oxygen [106]. The oxygen mass transfer coefficient depends on several factors, including, but not limited to, agitation rate, gassing rate, and sparger type, size, and position [107]. The most common cell cultures require $k_L a$ values between 5 and 10 hr^{-1} [19].

As shown in Figure 3.5, experimentally determined $k_L a$ values for the small 3 L chamber are in good agreement with published data for the Mobius® CellReady bioreactor [93], with a maximum difference of 25%. For the large 50 L chamber, $k_L a$ values are in even better

agreement with published results for the BIOSTAT® STR 50 L bioreactor (less than 15% deviation) but only for the model using a ring sparger with an 800 µm pore size.

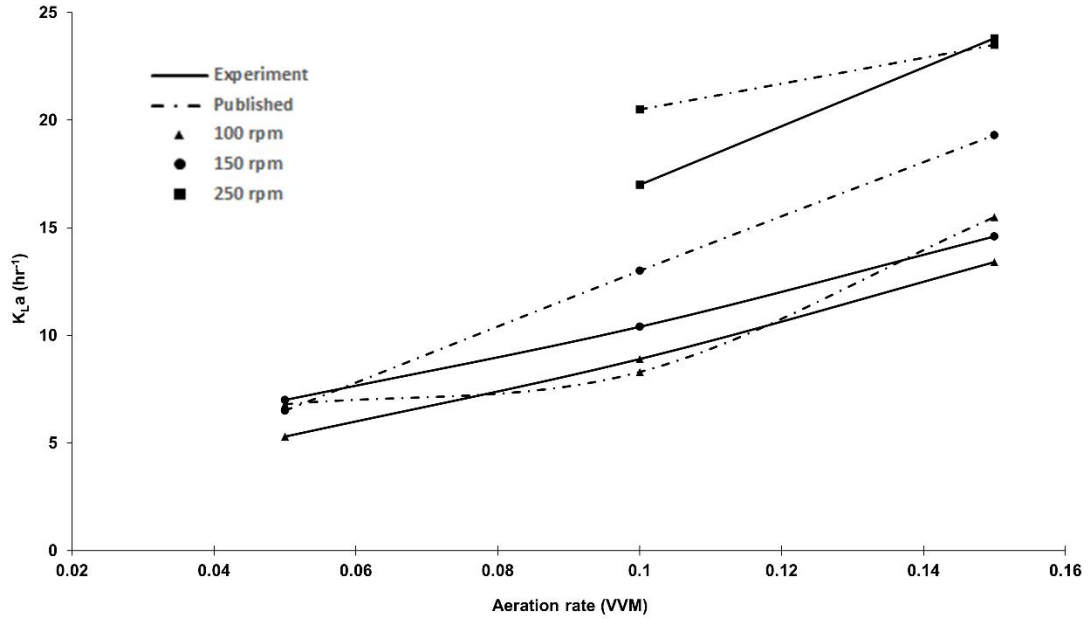


Figure 3.5. k_La values in the 3 L chamber at different aeration rates and tip speeds, compared to the experimental results for Mobius® CellReady 3 L.

Results for the prototype are significantly lower when compared to data for the BIOSTAT STR 50 L bioreactor model that uses a microsparger with 150 µm pore size (Figure 3.6). Sparger pore size clearly impacts k_La by affecting the bubble size and the resulting surface area available for mass transfer. Smaller bubbles are produced from spargers with smaller pores, which generates greater surface area at the gas-liquid interface and subsequently a higher oxygen transfer rate [19]. While this explains the higher k_La values for the BIOSTAT® STR 50 L bioreactor with a 150 µm pore size sparger compared to the bioreactor with an 800 µm pore size sparger, it does not explain why the 50 L chamber with a 10 µm pore size sparger had lower k_La values.

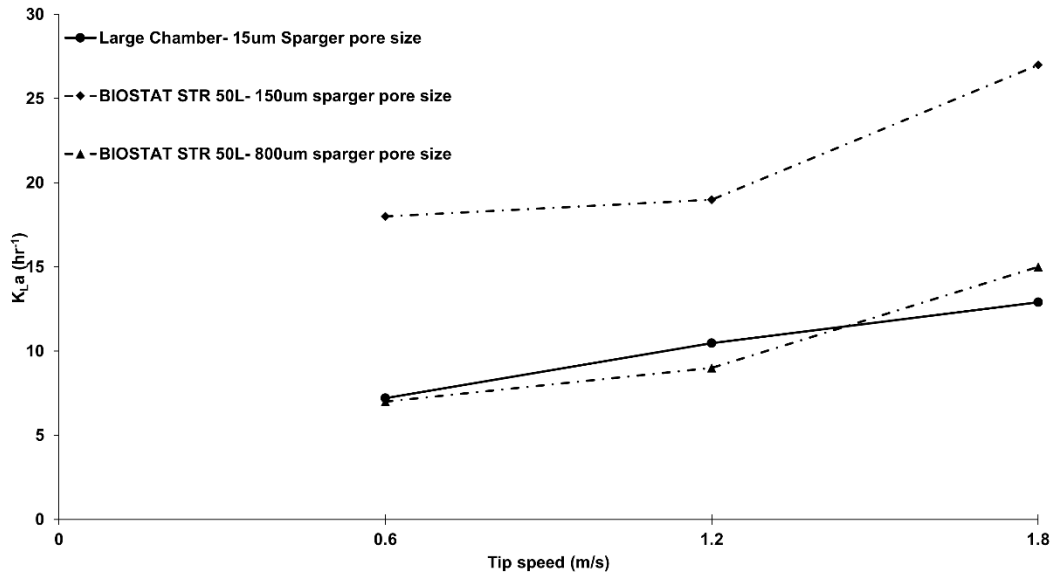


Figure 3.6. Calculated k_{La} values at 0.1 VVM aeration rate and different tip speeds in the large 50 L chamber and the BIOSTAT STR 50 L with the 800 μm pore size ring sparger and the 150 μm pore size microsparger.

Rewatkar et al. [108] studied the effect of different sparger designs on the fractional gas hold-up, which is the ratio of gas phase volume to the total fluid volume inside the reactor. The ring sparger, which is used in the BIOSTAT[®] STR 50 L bioreactor, was shown to have a consistent 20-30% improvement in gas hold up at different agitation rates, and hence greater k_{La} values. Also, Yawalkar et al. [109] reviewed a number of studies that directly correlated k_{La} to P/V . Yet another factor that affects k_{La} is the aspect ratio (H/T). A higher H/T yields a longer residence time of gas bubble and a higher k_{La} [110].

In order to understand the impact of these factors on our results, it is important to note that while our prototype 50 L chamber is constructed with a pipe sparger, the BIOSTAT[®] STR bioreactor has a ring sparger. The BIOSTAT[®] STR bioreactor also has a higher P/V at the same tip speed, and a higher H/T . All these factors can, to some extent, explain the enhanced oxygen mass transfer behavior of the BIOSTAT[®] STR reactor with the 150 μm pore sparger. While these

factors are probably compensated with the big difference in the sparger pore size between our reactor and the 800 μm sparger of the other BIOSTAT STR model.

The $k_L a$ determined at the tip speed 1.2 m/s in the prototype 50 L chamber is about 26% higher than the 8.3 hr^{-1} value reported at the same tip speed and aeration rate for the HyClone 50 L S.U.B, where a similar pipe sparger is used [96]. This improvement can be attributed to the smaller sparger pore size in our reactor (10 μm versus 15-30 μm in the HyClone 50 L S.U.B) and also to the higher impeller diameter to vessel diameter (D/T) ratio [111].

3.4 Optimization of the Manufacturing Process for a Second-Generation Prototype

A new method for fabricating a second-generation 2 L to 200 L, two-chamber prototype was conducted in collaboration with FlexConcepts, the same bag manufacturer that collaborated in fabricating the first-generation prototype. The new fabrication method allowed a fully automated manufacturing process of the prototype with two flexible chambers. A shaft carrying the impellers for both chambers was fabricated from FDA approved plastics (Appendices A.5 and A.6). The shaft was designed to pass through two polyethylene housing disks (Figure 3.7A). Each polyethylene housing is designed with an air/liquid tight seal and bearings for the rotating shaft to ensure aseptic conditions and to prevent culture leakage (Appendices A.3 and A.4). The two chambers of the prototype were fabricated as two separate flexible bags at FlexConcepts using their specialized machinery and the double layered plastic films (Appendices A.1 and A.2). The films were then welded to the polyethylene housings of the shaft. The upper surface of the lower housing was welded to the bottom of the smaller bag, while the bottom surface was welded to the top of the larger chamber to create the configuration of the two chambers one on top of the other (Figure 3.7B). The smaller chamber was then pushed downwards to create a sealed pocket to insert a heating blanket for the sake of temperature control inside the small chamber (Figure 3.7C).

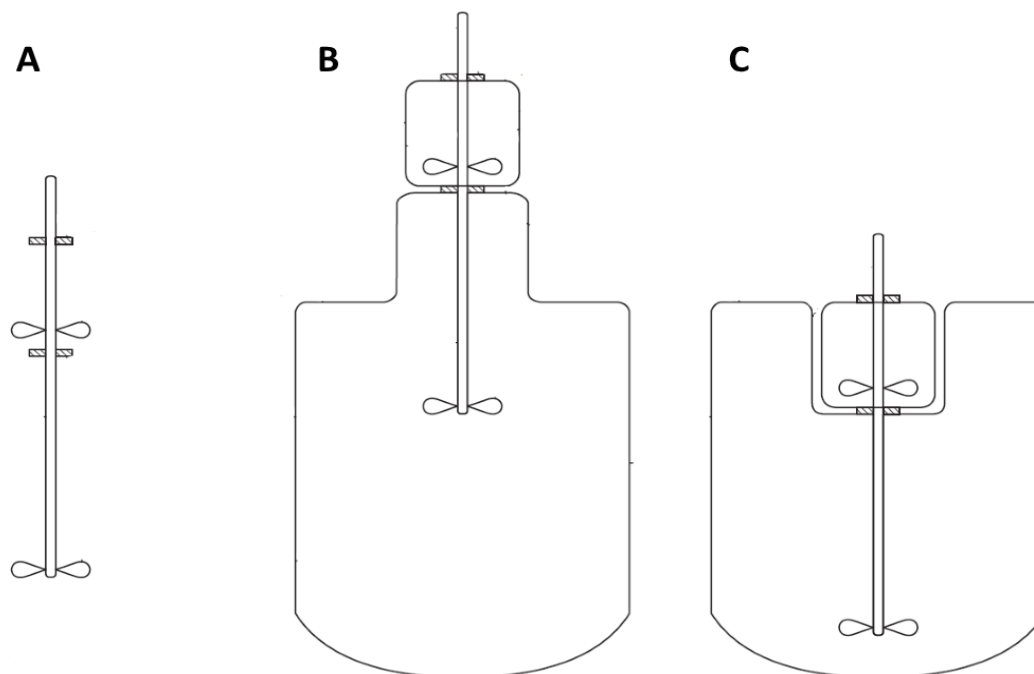


Figure 3.7. Sketch for the second-generation prototype fabrication parts and assembly. (A) a shaft carrying impellers for mixing both chambers going through polyethylene housings with air-tight seal and bearings, (B) two-flexible chambers welded to the polyethylene housings on the shaft, (C) the smaller chamber pushed downwards creating a sealed pocket.

3.5 Cell Culture Evaluation

Cell culture behavior of the developed two-chamber bioreactor shown in Figure 3.1 was evaluated by growing recombinant protein producing cells. The IgG producing CHO cell line (CRL-11397, ATCC) was grown in the two-chamber bioreactor. The culture was expanded in T-flasks up to 400 mL, then it was seeded in the smaller chamber of the bioreactor at a total volume of 2.5 L at a seeding density of 3.5×10^5 viable cells/mL. A BIOSTAT CULTIBAG control unit from Sartorius was connected to the optical sensors welded on the walls of each chamber and was used to take DO and pH measurements in the culture medium. The sparger inlet filters were connected to separate mass flow controllers which were coupled to compressed air, oxygen, and carbon dioxide cylinders. The flow rate of different gases into the culture medium was manually controlled according to pH and DO values recorded on the BIOSTAT control unit. In 48 hours,

the viable cell density was more than doubled reaching 8.0×10^5 cells/mL in the smaller chamber. The culture was transferred to the larger chamber and scaled up to 10 L. The culture was monitored for an additional 12 hours. At this point, the cell viability began to decline, and the manual control became impractical (cell growth curve is shown in appendix A.7). Further validation of the prototype cell culture behavior is required with automated culture control.

3.6 Conclusions

The multi-chamber single-use bioreactor presented in this paper is based on a novel concept for cell culture in the biopharmaceutical industry. In this study, we presented a two-chamber bioreactor that allows for cell culture expansion from 1 to 50 L in a single, closed system. This volume expansion is 10 times greater than the range currently offered by commercially available stirred tank bioreactors. The unique features associated with the bioreactor will save upstream equipment cost and space and reduce the risk of microbial contamination.

The two-chamber bioreactor is a simple demonstration of an approach that can be extended to more than two chambers. For example, a third chamber with a working volume range from 250 to 1,000 L can be integrated into the design presented in this study to form a three-chamber bioreactor with the capability of a thousand-fold increase of the cell culture volume in a single bioreactor. One may expect that such a design will be associated with additional challenges in manufacturing, sterilization and operation in terms of complexity and costs. Hence, a risk/cost-benefit analysis will be needed.

The early prototype presented in this study operates under conditions that follow general recommendations for cell culture bioreactors, and engineering characterization shows that the performance of the prototype is comparable to commercially available bioreactors. The purpose of this early prototype is to demonstrate proof of a novel approach to cell culture volume

expansion, and in general, the bioreactor is not limited to the configuration used in this study. For example, the bioreactor can be modified to accommodate other chamber volumes and geometries, as well as other mixing, heating, and sparging mechanisms. The approach to optimizing the design of the bioreactor can be simplified by evaluating proposed configurations using CFD simulations to predict engineering characteristics, where subsequently only the most promising candidates are experimentally validated using cell culture.

3.7 Acknowledgments

Funding: This work was supported by the Technology Business Development Program at Oklahoma State University.

3.8 Notation

a	[m ⁻¹]	interfacial area of air per unit volume of liquid
$C_{O_2}^*$	[kg/m ³]	dissolved oxygen saturation concentration in liquid phase
C_{O_2}	[kg/m ³]	dissolved oxygen concentration in liquid phase
D	[m]	impeller diameter
H	[m]	liquid height
$k_L a$	[s ⁻¹]	specific oxygen mass transfer coefficient
n	[s ⁻¹]	stirrer rotational speed
N_e	[-]	impeller power number
P	[W]	impeller power input
Re	[-]	Reynolds number
T	[m]	vessel diameter
V	[m ³]	volume of liquid

Greek symbols

ρ	[m/s]	density
θ_m	[s]	mixing time

CHAPTER IV

USING CFD SIMULATIONS AND STATISTICAL ANALYSIS TO CORRELATE OXYGEN MASS TRANSFER COEFFICIENT TO BOTH GEOMETRICAL PARAMETERS AND OPERATING CONDITIONS IN A STIRRED-TANK BIOREACTOR

This Chapter is published online in Biotechnology Progress Journal in February 2019 [112].

4.1 Introduction

The first single-use bioreactor was introduced in the late 1990s as a plastic bag that is mixed via wave motion [15]. Since then, single-use bioreactors have gathered a great deal of interest and been hugely successful in replacing their stainless-steel counterparts for upstream processing in the biopharmaceutical industry [16]. While wave-mixed bioreactors initially dominated the single-use technology market, stirred bag systems have gained in popularity and are being used in large numbers. The fact that stirred bags are more similar to the stainless-steel reusable bioreactors, where there is extensive experience, has facilitated their penetration of the market and their integration into modern manufacturing processes [19, 113, 114].

Single-use bioreactors are sterilized, ready-to-use, cultivation vessels. They are used once and then discarded after the end of the cultivation run. Processes based on single-use technology offer many advantages. The use of such disposable systems eliminates the need for cleaning-in-place, sterilization-in-place, and cleaning validation. The risk of cross-contamination and

production turnaround times are also reduced [90]. Further, single-use bioreactors reduce the validation time and shorten time to market [19], which is an enormous advantage given the extensive development and increased demand of recombinant protein therapeutics. In 2013, estimates indicated that compared to stainless-steel facilities, single-use operated facilities had annual production rates that were 27% greater and production costs that were 23% lower on a gram of mAb basis [24].

In addition to the above-mentioned advantages of single-use technology, we have proposed a new multi-chamber, single-use bioreactor that possesses additive advantages [115]. The proposed design involves chambers of different volumes, where a larger chamber encloses a smaller one, all presented as a single closed system that requires only one control unit and support structure. Thus, a 50 to 100-fold increase in the culture volume can be achieved in one single bag during the seed-train process. That is a substantial enhancement to the current limit of only 5-fold increase achievable in any stirred-tank single-use bioreactor on the market. The multi-chamber design allows a further reduction in the upstream processing costs. The cost reduction includes the cost associated with the purchase, qualification, and maintenance of equipment, as well as the cGMP factory footprint occupied by the different seed-train bioreactors and control units. The design also reduces the risk of microbial contamination by allowing transfer of the cell culture between the different chambers, through internal tubing, via gravity or peristaltic pumps, without the need of opening the system. Our early proof of concept work [115] was based on a single-use, two-chamber bioreactor design. The smaller chamber had a 3 L maximum operating volume and had a geometry similar to the Mobius® CellReady 3 L bioreactor, while the larger chamber had a 50 L maximum operating volume. The engineering characterization of the two chambers showed good agreement with other commercially available bioreactors with the same working volumes. However, the 50 L chamber required some design optimizations to improve the oxygen mass transfer (k_{La}) to be more in line with other bioreactors on the market.

The aim of the study presented here was to use computational fluid dynamics (CFD) simulations to model mixing and gassing in the 50 L chamber of the multi-chamber bioreactor and to validate the simulations with the published experimental data. The simulation model was then used to study the effect of different impeller and sparger sizes on k_{LA} , as well as the effect of using a ring sparger instead of the pipe sparger, which was used in the early 50 L prototype.

CFD is a powerful tool that has been consistently applied to model stirred-tank bioreactors. The CFD models can generate high-resolution localized data regarding some parameters that are hard or even impossible to measure, such as the distributions of shear stress and turbulent kinetic energy [73]. Many scientific papers have used CFD to model fluid flow and turbulence inside agitated systems [46-50]. Other studies used CFD to model multiphase flow including gas phase, particle tracking or reaction processes [52, 62-67]. The suitability of CFD models for engineering characterization of single-use bioreactors has also been demonstrated. Many case studies have been reviewed by Loffelholz et al. [84], as well as some other recent studies [85, 86]. These studies involved stirred-tank and wave-mixed bioreactors, as well as other bioreactor designs with uncommon mixing mechanisms like the oscillating disk with conical orifice in the Vibromix system and the air wheel in the PBS Biotech bioreactor. The case study of the PBS bioreactor was unique in the sense that the CFD simulations were used to develop the market ready bioreactor based on only a prototype, which relates to one scope of the present study regarding the multi-chamber bioreactor development. Applying CFD in the bioreactor development process led to a significant reduction in time and costs [84]. CFD has been also used to optimize cultivation and scale-up conditions in bioreactors by predicting the critical shear stress and hence proposing optimum impeller speeds for cell cultivation processes [87, 88].

In the present study, numerical simulations were performed using ANSYS Fluent 17.0 (ANSYS Inc., Canonsburg, PA). A Eulerian-Eulerian model was employed to model the multiphase flow combined with the *k-epsilon* dispersed turbulence model. A population balance

model (PBM) has been previously employed in multiphase simulations of stirred-tank reactors [116-118] and was used in this study to predict bubble size distribution in the stirred-tank reactor by considering bubble breakage and coalescence. The number and sizes of bins of the PBM for different agitation speeds were optimized by trial-and-error approach and were validated by experimental data generated from the 50 L chamber of the multi-chamber bioreactor. The model was then used to compare between a pipe sparger, which was used in the bioreactor prototype, and a ring sparger, in terms of the efficiency of oxygen mass transfer in the bioreactor. Oxygen mass transfer coefficient (k_La) is an indication of the oxygen transfer efficiency in the culture medium. A higher k_La value is required to ensure that the oxygen demand is met at higher cell densities, and to avoid excessive gassing which, in addition to the higher cost, may introduce excessive shear on the cells. Generally, while developing a new bioreactor, a design with a high (k_La) and a reasonable shear stress will enable growth of higher cell densities, reduce operating costs, and eventually result in a bioreactor that more favorably compares to commercially available top-tier bioreactors.

Different sparger and impeller sizes were also examined using the validated CFD model. Many studies, as reviewed by Markopoulos et al. [119], have correlated k_La to the operating conditions like power input per unit volume (P/V) and superficial gas velocity for a given bioreactor geometry. In this study, we present a model equation to correlate k_La in a stirred-tank bioreactor to different geometrical and operating factors. The developed model equation correlates k_La to geometrical factors (i.e. impeller-to-vessel diameter ratio, D/T , and sparger-to-impeller diameter ratio, d_{sp}/D), mixing factors (i.e. Reynolds number, Re), and gassing factors (i.e. volumetric gas flow per unit liquid volume, Q/V_L). The developed model equation can be used to help the selection of the proper sparger, impeller, and vessel geometries and dimensions to be constructed and integrated during the development process of stirred-tank bioreactors, especially the next generation multi-chamber bioreactor prototypes of different operating

volumes. The model can also be used to predict the oxygen mass transfer efficiency in stirred-tank bioreactors under variable operating conditions.

4.2 Bioreactor Geometry Reconstruction and Mesh Regeneration

The bioreactor under consideration was the 50 L chamber of the two-chamber, single-use bioreactor described earlier (Figure 4.1A) [115]. The chamber was a cylindrical vessel with a diameter (T) of 38.0 cm and a height of 67.0 cm. The liquid height at the maximum working volume was 42.0 cm which was the height considered in the CFD model. A three-blade impeller pitched at 30 degrees was carried on a central, top mounted shaft and was used to mix the fluid inside the bioreactor. The impeller diameter (D) was 22.8 cm. The air sparger was placed at the bottom center of the bioreactor. The sparger was a pipe with a length of 3.1 cm and constant pore sizes (d_h) of 10 μm . For CFD simulations, different impeller diameters were examined, as well as other pipe spargers of different lengths and ring spargers with variable diameters. Experiments and simulations were carried out at impeller tip speeds of 0.6, 1.2 and 1.8 m/s, which for the constructed prototype, corresponded to 50, 100 and 150 rpm, respectively. The air sparging rate was set at 0.02, 0.05 and 0.10 volume of air per volume of liquid per minute (VVM).

Booleans for the solid parts of the bioreactor (i.e. shaft, impeller, and sparger) were created so that only the fluid domains of the bioreactor were considered for the simulation. Two distinct fluid domains were created. A smaller domain, or the moving reference frame (MRF), was defined near the impeller and was set as a rotating region with a velocity corresponding to the impeller tip speed. The other volume, which was the stationary volume, was the volume away from the impeller.

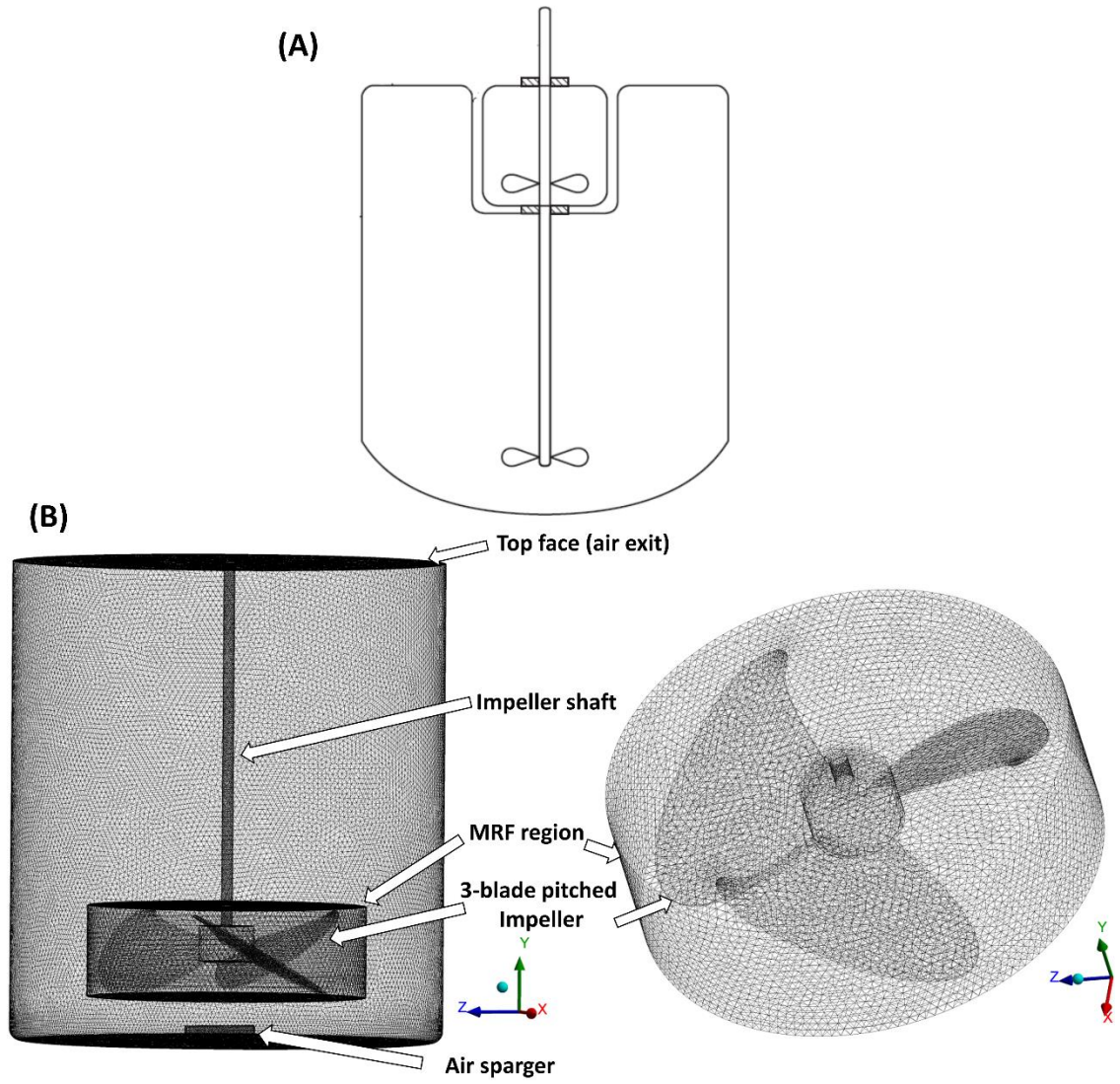


Figure 4.1. Illustration of the bioreactor geometry and mesh.

Unstructured tetrahedral meshes were generated using ANSYS Meshing (ANSYS Inc., Canonsburg, PA). Interfaces were defined at the joint boundaries of the two fluid domains allowing free flow across the two regions. The ANSYS meshing tool generated unstructured grids consisting of tetrahedral elements (Figure 4.1B). Mesh quality has been improved and checked to meet the requirement in ANSYS Fluent. Specifically, all mesh elements had skewness less than 0.83, and 98.4% of the elements had an aspect ratio between 1 and 2. A mesh independence test was performed to identify the optimum number of mesh elements that provides accurate results

and good computational efficiency. Multiple sets of mesh with different numbers of elements were generated, and simulations were run on each of them. The results were initially found to vary with the mesh element size until it reached a certain point where the results were constant and no longer dependent on the grid size. The k_{LA} value was the parameter selected to perform the mesh independence test. As shown in Figure 4.2, increasing the number of mesh elements beyond 1.48 million cells resulted in negligible differences in k_{LA} values, and thus the 1.48 million grid size was selected for all further simulations. For the mesh independence test, simulations were run at the bioreactor impeller speed of 150 rpm and an inlet air flow rate of 0.1 VVM. The final mesh (shown in Figure 4.1B) contains 1,487,040 elements and 266,038 nodes.

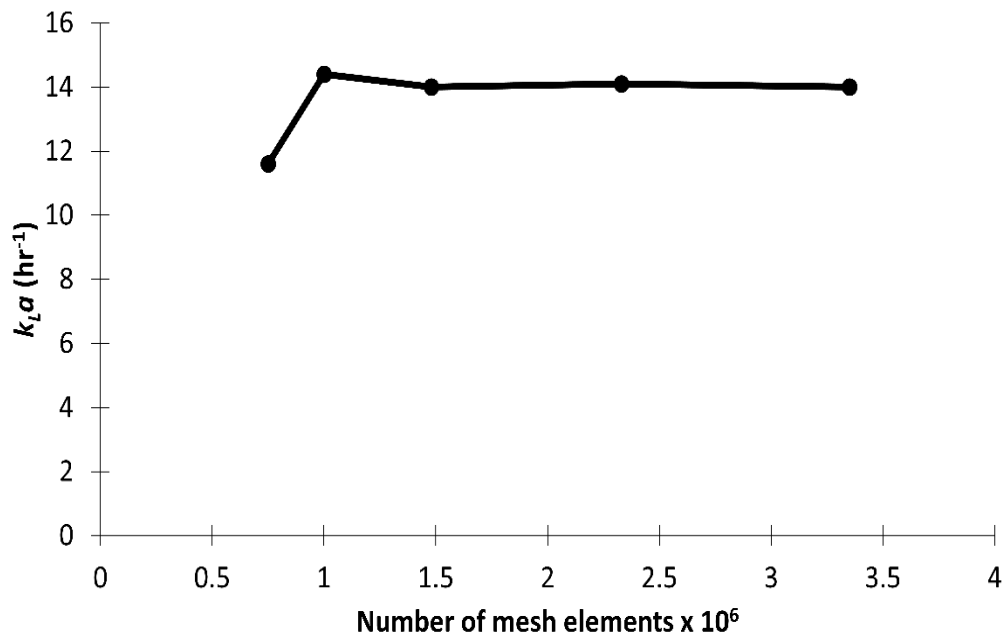


Figure 4.2. Mesh independence test where k_{LA} is plotted as a function of number of mesh elements. Simulations are carried out at impeller tip speed of 1.8 m/s and aeration rate of 0.1 VVM.

4.3 Numerical Setup

The CFD simulations were carried out using the ANSYS FLUENT 17.0 finite volume solver. The bioreactor vessel containing liquid mixed by an impeller and aerated from the bottom was represented by a multiphase gas-liquid system. The system was modeled using the Eulerian-Eulerian multiphase model, where water was the primary continuous phase and air was the secondary phase and was dispersed in water as air bubbles.

All walls were treated with no-slip boundary conditions. The sparger surface was treated as air velocity inlet, where the air volume fraction was set to unity. The bioreactor top was set as a degassing outlet to allow only air to escape from the bioreactor top boundary and not water. Properties of fluids in the simulations were set as follows: for water, $\rho_L = 998.2 \text{ kg/m}^3$, $\mu_L = 0.001 \text{ kg/m}\cdot\text{s}$, while for air $\rho_G = 1.225 \text{ kg/m}^3$, $\mu_G = 1.789 \times 10^{-5} \text{ kg/m}\cdot\text{s}$, and the water-air interfacial tension $\sigma_L = 0.072 \text{ N/m}$.

The phase-coupled SIMPLE algorithm was used for pressure velocity coupling. The second order upwind scheme was used for momentum discretization, and the first order upwind scheme was used for the turbulent kinetic energy (k) and turbulent dissipation rate (ϵ). QUICK scheme was used to solve for volume fraction while the Green-Gauss node-based method was used for gradient. For each simulation, single-phase flow was performed first by solving continuity and momentum equations. The single-phase solution was then used to initialize the multiphase solution. The time step was set to 0.01 s in single-phase simulations and 0.001 s in multiphase simulations. The maximum number of iterations per time step was set to 60. Convergence was determined by reaching residuals below 1×10^{-5} for all parameters and 1×10^{-4} for continuity and by reaching a constant k_{La} value over a significant number of time steps.

4.4 Governing Equations

4.4.1 Eulerian-Eulerian Multiphase Model

This model involves solving the Navier-Stokes equations assuming constant density and viscosity for both phases. The governing equations for mass and momentum conservation are

$$\frac{\partial}{\partial t}(\rho_i \alpha_i) + \nabla \cdot (\alpha_i \rho_i \mathbf{U}_i) = 0 \quad (\text{Equation 4.1})$$

$$\frac{\partial}{\partial t}(\rho_i \alpha_i \mathbf{U}_i) + \nabla \cdot (\rho_i \alpha_i \mathbf{U}_i \mathbf{U}_i) = -\alpha_i \nabla p + \nabla \cdot \boldsymbol{\tau}_{ef} + \mathbf{R}_i + \mathbf{F}_i + \alpha_i \rho_i \mathbf{g} \quad (\text{Equation 4.2})$$

where ρ_i , α_i , and \mathbf{U}_i are the density, volume fraction, and mean velocity vector of phase i , respectively, where the subscript i refers to either the liquid (L) or gas (G) phase. The terms p , \mathbf{R}_i , and \mathbf{F}_i represent the pressure, momentum exchange, and centrifugal forces. The term \mathbf{g} is acceleration due to gravity. The Reynolds stress tensor, denoted by $\boldsymbol{\tau}_{ef}$, was described by the k - ε turbulence model provided by FLUENT and was used with default settings [120].

The sum of both liquid and gas phase volume fractions remains unity in every cell domain as follows:

$$\alpha_L + \alpha_G = 1 \quad (\text{Equation 4.3})$$

The drag force acting on the air bubbles resulting from the relative velocity between the two phases is the most important interface force. The drag force for the secondary phase can be described as [121]

$$\mathbf{R}_G^{Drag} = \frac{18\alpha_G(1-\alpha_G)\mu_L C_D Re_p}{24d_p^2} (\mathbf{U}_G - \mathbf{U}_L) \quad (\text{Equation 4.4})$$

While the drag force for primary phase can be described as

$$\mathbf{R}_L^{Drag} = -\mathbf{R}_G^{Drag} \quad (\text{Equation 4.5})$$

While there are several drag law models provided by FLUENT, Kaiser [122] reported that the drag coefficients, C_D , predicted from nine different models were nearly identical at low particle Reynolds number, Re_p , and the drag coefficients only began to deviate when Re_p was close to 1,000. In our study, the maximum Re_p was 0.22, as calculated from Equation 4.7, which suggests that any of the drag law models can be used in our simulations with little concern of differences. The drag coefficient described by the Schiller and Naumann correlation [121] is frequently used in literature to simulate stirred-tank bioreactors [93, 116, 117], and was selected in our study:

$$C_D = \begin{cases} \frac{24(1+0.15Re_p^{0.687})}{Re_p} & Re_p \leq 1,000 \\ 0.44 & Re_p > 1,000 \end{cases} \quad (\text{Equation 4.6})$$

The particle Reynolds number [123] is

$$Re_p = \frac{\rho_L |U_G - U_L| d_p}{\mu_L} \quad (\text{Equation 4.7})$$

4.4.2 Turbulence Model

Because the volume fraction and the density of the secondary phase is low, and the density difference between the two phases is high, the dispersed k - ϵ turbulence model was used. In this dispersed k - ϵ model, the turbulence of dispersed phase is not considered, and the flow of this secondary phase is considered to be laminar [124].

The liquid phase turbulence viscosity is described as [125]:

$$\mu_{t,L} = \rho_L C_\mu \frac{k_{Liq}^2}{\epsilon_L} \quad (\text{Equation 4.8})$$

where the turbulent kinetic energy term for the liquid phase (k_{Liq}) should not be confused with the convective mass transfer coefficient (k_L) that is a part of the oxygen mass transfer coefficient

(k_L). Within Equation 4.8, the transport equations for the turbulent kinetic energy, k , and the turbulent energy dissipation, ε , are given by

$$\frac{\partial(\rho_L \alpha_L k_{Liq})}{\partial t} + \nabla \cdot (\rho_L \alpha_L k_{Liq} \mathbf{U}_L) = \nabla \cdot \left(\alpha_L \frac{\mu_{t,L}}{\sigma_k} \nabla k_{Liq} \right) + \alpha_L G_{kL} - \alpha_L \rho_L \varepsilon_L + \alpha_L \rho_L \Pi_{kL}$$

(Equation 4.9)

$$\frac{\partial(\rho_L \alpha_L \varepsilon_L)}{\partial t} + \nabla \cdot (\rho_L \alpha_L \varepsilon_L \mathbf{U}_L) = \nabla \cdot \left(\alpha_L \frac{\mu_{t,L}}{\sigma_\varepsilon} \nabla \varepsilon_L \right) + \alpha_L \frac{\varepsilon_L}{k_{Liq}} (C_{1\varepsilon} G_{kL} - C_{2\varepsilon} \rho_L \varepsilon_L) + \alpha_L \rho_L \Pi_{\varepsilon L}$$

(Equation 4.10)

where G_{kL} is the rate of production of k , Π_{kL} and $\Pi_{\varepsilon L}$ account for the influence of dispersed phase on the continuous phase [126], while C_μ , $C_{1\varepsilon}$, $C_{2\varepsilon}$, σ_k , and σ_ε are model parameters given the values 0.09, 1.44, 1.92, 1.0, and 1.3, respectively [120].

4.4.3 Population Balance Model

While constant bubble size models are simple and require less computational time, they do not accurately represent the physical system [125, 127]. Bubbles are discharged from the sparger with a uniform diameter. Once they are in the medium, however, the bubbles interact with the moving primary phase and undergo breakup and coalescence. Bubble breakup occurs when the liquid disruptive forces overcome the bubble surface tension, while coalescence happens when bubbles collide strongly enough to break the bubble thin film. A population balance model provides more accurate information by predicting coalescence and breakup mechanisms and providing information on the bubble size and the bubble size distribution within the bioreactor [68, 127, 128]. In this study, the method of classes [129, 130] was used for discretizing and solving the population balance partial differential equation, which can be written as follows:

$$\frac{\partial(\rho_G n_i)}{\partial t} + \nabla \cdot (\rho_G \mathbf{U}_{G,i} n_i) = \rho_G (B_{iC} - D_{iC} + B_{iB} - D_{iB}) \quad (\text{Equation 4.11})$$

In this equation, n_i is the number of bubbles in the bubble class i , $U_{G,i}$ is the velocity vector of gas phase bubbles in the class i , B_{iB} and B_{iC} are the bubble birth rates due to breakage and coalescence, and D_{iB} and D_{iC} are the bubble death rates due to breakage and coalescence, respectively. These terms are modeled as functions of bubble volumes V' as follows [129]:

$$B_{iC} = \frac{1}{2} \int_0^V a(V - V', V') n(V - V', t) n(V', t) dV' \quad (\text{Equation 4.12})$$

$$D_{iC} = \int_0^\alpha a(V, V') n(V, t) n(V', t) dV' \quad (\text{Equation 4.13})$$

$$B_{iB} = \int_V^\alpha m(V') b(V') p(V, V') n(V', t) dV' \quad (\text{Equation 4.14})$$

$$D_{iB} = b(V) n(V, t) \quad (\text{Equation 4.15})$$

In these equations, $a(V, V')$ is the coalescence rate between the different sized bubbles of volumes V and V' , $b(V')$ is the breakage rate of bubble with volume V' , $m(V')$ is the number of daughter bubbles formed due to fragmentation from bubbles of volume V' , $n(V, t)$ is the number of bubbles of volume V at time t , and $p(V, V')$ is the probability density function to determine offspring bubbles of volume V generated from bubbles of volume V' .

Because it is more useful to work in terms of the volume fraction of a particular bin of bubbles (f_i) than the number of bubbles in that bin (n_i), it is convenient to express Equation 3.11 in different terms. With the volume fraction of bubble size i defined as

$$\alpha_i = n_i V_i \quad (\text{Equation 4.16})$$

and f_i defined as the ratio of the volume fraction of the i^{th} bin to the total gas volume fraction,

$$f_i = \frac{\alpha_i}{\alpha_G} \quad (\text{Equation 4.17})$$

and

$$\sum_i f_i = 1 \quad (\text{Equation 4.18})$$

The population balance equation (Equation 4.11) can be written in terms of f_i and α_G :

$$\frac{\partial(\rho_G f_i \alpha_G)}{\partial t} + \nabla \cdot (\rho_G \mathbf{U}_{G,i} f_i \alpha_G) = \rho_G V_i (B_{iC} - D_{iC} + B_{iB} - D_{iB}) \quad (\text{Equation 4.19})$$

Sauter mean diameter (d_{32}) was used as the input bubble diameter in the simulation and was used to couple the PBM with the fluid dynamics [129]. The Sauter mean diameter is given by

$$d_{32} = \frac{\sum n_i d_i^3}{\sum n_i d_i^2} \quad (\text{Equation 4.20})$$

Many breakage and coalescence models for bubble flow are available. These models, however, are quite similar with some minor differences in the model constants or assumptions used to develop the model [62]. While the discussion of aggregation and breakage kernels is beyond the scope of this paper, it is worth mentioning that several studies [131-134] have detailed comparisons between the different breakage and coalescence models, including those proposed by Prince and Blanch [135], Luo and Svendsen [136], Luo [137], Chesters [138], Martínez-Bazán et al. [139], Alopaeus et al. [140], and Lehr et al. [141]. The findings from these studies suggest that there is little difference between the mean flow, gas hold-up and bubble Sauter mean diameter predicted by the different models, while there is some difference in the predicted bubble size distribution.

In this study, The FLUENT embedded Luo-Svendsen [136] and Luo [137] models were used to model both the breakage and coalescence of bubbles, respectively. The models have been frequently used in literature to simulate stirred-tank bioreactors using FLUENT software [116, 117]. In the breakage model, only turbulent eddies with a scale smaller than the bubble diameter

are considered to cause the bubbles to break while larger scale eddies are only considered to convect the bubbles.

4.4.4 Mass Transfer Coefficients and Bubble Diameter

The models used by Rathore et al. [116] were based on Higbie's penetration theory [142] and were used to theoretically estimate the mass transfer coefficient (k_L) and the interfacial area available for mass transfer (a) as follows:

$$k_L = \frac{2}{\pi} \sqrt{D_{O_2}} \left(\frac{\varepsilon \rho_L}{\mu_L} \right)^{\frac{1}{4}} \quad (\text{Equation 4.21})$$

$$a = \frac{6\alpha_G}{d_{32}} \quad (\text{Equation 4.22})$$

where D_{O_2} is the molecular diffusivity of oxygen and is equal to 1.97×10^{-9} m²/s [68]. Both models were used as user defined functions in FLUENT to predict $k_L a$.

The original diameter (d_p) of the bubbles coming out from the sparger holes of diameter d_h was modelled by [135, 143]:

$$d_p = \left(\frac{6\alpha d_h}{g(\rho_L - \rho_G)} \right)^{1/3} \quad (\text{Equation 4.23})$$

The oxygen mass transfer coefficient $k_L a$ was experimentally determined by the gassing out method as previously described for the 50 L chamber of the multi-chamber single-use bioreactor [115].

4.5 Statistical Analysis and Correlation Equation

A randomized response surface method (RSM) was applied to study the effect on $k_L a$ of the sparger-to-impeller diameter ratio (d_{sp}/D), impeller-to-vessel diameter ratio (D/T), Reynolds number (Re), and the gas flow rate per unit liquid volume (Q/V_L). The simulation results used in

the analysis were performed at d_{sp}/D ratios: 0.086, 0.173, 0.259, 0.500 and 0.800; D/T ratios: 0.2, 0.4 and 0.6; Re numbers within the range 20,000 – 100,000; and Q/V_L : 1.2, 3.0, and 6.0 liters of gas/ liter of liquid/ hour. A total of 16 simulation results at different levels of the four studied factors were evaluated by an analysis of variance (ANOVA) statistical test. A quadratic model equation was generated to correlate the test factors to k_{LA} values. All data were analyzed using Design-Expert software, version 11 (Stat-Ease, Inc., Minneapolis, MN).

4.6 Results and Discussion

4.6.1 Single-Phase Flow Pattern

As shown in Figure 4.3, the velocity contours and vectors show the flow pattern at a mid-plane of the 50 L bioreactor. The fluid is discharged from the impeller tip toward the vessel wall. As the fluid hits the wall, it is divided into two loops that recirculate at the top and the bottom of the stirrer. This flow pattern is consistent with what was simulated in the Mobius[®] CellReady bioreactor with a similar 3-blade pitched impeller [86, 93]. Those published flow simulations were validated by particle image velocimetry (PIV) [86] and by visual observation of the trajectory of small plastic particles suspended in the bioreactor [93].

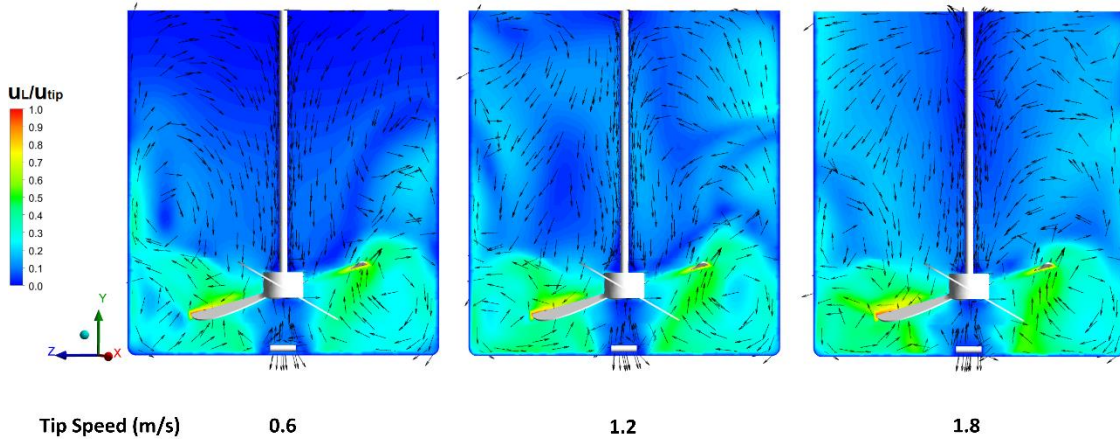


Figure 4.3. Contours and vector plots of fluid velocity in a single-phase flow at different impeller tip speeds. Velocity of liquid (u_L) is shown normalized to the tip speed (u_{tip}).

The highest velocity magnitude was shown at the closest proximity to the impeller tip and the velocity gradient migrated away from the tip and across the boundary between moving reference frame and the stationary domain, thus reflecting what we know to be representative of the physical system. This observation was true for all the three tip speeds tested. The top circulation loop showed lower velocities than the lower loop which was also consistent with what was previously reported for the Mobius[®] CellReady bioreactor.

4.6.2 Multiphase Fluid Simulation and k_{LA} Prediction

Although assuming a constant bubble diameter throughout the bioreactor operation saves computational effort and has been successfully used in some studies [93, 144], our k_{LA} prediction from a constant bubble size simulation was substantially different than the experimental results. At 0.6 impeller tip speed and 0.1 VVM, the experimental k_{LA} measurement was 7.3 hr^{-1} while the k_{LA} predicted from the constant bubble size simulation was 18.2 hr^{-1} . The PBM simulation, with bin sizes displayed in Table 4.1, predicts a more realistic k_{LA} value of 8.0 hr^{-1} .

4.6.3 Model Validation and Optimization of Bin Sizes

The agitation speed and aeration rate are expected to affect the bubble size and bubble size distribution within the bioreactor, and a single PBM model is incapable of accurately predicting the bubble size and size distribution at all of these operating conditions. In our study, therefore, the number and sizes of bins were optimized for the different operating conditions using a trial-and-error method as has been reported by Sarkar et al. [117] For each impeller tip speed, a different number of bins of different bubble diameters were tried, and the PBM model was validated by predicting k_{LA} values within 10% deviation from the experimental results at various tip speeds and aeration rates, as shown in Figure 4.4.

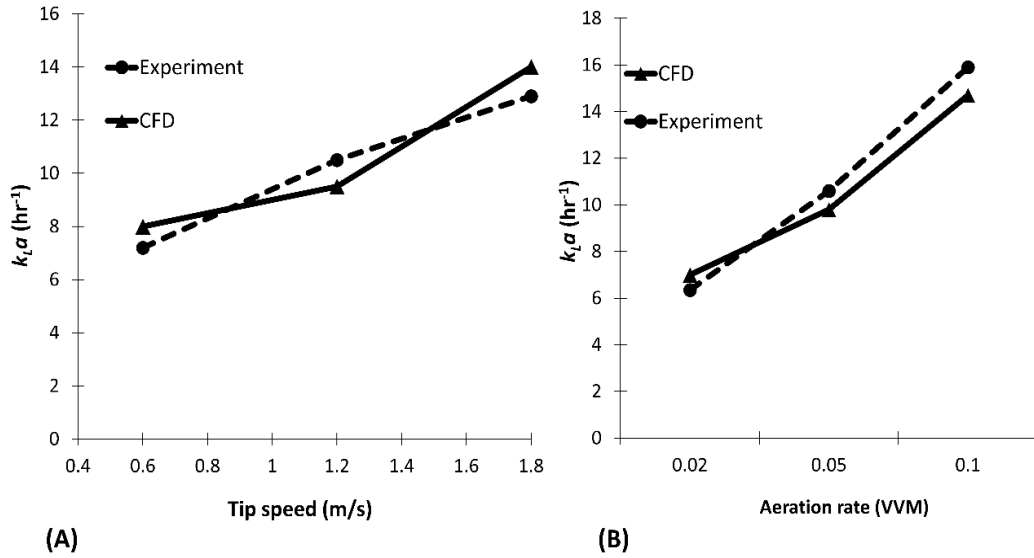


Figure 4.4. PBM model validation. (A) validation versus $k_L a$ experimental data obtained at different impeller tip speeds and a constant aeration rate of 0.1 VVM, (B) validation versus $k_L a$ experimental data obtained at different aeration rates and a constant impeller tip speed of 1.8 m/s.

The optimized bin number and sizes at different impeller tip speeds are shown in Table 4.1, where the original bubble diameter emerging from the sparger predicted from Equation 4.23 was always set as the middle bin allowing for equal chances of breakage and coalescence in both larger and smaller bins. While the bubble diameter predicted from Equation 4.23 was 0.88 mm, the Sauter mean diameter predicted from the PBM simulations was always larger than 0.88 mm, which indicated that coalescence dominated over breakage.

Table 4.1. Number and size of bins used in the Population Balance Model to simulate the multiphase flow at different impeller tip speeds.

Tip speed (m/s)	1.8	1.2	0.6
	Bin bubble diameter (mm)		
Bin-0	7.04	2.66	1.88
Bin-1	4.98	2.02	1.46
Bin-2	3.52	1.53	1.13
Bin-3	2.49	1.16	0.88
Bin-4	1.76	0.88	0.68
Bin-5	1.24	0.67	0.53
Bin-6	0.88	0.50	0.41
Bin-7	0.62	0.38	
Bin-8	0.44	0.29	
Bin-9	0.31		
Bin-10	0.22		
Bin-11	0.16		
Bin-12	0.11		

4.6.4 Effect of Sparger Shape on k_La

Pipe spargers resulted in approximately 30% lower k_La values than the ring spargers of the same surface area, as shown in Figure 4.5A, where simulations were run at an impeller tip speed of 1.2 m/s and an aeration rate of 0.1 VVM. A higher gas volume fraction was observed with the ring sparger simulations, as shown in Figure 4.5B, which can be attributed to the fact that the ring sparger configuration produces more bubbles at a closer proximity to the impeller tip.

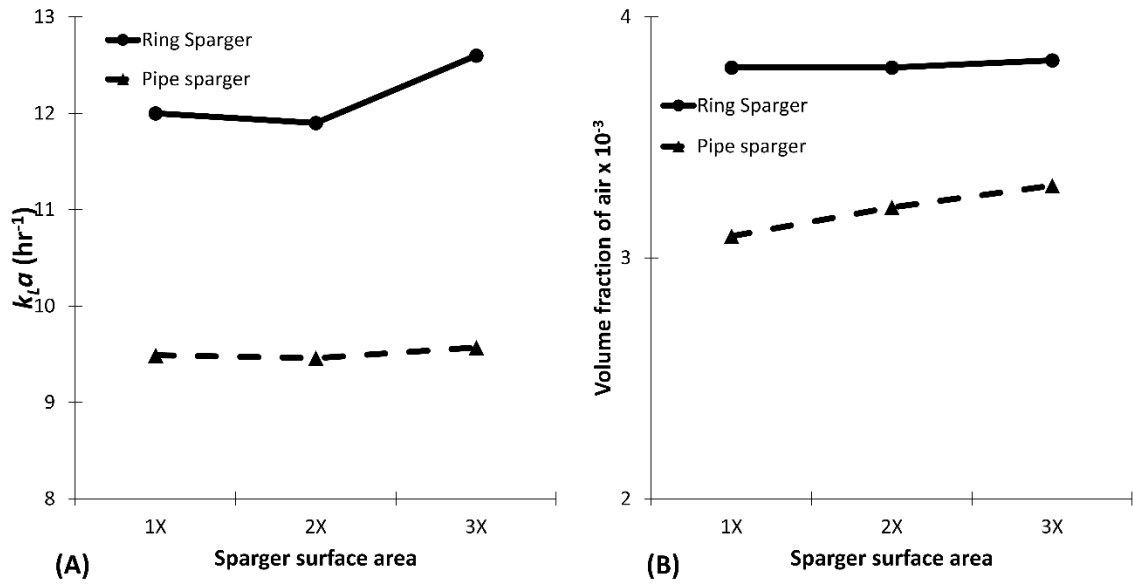


Figure 4.5. Comparison between pipe and ring spargers of same sparging surface area (1X is equivalent to the surface area of the sparger used in the prototype). (A) effect of sparger geometry on k_{La} , (B) Effect of sparger geometry on air volume fraction.

The fluid at the impeller tip experiences higher turbulence and better distribution across the bioreactor vessel, which can be observed from the top view of the vessel showing dispersed gas (Figure 4.6). In agreement with the simulation results, a previous experimental study showed similar results [108]. The study showed higher gas hold-up with the ring sparger compared to the pipe sparger over a wide range of impeller speeds and gas velocities. Lower impeller speeds showed 25% improvement in gas hold-up with the ring sparger and 18% improvement at higher impeller speeds.

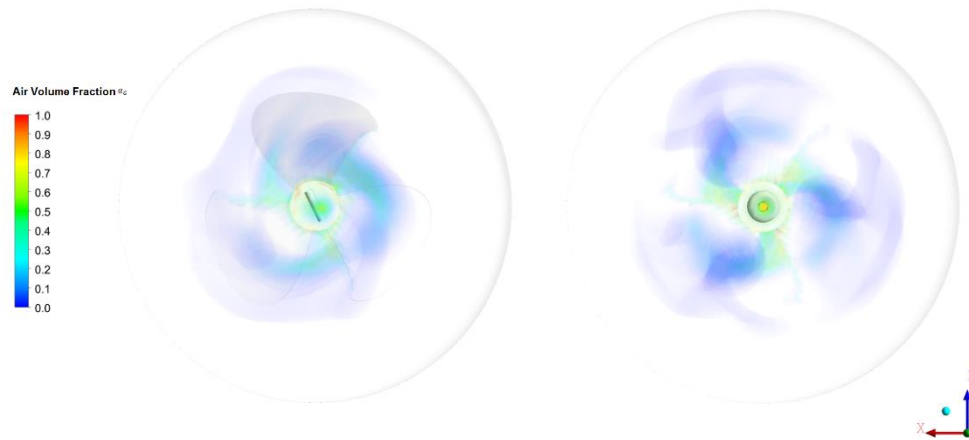


Figure 4.6. Top view of the air volume fraction inside the bioreactor with a pipe sparger (left) and a ring sparger (right).

4.6.5 Effect of Sparger Size on k_{LA}

Different sizes of spargers were tested to examine the effect of the sparger size on k_{LA} . Simulations were run at a stirrer tip speed of 1.2 m/s and a gassing rate of 0.1 VVM. As shown in Figure 4.7A, better k_{LA} values were achieved by increasing the sparger size until some point where the use of bigger spargers led to a sharp drop in k_{LA} . The trend of the k_{LA} values with increased sparger size was consistent with the trend of the volume fraction of air (Figure 4.7B). The best k_{LA} value was achieved when the ratio between the sparger diameter and the impeller diameter (d_{sp}/D) was 0.8. At this d_{sp}/D ratio, a 16% increase in the k_{LA} value was observed over the smallest sparger size tested, which had a d_{sp}/D ratio of 0.086. A sharp reduction of 43% in k_{LA} was observed when the d_{sp}/D was increased from 0.8 to 1.0.

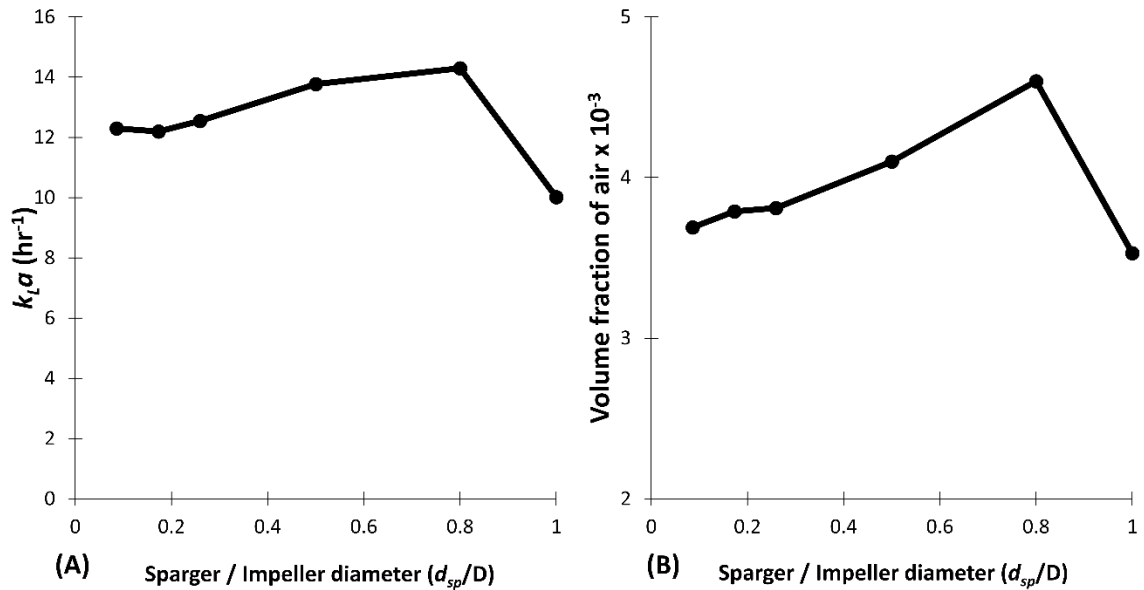


Figure 4.7. Effect of ring sparger diameter on (A) k_{La} and (B) air volume fraction.

The air bubble size distribution at a mid-plane of the bioreactor is shown in Figure 4.8, where it can be observed that at the small sparger diameter, the air bubbles are purged toward the center of the vessel where the fluid velocity and turbulence is low. The bubbles are thus prone to coalesce and to escape the vessel quickly from top. In the best case, the sparger diameter to the impeller diameter ratio was equal to 0.8, and a fraction of the bubbles is shown to be forced towards the impeller tip where the velocity and turbulence are at their maximum, thus causing the bubbles to break. The smaller bubbles are thrown toward the vessel wall and residence time of the bubbles inside bioreactor is increased. A fraction of the bubbles is also pushed towards the center of the vessel, where they coalesce and rise upward. This combination of events allows a better distribution of gas inside the vessel, which is reflected in the higher gas volume fraction. In contrast, at a sparger diameter that is equivalent to the impeller diameter, the gas bubbles are mostly dispersed outward by the impeller and are not efficiently distributed in the center of the vessel. That poor distribution of gas bubbles inside the bioreactor leads to a lower gas volume fraction and hence a lower k_{La} . The simulation results are supported by experimental results

reported by Rewatkar et al. [108] where a ring sparger of a diameter that is 0.8 of the impeller diameter showed a higher gas hold-up over a wide range of impeller speeds compared to other ring spargers with a diameter that was either half or equal to the diameter of the impeller. The d_{sp}/D ratio of 0.8 was also recommended by McFarlane et al. [145] to enhance gas handling capability and energy efficiency in dispersing gas in stirred-tank bioreactors. Birch and Ahmed [146] also showed that the gas hold-up dropped significantly when the diameter of the ring sparger exceeded the diameter of the impeller.

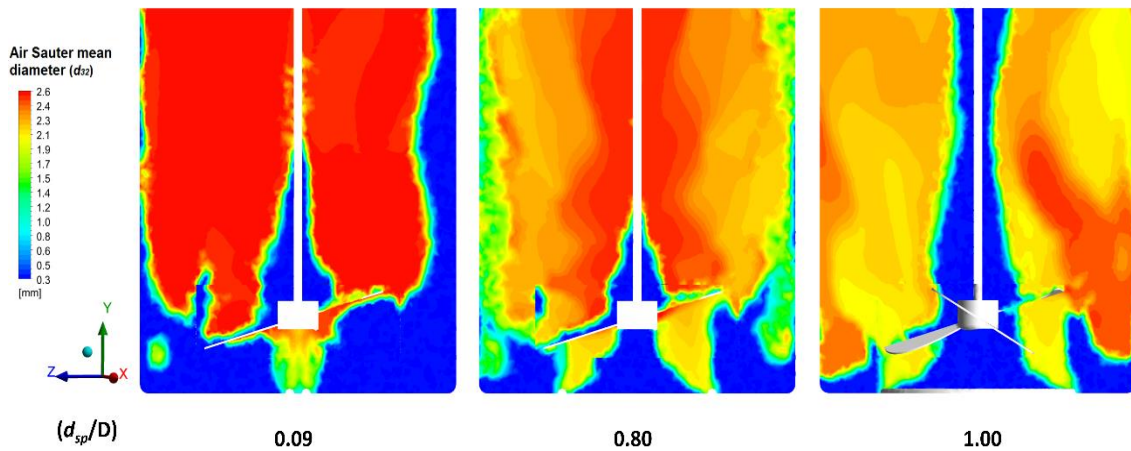


Figure 4.8. Contour plots of bubble size distribution at d_{sp}/D ratio of 0.09 (left), 0.8 (middle), and 1.0 (right).

4.6.6 Effect of Impeller Diameter on k_{LA}

A number of studies, reviewed by Markopoulos et al. [119], correlated k_{LA} to the power input per unit volume (P/V), which was directly proportional to the fifth power of the impeller diameter according to the following equation:

$$P/V = \frac{N_e \cdot \rho \cdot n^3 \cdot D^5}{V} \quad (\text{Equation 3.2})$$

In contrast García-Cortés et al. [147] reported a correlation where k_{LA} was directly proportional to the impeller-to-vessel diameter (D/T) ratio raised to the power of 2.8. In the

present study, simulations were consistent with the aforementioned findings in the sense that the larger impeller diameter produced higher k_{La} values. For a constant d_{sp}/D ratio of 0.8, the k_{La} value at a 0.6 D/T ratio was higher than at a 0.4 D/T ratio by more than 60% and was more than double compared to a D/T ratio of 0.2 (Figure 4.9).

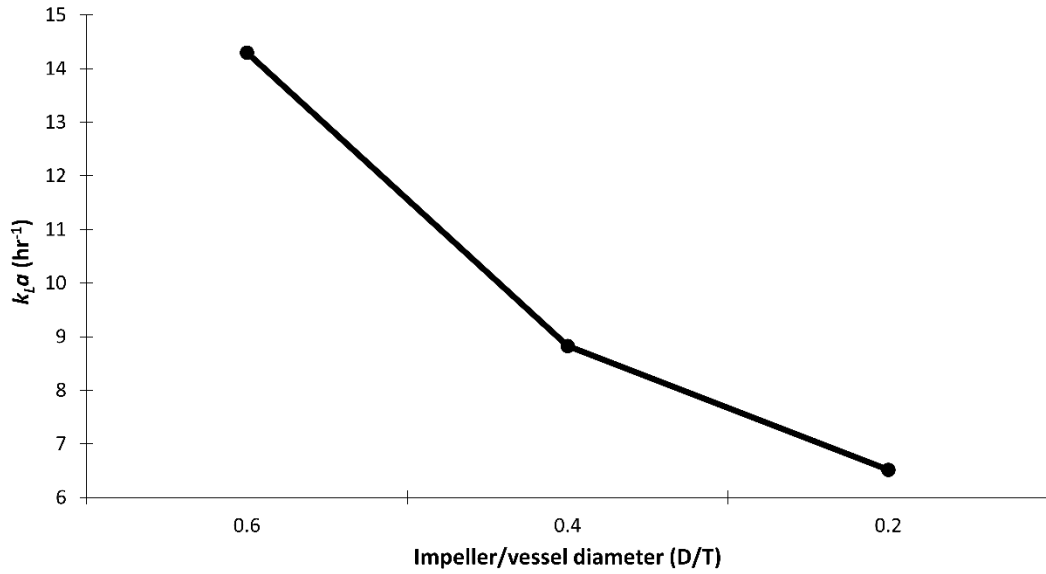


Figure 4.9. Effect of impeller diameter to vessel diameter ratio (D/T) on k_{La} .

The mid-plane contours of the gas volume fraction (Figure 4.10) show a clear enhancement in gas distribution inside the vessel with increasing impeller diameter. The better gas distribution can be related to the enhanced mixing behavior, where a larger impeller-to-vessel diameter ratio has been reported to enhance mixing behavior with any type of agitator [98].

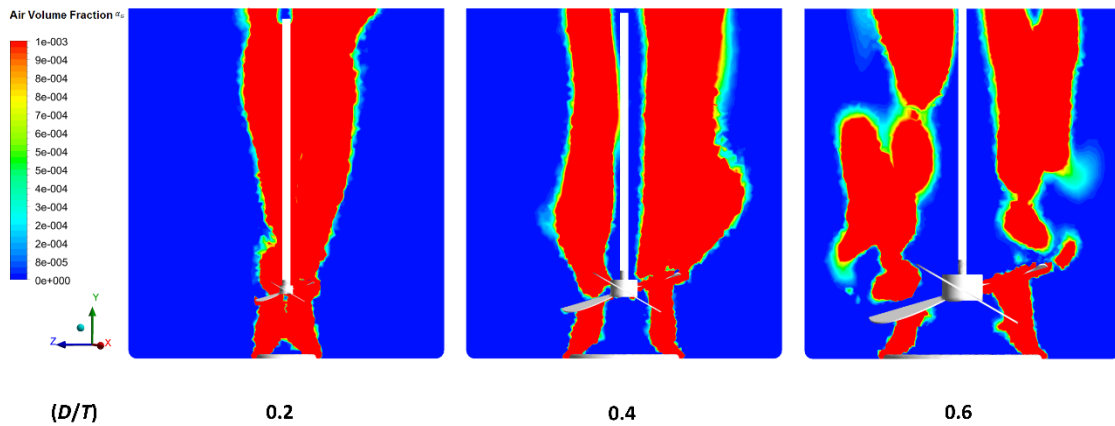


Figure 4.10. Contours of air volume fraction (α_G) at the bioreactor midplane with different impeller diameters ($D/T = 0.2, 0.4,$ and 0.6). In all cases d_{sp}/D is 0.8 , the tip speed is 1.2 m/s, and the aeration rate is 0.1 VVM.

4.6.7 Statistical Analysis and Model Equation

The ANOVA test results were helpful to evaluate the accuracy of the applied model. A correlation coefficient (R^2) of 0.9650 , which was quite close to the adjusted R^2 value of 0.9417 , indicated that the model showed a true relationship between the response and the independent variables within the tested range.

A predicted R^2 of 0.8896 , with less than 0.2 difference from the adjusted R^2 (as suggested by the Design-Expert Software), as well as a good fit between simulation results and the model predictions, shown in Figure 4.11A, indicated that the model is a good predictor. The small standard deviation (0.845) revealed the reproducibility of the model, and the small p-value (<0.0001) indicated that the model is highly significant. Contour line maps, shown in Figure 4.11(B-G), show the effect of every two tested variables on the response (k_{LA}).

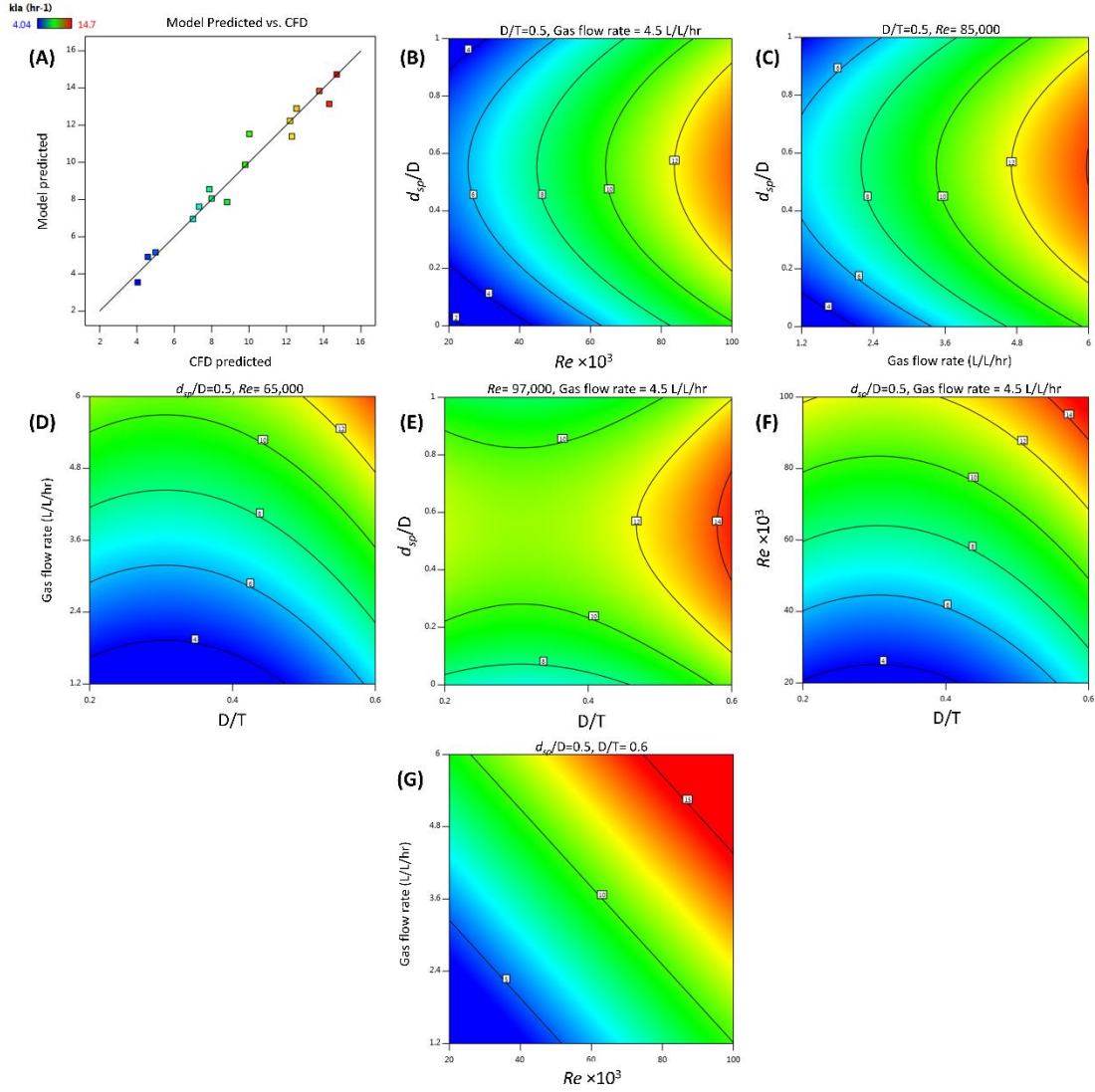


Figure 4.11. (A) Linear plot of model predicted versus CFD predicted k_{La} values. (B-G) Contour line maps showing the effect of different variables d_{sp}/D , D/T , Re , and gas flow rate on k_{La} .

The final model equation correlates k_{La} to the four tested factors within the ranges commonly used in cell culture applications and can be written as:

$$k_{La} = -7.4353 + 0.102752 (Re) - 16.86911 \left(\frac{D}{T}\right) + 12.6307 \left(\frac{d_{sp}}{D}\right) + 1.61915 \left(\frac{Q}{V_L}\right) + 32.10674 \left(\frac{D}{T}\right)^2 - 11.4995 \left(\frac{d_{sp}}{D}\right)^2 \quad (\text{Equation 4.25})$$

Based on the above model analysis, the response surface model was suitable for correlating k_{LA} to both geometrical and operating parameters and thus can be used to predict k_{LA} in stirred-tank bioreactors and to optimize the bioreactor geometry and operating conditions.

4.7 Conclusions

High efficiency of oxygen mass transfer in a bioreactor is essential for a successful cell culture process. Oxygen mass transfer coefficient (k_{LA}) is a widely used parameter to evaluate the design and performance of a bioreactor. Over the course of designing a new bioreactor, an exceedingly large number of combinations of different geometries and operating conditions may be required to be evaluated, which makes the experimental evaluation of all possible configurations almost impossible. Thus, CFD is a powerful tool that has been often recruited to help design and optimize bioreactor performance, requiring less time and fewer experiments.

In this study, we presented a CFD model to predict k_{LA} in a stirred-tank bioreactor for mammalian cell culture, and the model was validated by experimental k_{LA} measurements. A population balance model that accounted for air bubble coalescence and breakup was shown to be essential for an accurate prediction of the multiphase flow inside the bioreactor. The validated CFD model was used to study the effect on k_{LA} of various sparger geometries and sizes, as well as different impeller sizes. A ring sparger was shown to exhibit a superior performance over the pipe sparger in terms of k_{LA} and gas hold-up, with an optimum diameter that is 80% of the impeller diameter. Reducing the impeller diameter was also shown to decrease k_{LA} inside the stirred-tank bioreactor. The CFD model was also used to develop a formula to correlate k_{LA} to sparger size, impeller size, and mixing and gassing conditions. While k_{LA} has been a primary factor in evaluating stirred-tank bioreactors, existing literature only correlates k_{LA} to the operating conditions and a geometry that is assumed to be fixed. While these correlations are useful for optimizing an existing bioreactor, they are of limited use when designing a bioreactor with a novel geometry. Designing a new bioreactor vessel requires selecting the proper hardware (i.e.

impeller or sparger), which negates the assumption of constant geometry and makes the existing correlations useless. The original scope of this study was to reduce the effort and time required to design and optimize our multi-chamber single-use bioreactor, however, the developed formula can also be extended to optimize and predict the performance of other stirred-tank reactors.

4.8 Notation

D = Diameter of impeller (m)

T = Diameter of vessel (m)

d_{sp} = Diameter of ring sparger (m)

d_h = Diameter of the holes in the sparger (m)

Q = Gas flow rate (L/s)

VVM = Volume of air per volume of liquid per minute

ρ_i = Density of phase i (kg/m^3), Where $i = \text{G}$ (gas) or L (liquid) phase

μ_i = Molecular viscosity of phase i ($\text{kg}/\text{m}\cdot\text{s}$)

σ_L = Water-air interfacial tension (N/m)

k = Turbulent kinetic energy (m^2/s^2)

ε = Turbulent energy dissipation rate (m^2/s^3)

α_i = Volume fraction of phase i

\mathbf{U}_i = Velocity vector of phase i (m/s)

p = Pressure (N/m^2)

$\boldsymbol{\tau}_{\text{ef}}$ = Stress tensor (N/m^2)

\mathbf{R}_i = Interphase momentum exchange term (N/m^3)

\mathbf{F}_i = Centrifugal forces (N/m^3)

\mathbf{g} = Acceleration due to gravity (m/s^2)

C_D = Drag coefficient

Re_P = Reynolds number

$\mu_{t,L}$ = Liquid phase turbulent viscosity (kg/m.s)

$C_\mu, C_{1\varepsilon}, C_{2\varepsilon}, \sigma_k, \sigma_\varepsilon$ = Model parameters given the values 0.09, 1.44, 1.92, 1.0, and 1.3, respectively

G_k = The rate of production of turbulent kinetic energy (m^2/s^4)

$\Pi_{kL}, \Pi_{\varepsilon L}$ = Terms accounting for influence of continuous phase on dispersed phase

n_i = Number density of bubbles in the i^{th} bubble class

B_{iB} = Birth rate due to breakage ($\text{m}^{-3}\text{s}^{-1}$)

D_{iB} = Death rate due to breakage ($\text{m}^{-3}\text{s}^{-1}$)

B_{iC} = Birth rate due to coalescence ($\text{m}^{-3}\text{s}^{-1}$)

D_{iC} = Death rate due to coalescence ($\text{m}^{-3}\text{s}^{-1}$)

$a(V, V')$ = Coalescence rate prevalent between different sized bubbles of volumes V and V' (s^{-1})

$b(V')$ = Breakage rate of bubble with volume V' (s^{-1})

$m(V')$ = Number of daughter bubbles formed due to fragmentation from bubbles of volume V'

$n(V, t)$ = Number of bubbles of volume V at time t

$p(V, V')$ = Probability density function to determine offspring bubbles of volume V generated from bubbles of volume V'

f_i = Ratio of volume fraction of i^{th} group bubbles and total gas volume fraction

d_{32} = Sauter mean diameter of air bubbles

D_{O_2} = Molecular diffusivity of O_2 (m^2/s)

$k_L a$ = Volume averaged mass transfer coefficient (s^{-1})

a = Interfacial area (m^2)

d_p = Bubble diameter (m)

P = Impeller power input (W)

V = Volume of liquid (m^3)

n = Stirrer rotational speed (s^{-1})

N_e = Impeller power number

CHAPTER V

COMMERCIALIZATION PLAN FOR THE MULTI-CHAMBER SINGLE-USE BIOREACTOR

5.1 Summary

A multi-chamber single-use bioreactor is an innovative solution to streamline biopharmaceutical manufacturing by reducing fixed costs, variable costs, production space, and the risk of microbial contamination which can lead to complete loss of product. In this chapter, a full commercialization plan is presented. The plan is proposed to be executed by Multivate LLC, a limited liability company that licenses the OSU owned technology of the multi-chamber bioreactor.

Like yeast is grown in fermenters to produce alcohol, mammalian cells are grown in vessels called bioreactors to produce pharmaceutical drugs. Mammalian cells are the dominant platform to produce biopharmaceutical drugs, including recombinant proteins and antibodies. Mammalian cell cultures require a tedious, expensive, and risky scale-up process to get to production scale volumes. A cell culture starts as just a few milliliters and take weeks to divide and grow to reach thousands of liters at the production scale. A traditional single-use bioreactor is designed as a single compartment bag with a maximum turndown ratio (i.e., the ratio between the maximum and the minimum working volume of the bag) of 5:1. This volume limitation for cell

cultivation inside a single bioreactor necessitates the use of multiple bioreactors with different working volumes throughout the scale-up process.



Figure 5.1. A typical seed-train process with multiple vessels of different volumes, multiple support structures, and control units. The marks X indicate intermediate bioreactor steps that could potentially be eliminated by using the multi-chamber bioreactor technology.

Our novel multi-chamber single-use bioreactor allows this entire process to be completed in a single container. Thus, by using our bags, biopharmaceutical manufacturers can eliminate independent, traditional bioreactor units and can save at least \$200,000 in fixed costs. The savings can be multiplied by the number of intermediates eliminated. Moreover, the simplified process can save customers variable costs of \$100,000 each year of bags, as well as up to \$100,000 annually by reducing labor requirements. Finally, reducing the risk of a contamination can potentially prevent lost revenue resulting from the loss of an entire batch of product. The cost of bag failure is estimated between \$100,000 and \$1,000,000 per bag [148]. The proposed bioreactor also adds the value of freeing production space for additional upstream processes. So, instead of using three pieces of equipment to produce only one batch, our customers can use three pieces of Multivate's equipment and produce three batches, simply allowing for a three-fold increase in production volume.

Mission: The mission of Multivate is to create an innovative high-quality solution to make the biopharmaceutical manufacturing process simpler and more cost effective.

Vision: The longstanding vision of Multivate is to become the new standard and leading single-use bioreactor bag manufacturer in the biopharmaceutical industry. This is through providing our customers with the unique solution that will make their mammalian cell culture process cheaper, simpler, less risky, and more elegant.

5.2 Company Overview

Multivate, LLC, is an Oklahoma based student startup limited liability company launched in November 2017. Multivate's multi-chamber single-use bioreactor technology is invented by the company's CTO. The technology is patent pending. The full utility patent was filed by Oklahoma State University in April 2018. While the company founders are still working on developing the technology as a part of their degree requirements, the university is open to discuss exclusive options with Multivate's management team to license the technology at the time of their graduation.

5.2.1 Business Opportunity

Mammalian cells used in the production of biopharmaceuticals take a long time to divide. This makes the upstream processing, starting from a seed vial containing a few milliliters of target cells to reach the 100's or 1,000's of liters required to achieve production scale, too lengthy and laborious.

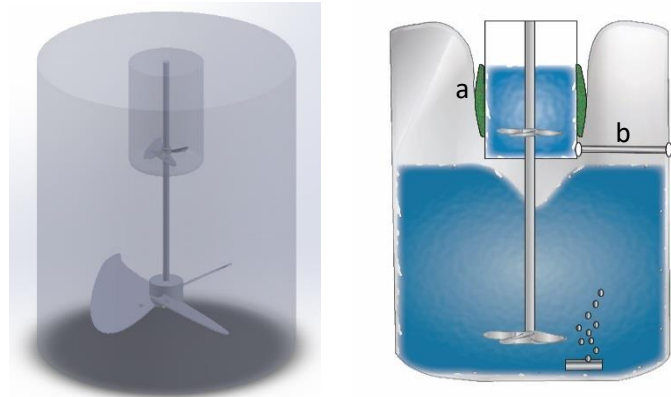


Figure 5.2. A 3D structure and a side view cartoon for a two-chamber bioreactor. (A) heating jacket in a tight sealed pocket, **(B)** internal tubing to aseptically connect optical fibers to optical sensors on the smaller chamber.

A single-use bioreactor system typically consists of a fixed support structure and a control unit. The bioreactor is a disposable bag that is inserted in the support structure and connected to the control unit which has the process control software installed. The bag is used only once and is then disconnected and disposed of when the batch is complete. A traditional single-use bag is designed as a single compartment bag with a maximum turndown ratio of 5:1 for stirred-tank reactors. This volume limitation for cell cultivation inside a single, disposable bag necessitates the use of multiple bags with different working volumes throughout the seed-train process, which is the process of scaling-up the cell culture until inoculating the production scale bioreactor. Each of these intermediate bags typically requires its own control unit and support structure. In addition to the high cost, this large amount of equipment requires significant production floor space, as well as a regular maintenance, qualification, and documentation upon operation. Moreover, a stepwise seed-train process requires connecting separate bags each time the cultivated cells and nutrient medium are transferred from the smaller to a larger bag, a procedure that requires highly trained personnel working under aseptic conditions.

The multi-chamber patent pending design, consists of an outer bag, or chamber, enclosing one or more additional smaller chambers. Together, all chambers require only a single control unit and supporting structure that fits the dimensions of the largest chamber. All chambers

are connected through internal tubing allowing transfer of culture from the smaller chamber to the larger one to occur via gravity or peristaltic pumps without the need of opening the system and risking microbial contamination.

5.2.2 The Value Proposition

By adopting Multivate technology, the multi-chamber single-use bioreactor bag allows our customers to complete multiple steps of the seed-train process in a single container. This revolutionary solution reduces overall manufacturing costs significantly. At least \$200,000 of fixed costs associated with the purchase and qualification, in addition to the costs of the cGMP footprint of equipment can be saved. The more intermediate equipment to be eliminated, the more savings are to be achieved. Our research estimated variable costs savings between \$50,000 and \$100,000 each year of bags purchase, as well as \$50,000-100,000 annual savings by reducing labor requirements. Moreover, reducing risk of contamination can potentially prevent lost revenue resulting from the loss of an entire batch of product. Freeing production space for additional seed-trains could also allow for 2-3-fold increase in production volume.

5.3 Market Analysis

Multivate considers the market secure, rapidly growing, and accessible for entry.

5.3.1 Market Trend

The single-use bioreactors market is expected to grow from \$818 million in 2016 to \$2.7 billion in 2022 at a CAGR of 22% [149]. Our addressable market will be the mammalian cell culture bioreactors, which accounts for over 70% of the total bioreactor market share [150]. One reason for the rapid market growth over the next few years is that before 2020, \$67 billion worth of biopharmaceuticals will lose patent protection and will be exposed to manufacturing competition [151]. This means more companies will compete to manufacture these drugs and to take their

share in this huge and fast-growing market. Only in the United States, there are more than 180 companies that are currently involved with at least one major biosimilar (i.e. generic) in their pipeline [152]. The number is expected to increase because of the great opportunity for small pharmaceutical companies and start-ups, which will primarily use single-use technology. This is because the single-use technology provides decreased capital expenditures and operating costs due to the reduction of cleaning, sterilization, and validation steps. In addition, processes based on single-use equipment are more flexible, require shorter set-up times, and have significantly reduced cross-contamination risk, all of which translates to a faster time to market and more robust and reliable production.

5.3.2 Market Size

Currently, there are about 500 manufacturing companies worldwide, each may have between 1 and 20 manufacturing sites. Assuming only 2 sites per company, and two equipment per site, this gives a total market of 2,000 equipment (\$300 million total market of equipment), and with an average of \$135,000 annual purchase of bags per equipment, it is a total market of \$270 million/year for bags.

5.3.3 Target Entry Market

The percentage of biopharmaceutical facilities performing all production in-house declined by more than 11% in between 2006 and 2014. The outsourced upstream processes alone have more than doubled from 17.1% to 43.2% between 2010 and 2013 [153]. Contract manufacturing organizations (CMOs) are more efficient developers of biopharmaceuticals because they usually have wider experience with a variety of products and their bioprocessing than most product sponsors. Therefore, Multivate has chosen to target CMOs as beachhead customers. In the United States alone, we identified at least 100 CMOs that produce biopharmaceutical drugs. Multivate has met with some regional CMOs who expressed significant

interest. Cytovance Biologics in Oklahoma and Fujifilm Diosynth in Texas expressed willingness to have onsite demonstrations and evaluation trials of our product once it is fully developed. Another thing we learned from our interviews with industry experts is that at early stages of development, companies will tend to perform their own manufacturing trials in an attempt to keep control on their process as much as they can before contract manufacturing. This is one reason for the growing trend of mobile cleanrooms and fully equipped, modular flexible facilities. This also validates our value proposition of the industry need to reduce footprint and fixed costs. As a result, our entry market will also target the early stage developers who are trying to develop their process before contract manufacturing.

5.3.4 Market Opportunity Validation

Multivate management team has conducted over 60 interviews with professionals in the industry throughout the business planning process. The team continues to learn more through the ongoing interviews as the research continues. Our interviews covered a variety of segments in the industry. Customers always mentioned they would like to free more space to add more projects or to reduce traffic and personnel/materials flow by including both upstream and downstream processing in the same room. Almost all interviewees identified at least one of our value propositions as a solution to a current pain. A summary of some key feedbacks gained from our interviews is highlighted in Table 5.1. All this information demonstrates that the project has the support of biopharmaceutical manufacturing companies, and that it offers a solution to recognized needs.

Table 5.1. Key feedback notes on the value propositions from industry professionals

Company	Position	Feedback
Fujifilm Diosynth Biotech, TX	Manufacturing Director	“Floor space is important. If we can place both the upstream and the downstream equipment in the same room, it will be a big advantage. We will be happy to have your prototype, once ready, for trials on our projects.”
Rhein Minapharm Biogenetics	R&D Manager	“If you can really offer this product, sure, I will give it a try.”
Kuhner Shaker	Head of Development	“I have never met a customer who is not interested in saving footprint.”
National Center for Therapeutics Manufacturing	Research Associate	“The culture transfer required as part of the seed-train process is a substantial pain. It takes a lot of time and it is risky. I am excited to try your bioreactor.”
BioPlan Associates, Inc.	President and Managing Partner	“All your value propositions are needed in the industry.”

5.4 Competition

5.4.1 Current Competitors

Current competing technologies are all single compartment reactors with a limited turndown ratio. Thus, requiring multiple reactor bags, support structures, and controllers to operate a complete upstream production process. The biggest four players in the single-use bioreactor market are: *Sartorius AG, GE healthcare, Merck Millipore and Thermofisher.*

These companies command most of the market share. These companies are tackling current problems like the footprint, high fixed costs, and contamination risk through different approaches. For instance, GE and Sartorius developed fully equipped, modular flexible facilities to reduce fixed costs and time to market compared to conventional facilities. Their solution, however, does not fit customers who already have their facilities established and running, and are

only willing to introduce more products. Competitors are also devoting more efforts to developing perfusion reactors to save footprint by performing the seed-train process in one reactor through a continuous process. Perfusion reactors, however, are significantly more complex to operate and will add at least 3-4 days to the process. Reducing contamination risks during transfer has been tackled by making sterile connections using external equipment like BioWelder/Biosealer from Sartorius. Yet we believe that the industry problems need to be solved by reducing the number of equipment used, not by adding more of them. Our patent pending design has unique features that offers solutions to all above mentioned problems in a single product while still gaining the interest of the broadest spectrum of customers.

5.4.2 Future Competitors

Continuous innovation and technological advancements will present new competitors for Multivate to stay aware of. Cell-tainer is an example of a small and growing company on the market. Cell-tainer® is a wave rocking bioreactor that is currently available in the market with the capability of expanding the cell culture volume by approximately 100-fold in the same bag (i.e., turndown ratio of ~100:1. However, the unusual mixing principle and restricted scalability of a wave-rocking bioreactor often limits its use to low volumes (200 L maximum) and simple applications such as seed-train expansion. The stirred tank reactors are more preferred in production scale than the wave-rocking bioreactors due to their higher volume capacity, smaller footprint, and conventional mixing mechanism. Another potential competitor is Kuhner Shaker, which recently introduced disposable bioreactor systems that are based on orbitally shaking mixing mechanism. The new shaking mechanism reduces the cost of bag manufacturing significantly, compared to stirred tank reactors, since there is no need to introduce any kind of shafts, impellers or gas spargers. Although the mixing technology used by Kuhner Shaker sounds interesting, yet it has not proven itself in the market where wave motion and stirred-tank reactors still dominates.

5.5 Description of Product

5.5.1 Products Offered and State of Development

The multi-chamber design consists of an outer bag, or chamber, enclosing one or more additional smaller chambers. Together, all chambers require only a single control unit and supporting structure that fits the dimensions of the largest chamber.

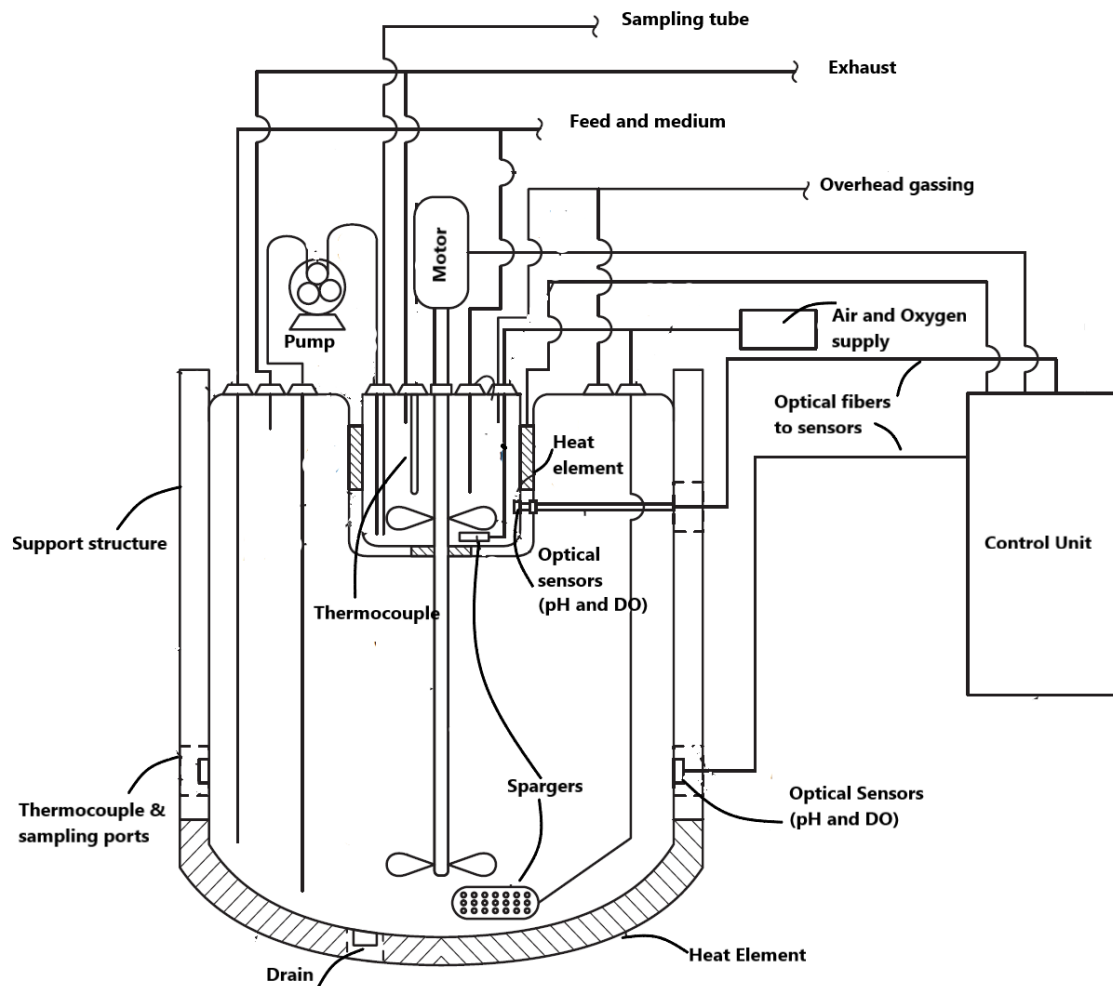


Figure 5.3. Detailed structure of a two-chamber single-use bioreactor.

All chambers are connected through internal tubing. The culture can be transferred from one chamber to another through these tubing via gravity or by using peristaltic pumps without the need of opening the system and risking microbial contamination. A top-mounted shaft with impellers goes from the top of the multi-chamber bag across the base of all smaller chambers through an air-tight sealing to serve for mixing in all chambers.

Multivate offers multi-chamber single-use bioreactor bags that are distributed pre-sterilized and ready to install and use. A series of two-chamber bags of different volumes will be marketed as Multivate 3/50, 10/200 and 50/1,000. As well as a three-chamber Multivate 5/100/2,000 bag. The numbers in the series name refer to the maximum working volume in each chamber, and each chamber typically has a turndown ratio of 5:1. For example, a 10/200 bag has a smaller chamber of a maximum working volume of 10 liters and a large chamber of a maximum working volume of 200 liters. An operator can start the culture in the smaller chamber at 2 L volume and scale it up to 10 L when the cell density reaches the desired value, then the culture can be internally transferred to the larger chamber at a volume of 40 L and then finally scaled up to 200 L in the larger chamber. Thus, a turndown ratio of 100 (from 2 L to 200 L) can be achieved in the Multivate bag. We will also offer control units and support structures to the single-use bags. A 200 CU, and a 2,000 CU, to operate and control bags up to 200 L and 2,000 L, respectively. The bags and control units will be outsourced for manufacturing.

5.5.2 Product Development Milestones

Multivate has working alpha prototypes. The prototypes were tested in terms of mixing and gas transfer efficiencies. The prototypes were also proven to grow mammalian cells that produce a recombinant IgG antibody. In the first year of operation, Multivate is targeting to produce an industry ready product by achieving specific milestones shown in Table 5.2.

Table 5.2. Milestones for multi-chamber single-use bioreactor product development

Product Development Tasks	Q1	Q2	Q3	Q4
Construction of industry deployable beta product				
Customer trials				
Iterations (Design or Process)				
Final industry ready product				

5.5.3 Pricing Strategy

Based on actual quotes we collected from current vendors, our prices are very competitive to the current options on market. Multivate prices the equipment and the bags with production, sterilization, testing, packaging costs, and customer value in mind. We also consider the price of competitors' bags and equipment. We price the bioreactor bags between \$4,000 and \$14,000 according to their volume. Our product prices are about 10% less than the average market price of the bags of the same volume. For example, the average 1,000 L bag price is \$8,000 and a 50 L bag price is \$3,000, so we are pricing our Multivate 50/1,000 two-chamber bag at \$10,000 which is about 10% less than the price of the two individual bags sold separately. For the equipment, the market price of control units varies between \$100,000 and \$400,000 according to the volume of bags it is used for. We price our equipment at \$150,000 with the option of a 1-month trial before purchase or a 1-year financing option. These options are important to attract new customers, taking into consideration that once they purchase the equipment, they will be committed to continually purchase our bags. All equipment and bag selling prices have 300% markup over the COGS.




Bags		1L-50L 2L-200L 10L-1000L	\$4K \$5.5K \$10K
		2L-100L-2000L	\$14K
Control Units		200 L 2000 L	\$150K
All at 400% markup over COGS			

Figure 5.4. Products offered and pricing.

5.6 Operations and Management

5.6.1 Operations Model

In our model, our bags are outsourced for manufacturing, sterilization, and testing for leakage and integrity at FlexConcepts, a bioprocessing bag manufacturer based in Utah State. We have worked with FlexConcepts to design and manufacture our two-camber 3/50 and 10/200 L prototypes and to put the design for the other volume models. Equipment will be outsourced for manufacturing at PendoTech, a company based in New Jersey. Pendotech proposed a customized bioreactor control unit that can fit and operate our unique bag design. Outsourced manufacturing will give Multivate the freedom to operate without purchasing large assets within the first few years. All Multivate bag series and equipment will be sold directly to our biopharmaceutical manufacturing customers. Our engineers will provide customers with on-site training, demos, and an ongoing technical support and troubleshooting which is a cornerstone for the continued success of our company. The continuous technical support is also important to make sure the customers are making the best use of our products. By the end of year 6, we anticipate having 206 equipment in the field creating over \$44 million in total sales and \$20 million in net profit.

5.6.2 Risks and Contingencies

Risk 1: From the operations stand point, we could incur a procurement problem if FlexConcepts, the manufacturer of our bags, is unable to fulfill orders. While this is unforeseeable, Multivate is prepared and already has quotes from other manufacturers. While FlexConcepts quote is the lowest, we believe that other offers can be negotiated when it is time to go for one of them, thus, to keep our profit margins unaffected.

Risk 2: One barrier for biopharmaceutical manufacturers against adopting new technologies offered by start-ups is the uncertainty that these start-ups can survive, keep up with their customers' demand, and deliver orders on time. For that reason, we will work closely with our customers to understand their needs and put an estimated plan for annual consumption. Customers who are worried about their order lead time can place orders for their annual needs with a quarterly or a half annual delivery plan.

Risk 3: Most customers require a comprehensive proof that the new bioreactor will work perfectly with their projects. This requires generating large amounts data using different cell lines that produce different proteins of interest at different culture conditions. While this will be very costly and time consuming, it still does not guarantee the generated data will be sufficient to convince every customer. Therefore, we believe that the best way is to give our potential customers a 1-month demonstration/trial period to test their specific projects on our products.

5.6.3 Management Team

5.6.3.1 Chief Officers

Austin Beaver, a mechanical engineering senior with minor in entrepreneurship, manages Multivate business development team as CEO. In 2012, Austin started a residential and commercial window cleaning company, which has grown to employ 8 college students and serve

over 120 customers in central Oklahoma and north Texas. Through heavy campus involvement, leadership positions, and experience in management, Austin has developed communication, execution, and leadership skills in addition to his experience with startups and engineering knowledge.

Momen Amer is the inventor of the multi-chamber bioreactor concept. He is currently a chemical engineering PhD student. His PhD work is all dedicated to design, develop, and test his invention, which is eventually the Multivate's product. Momen has a bachelor's degree in pharmaceutical sciences and a master's degree in biotechnology. He spent 5 years working in biopharmaceutical companies in both R&D and production facilities, which allowed him to develop an extensive experience working with all kinds and scales of single-use bioreactors for mammalian cell culture. Momen is acting as the CTO of Multivate.

Yasmine Gabal, a Chemical Engineering PhD student holding a bachelor's and a master's degrees in pharmaceutical sciences, is our COO. Yasmine exhibits excellent communication skills and a clear understanding of both the business and technical aspects of our product, which she uses to actively assist in the logistics and technical sales.

We are looking to add a sales professional with recorded experience and passion for the improvement of the biomanufacturing processes.

5.6.3.2 Advisory Board

Susann Koch has over 25 years of experience in cell culture and biopharmaceutical industry. She held managerial positions in top biopharmaceutical companies in 3 continents.

Josh Ramsey is a chemical engineering professor. He is a co-inventor of Multivate's technology and has been working in the product development during the past 4 years.

Richard Gajan has over 15 years in business advising. Richard served as a venture advisor for I2E, Inc., a high-profile Oklahoma organization that helps create high technology companies. During a period of 5 years, he guided 27 I2E clients in launching businesses that collectively raised \$13 million in equity funding and \$4.5 million in grants.

5.7 Marketing and Sales Strategy

5.7.1 Sales Approach

Multivate adopts a B2B concept with a direct sales approach to sell the Multivate bags and equipment to biopharmaceutical manufacturers. We will initially target CMOs and start-up self-manufacturers. Our sales personnel will interact with potential customers, develop a relationship, and share the unique value propositions we offer. We have already interviewed around 60 potential customers and we had interest from nearly all of them in the technology and the solution it offers to current problems in industry practices.

We identified a total of 500 biopharmaceutical manufacturers. The number of manufacturing sites for each of company varies widely from 1 up to 20 sites according to the company size. Our sales strategy assumes only 2 manufacturing sites per company, and targets selling two pieces of equipment to each site. Thus, out of the total 1,000 sites, we have a total served market size of 2,000 equipment. In the first year of sales, we will hire one sales person, the number will increase to 20 in five years. Each sales person will be responsible for 30 manufacturing sites, and he is expected to convince 6-10 sites to have an on-site trial for our product. Out of these trials we expect 20% closing rate in the first year which will increase up to 70% in year 5 with gaining more reputation and proving ourselves in the market, and also because we expect our existing customers to order their second or third equipment with no need for further onsite trials. Every closed sale generates a single equipment purchase of \$150,000 and a recurring annual bag purchase of \$135,000.

Because of the high technicality and sometimes the customization of bags required by the customers to fit their specific projects, our sales force will always be partnered with a product engineer. The salesmen will make initial contact with customers through trade shows, referrals, and cold calls. We will follow up with them via emails and phone calls to their production and purchasing departments. Once we find a customer that agrees to test our products, the technical sales team is responsible for transferring materials and data to and from the customer and to arrange for a one- or two-days on-site demonstration and training the customer's technicians to set-up, operate, and control the process with our equipment and bag products. Trial periods of 1 month will be granted to our potential customers. For the trial, the equipment will be shipped and loaned to customer at no charge, while the bags will be sold to the customers at their manufacturing costs. The same technical and sales team will be responsible for following up with the customers, make sure they are conducting trials on our product and help them with any technical problems or concerns. The team will also be responsible to keep contact with the customers after the end of the trial period to assess the feedback, offer solutions to whatever concerns they have, and close the deal with satisfied customers who want to make the purchase. The entire sales process is expected to take approximately nine months from initial contact to first sale. Based on our industry knowledge and sales forecasts, one customer account will have a single purchase of equipment of \$150,000 value, then a recurrent annual purchase of \$80,000-\$110,000 for a small volume bags and \$140,000-\$210,000 for a large volume manufacturing account. Once our product is adopted into biopharmaceutical manufacturing, we estimate a total of 206 equipment sold and over \$44 million in sales by year 6.

5.7.2 Marketing

For the industry we plan to enter, demonstrations, equivalency studies, and reputation are the most important factors in attracting customers. Our B2B marketing strategy includes scientific publications, trade shows, conferences, and on-site trials.

Attending and participating in industry trade shows will aim to provide demonstrations to engage our customers. This strategy will allow us to interact with high and low volume manufacturers. From there, we will develop the next step with interested customers for an on-site demo/trial. Our goal is to create ease in finding more information about our product and its capabilities through publishing articles and advertisements in trade magazines. We plan to gain credibility by having articles of validation and equivalency studies comparing our product to the competitor products published in the bioprocessing industry leading magazines like *bioprocessing international* and *Biopharm International*. BPI and ISPE are very well-attended trade shows happening throughout the year to highlight industry innovations and progress. We will use these campaigns to feature the values of saving fixed and recurrent costs as well as streamlining the process through our innovative bioreactor design. We plan to purchase key words through Google ad words, which will allow Multivate to capitalize on Google searches related to single-use bioreactors.

5.8 Investment Opportunity

Multivate seeks \$600,000 in investment and is offering 25% stake of ownership to angel investors and funding groups. Our hope is to secure an investor who would accept a position on the board of directors and actively help connect the management team with industry professionals to help launch Multivate. The ownership and equity structure pre- and post-investment is indicated in Table 5.3.

Table 5.3. Cap Table with round 1 of investment

Owners	Percent Ownership	
	On Founding	Round 1
Momen Amer, CTO	50.0%	33.0%
Austin Beaver, CEO	25.0%	18.0%
Yasmine Gabal, COO	25.0%	18.0%
Investor 1	0.0%	25.0%
Option Pool	0.0%	6.0%
Total	100.0%	100.0%

5.9 Exit Strategy

Multivate anticipates being purchased by a large single-use bioreactor manufacturer. In the 2017 BioProcess International conference, we already drew the attention of industry big players and experts. We were approached by Sartorius and asked to initiate discussions about possible collaboration. We were also approached by early investors in Accelerex (the first stirred-tank single-use bioreactor, now acquired by GE) and we were offered help to find partners or licensees for our technology.

5.10 Financials

5.10.1 Research Grants and Awards

Multivate's technology has raised a total \$370,000 of non-dilutive funds since 2015 to develop its product. Round 1 of \$21,250 was granted to develop and characterize the two-chamber prototype. Then, a second grant of \$25,000 was awarded to evaluate cell culture behavior in the prototype. Both grants were awarded by the Technology Development Center at

Oklahoma State University. Through Oklahoma Applied Research Support (OARS) program, we received \$300,000 grant to custom manufacture the control equipment and large volume prototypes. Multivate team also secured a \$3,000 through NSF I-Corps program which was used to conduct customer interviews, and to attend trade shows for marketing, in addition to \$18,000 in awards from business plan competitions.

Table 5.4. Sources and use of funds received

Source	Amount Received
OCAST OARS Research Grant	\$300,000
OSU Technology Business Development Program	\$21,250
OSU Technology Business Development Program	\$25,000
Second Place Award (LOVE's Business Plan Competition)	\$10,000
First Place Award (OSU Business Plan Competition)	\$8,000
National Science Foundation I-CORP Regional Program	\$3,000

5.10.2 Income Statement

The following income statement is a detailed projection of Multivate's first 6 years of operations upon investment funding. These projections are based on securing several biopharmaceutical manufacturers who will buy directly from us and adopt the Multivate technology in their process. Assumptions were made based on 60 customer discovery interviews.

Table 5.5. Projected income statement

Sales Forecast	Year 1	Year 2	Year 3	Year 4	Year 5	Year 6
ASSUMPTIONS:						
Number of New Equipment Orders	0	2	10	26	56	112
Total Number of Equipment in Field	0	2	12	38	94	206
Equipment						
Control Unit	0	2	10	26	56	112
Bags						
3/50L	0	8	48	152	376	824
10/200L	0	8	48	152	376	824
50/1000L	0	8	48	152	376	824
5/100/2000L	0	8	48	152	376	824
Revenue						
Grant Funding	\$ 300,000					
Control Unit	\$ -	\$ 300,000	\$ 1,500,000	\$ 3,900,000	\$ 8,400,000	\$ 16,800,000
Total Equipment Sales	\$ -	\$ 300,000	\$ 1,500,000	\$ 3,900,000	\$ 8,400,000	\$ 16,800,000
Bags						
3/50L	\$ -	\$ 32,000	\$ 192,000	\$ 608,000	\$ 1,504,000	\$ 3,296,000
10/200L	\$ -	\$ 44,000	\$ 264,000	\$ 836,000	\$ 2,068,000	\$ 4,532,000
50/1000L	\$ -	\$ 80,000	\$ 480,000	\$ 1,520,000	\$ 3,760,000	\$ 8,240,000
5/100/2000L	\$ -	\$ 112,000	\$ 672,000	\$ 2,128,000	\$ 5,264,000	\$ 11,536,000
Total Bag Sales	\$ -	\$ 268,000	\$ 1,608,000	\$ 5,092,000	\$ 12,596,000	\$ 27,604,000
Total Sales	\$ 300,000	\$ 568,000	\$ 3,108,000	\$ 8,992,000	\$ 20,996,000	\$ 44,404,000
Cost of Goods Sold						
Control Unit	\$ -	\$ 75,000	\$ 375,000	\$ 975,000	\$ 2,100,000	\$ 4,200,000
3/50L	\$ -	\$ 8,000	\$ 48,000	\$ 152,000	\$ 376,000	\$ 824,000
10/200L	\$ -	\$ 11,000	\$ 66,000	\$ 209,000	\$ 517,000	\$ 1,133,000
50/1000L	\$ -	\$ 20,000	\$ 120,000	\$ 380,000	\$ 940,000	\$ 2,060,000
5/100/2000L	\$ -	\$ 28,000	\$ 168,000	\$ 532,000	\$ 1,316,000	\$ 2,884,000
Cost Of Goods Sold Material	\$ -	\$ 142,000	\$ 777,000	\$ 2,248,000	\$ 5,249,000	\$ 11,101,000
New Customer Bonus	\$ -	\$ 20,000	\$ 100,000	\$ 260,000	\$ 560,000	\$ 1,120,000
Commission on Bags	\$ -	\$ 8,040	\$ 48,240	\$ 152,760	\$ 377,880	\$ 828,120
Royalty Fee OSU (2.5% of Revenue)	\$ -	\$ 14,200	\$ 77,700	\$ 224,800	\$ 524,900	\$ 1,110,100
Cost Of Goods Sold Total	\$ -	\$ 184,240	\$ 1,002,940	\$ 2,885,560	\$ 6,711,780	\$ 14,159,220
Gross Profit On Sales	\$ 300,000	\$ 383,760	\$ 2,105,060	\$ 6,106,440	\$ 14,284,220	\$ 30,244,780
General and Administrative Expenses						
Number of Business Managers	1	1	1	2	3	3
Business Manager Salary	\$ -	\$ 75,000	\$ 75,000	\$ 170,000	\$ 300,000	\$ 300,000
Number of Technical Managers	1	1	1	1	2	3
Technical Manager Salary	\$ -	\$ 75,000	\$ 75,000	\$ 85,000	\$ 200,000	\$ 300,000
Number of Engineers	1	1	2	3	6	10
Engineer Salary	\$ -	\$ 75,000	\$ 150,000	\$ 255,000	\$ 510,000	\$ 850,000
Number of Salespeople	-	1	4	8	14	20
Sales Salary	\$ -	\$ 50,000	\$ 200,000	\$ 400,000	\$ 700,000	\$ 1,000,000
Number of Staff	-	1	3	6	10	22
Staff Salary	\$ -	\$ 30,000	\$ 90,000	\$ 180,000	\$ 300,000	\$ 660,000
Total Personnel	3	5	11	20	35	58
Taxes and Benefits	\$ -	\$ 82,500	\$ 150,000	\$ 273,000	\$ 513,000	\$ 735,000
R&D Expenses	\$ 250,000	\$ 150,000	\$ 100,000	\$ 100,000	\$ 60,000	\$ 60,000
Office and Manufacturing Rent Expense	\$ -	\$ 50,000	\$ 50,000	\$ 100,000	\$ 200,000	\$ 200,000
Marketing	\$ 50,000	\$ 80,000	\$ 200,000	\$ 360,000	\$ 600,000	\$ 840,000
Equipment for use in demos	\$ 37,500	\$ 75,000	\$ 300,000	\$ 600,000	\$ 1,050,000	\$ 1,500,000
Travel	\$ 10,000	\$ 25,000	\$ 100,000	\$ 200,000	\$ 350,000	\$ 500,000
General Counsel & Legal Expense	\$ 9,000	\$ 17,040	\$ 93,240	\$ 269,760	\$ 629,880	\$ 1,332,120
Insurance	\$ 2,000	\$ 11,360	\$ 62,160	\$ 179,840	\$ 419,920	\$ 888,080
Depreciation & Amortization		\$ 5,400	\$ 15,800	\$ 36,067	\$ 61,333	\$ 96,600
Office Expenses	\$ 8,400	\$ 10,000	\$ 22,500	\$ 45,000	\$ 90,000	\$ 90,000
Miscellaneous	\$ 9,000	\$ 11,513	\$ 63,152	\$ 183,193	\$ 428,527	\$ 907,343
Total SG&A Expenses	\$ 375,900	\$ 822,813	\$ 1,746,852	\$ 3,436,860	\$ 6,412,660	\$ 10,259,143
Net Income (Loss)	\$ (75,900)	\$ (439,053)	\$ 358,208	\$ 2,669,580	\$ 7,871,560	\$ 19,985,637

Table 5.6. Statement of cash flows

	Year 1	Year 2	Year 3	Year 4	Year 5	Year 6
Operating Activities						
Net Income (loss)	(75,900)	(439,053)	358,208	2,669,580	7,871,560	19,985,637
Charges to net income (loss) not affecting cash						
Depreciation		5,400	15,800	36,067	61,333	96,600
Increase (decrease) in current liabilities						
Accounts Receivable		(47,333)	(211,667)	(537,667)	(1,212,000)	(2,488,333)
Accounts Payable	12,530	33,321	125,201	277,917	607,017	1,150,877
	12,530	(14,012)	(86,465)	(259,750)	(604,983)	(1,337,457)
Net Cash Provided By (Used In) Operating Activities	(63,370)	(447,665)	287,543	2,445,897	7,327,910	18,744,780
Investing Activities						
Laptops, cell phones, etc...	(6,000)	(6,000)	(4,000)	(4,000)	(4,000)	(4,000)
Equipment	(37,500)	(75,000)	(75,000)	(75,000)	(75,000)	(75,000)
Demo Equipment	(37,500)	(75,000)	(225,000)	(300,000)	(450,000)	(450,000)
Net Cash Provided By (Used In) Investing Activities	(81,000)	(156,000)	(304,000)	(379,000)	(529,000)	(529,000)
Financing Activities						
Grant Money	300,000					
Common Stock Sales	-	-	-	-	-	-
Preferred Stock Sales	600,000	-	-	-	-	-
Long Term Loan						
Dividend Payments for Tax Liability	-	-	(107,462)	(800,874)	(2,361,468)	(5,995,691)
Net Cash Provided By (Used In) Financing Activities	900,000	-	(107,462)	(800,874)	(2,361,468)	(5,995,691)
Net Increase (Decrease) In Cash	755,630	(603,665)	(123,920)	1,266,023	4,437,442	12,220,089
Cash - Beginning of Period	-	755,630	151,965	28,045	1,294,068	5,731,510
Cash - End of Period	755,630	151,965	28,045	1,294,068	5,731,510	17,951,599

Table 5.7. Balance sheet

ASSETS	2018	2019	2020	2021	2022	2023
Current Assets						
Cash	755,630	151,965	28,045	1,294,068	5,731,510	17,951,599
Total Current Assets	\$ 755,630	\$ 151,965	\$ 28,045	\$ 1,294,068	\$ 5,731,510	\$ 17,951,599
Fixed Assets						
Equipment	37,500	112,500	187,500	262,500	337,500	412,500
Demo Equipment	37,500	112,500	337,500	637,500	1,087,500	1,537,500
Technology (Laptops, Cellphones...etc)	6,000	12,000	16,000	20,000	24,000	28,000
Accumulated Depreciation & Amortization	-	(5,400)	(21,200)	(57,267)	(118,600)	(215,200)
Net Equipment	\$ 81,000	\$ 231,600	\$ 519,800	\$ 862,733	\$ 1,330,400	\$ 1,762,800
TOTAL ASSETS	\$ 836,630	\$ 383,565	\$ 547,845	\$ 2,156,801	\$ 7,061,910	\$ 19,714,399
LIABILITIES & SHAREHOLDER EQUITY						
Liabilities						
Accounts Receivables		(47,333)	(259,000)	(796,667)	(2,008,667)	(4,497,000)
Accounts Payable	12,530	45,851	171,052	448,969	1,055,986	2,206,863
Loan						
Total Liabilities	\$ 12,530	\$ (1,482)	\$ (87,948)	\$ (347,698)	\$ (952,681)	\$ (2,290,137)
Equity						
Common Stock Sales	-	-	-	-	-	-
Preferred Stock	600,000	600,000	600,000	600,000	600,000	600,000
retained earnings	(75,900)	(514,953)	(264,207)	1,604,499	7,114,591	21,104,537
Total Shareholder's Equity	\$ 524,100	\$ 85,047	\$ 335,793	\$ 2,204,499	\$ 7,714,591	\$ 21,704,537
TOTAL LIABILITIES & SHAREHOLDER EQUITY	\$ 536,630	\$ 83,565	\$ 247,845	\$ 1,856,801	\$ 6,761,910	\$ 19,414,399

5.10.3 Projections and Assumptions

- Based on our industry knowledge and sales forecasts, each account will have a single purchase of equipment of \$150,000 value, then a recurrent annual purchase of approximately \$135,000 of bags. All Multivate products are sold at 300% markup over the COGS. We estimate a total of 206 equipment sold, over \$44 million in sales, and \$20 million in net profit by year 6, and breakeven in year 3. We assume an even number of sales for all our bag and equipment sizes.
- We assume an annual bag purchase for each customer of 16 bags, which represents the average number of annual production batches in the industry (3 weeks/batch).
- During year 1 of operation, efforts will be dedicated to developing, and testing all Multivate series bags and equipment. No sales are expected in year 1.
- In the fifth year of sales, we will have 20 salespersons in total. Salesmen will receive a \$10,000 bonus upon closing a deal with every new equipment, and a 3% commission on annual bag sales. They will also receive an annual base salary of \$50,000.
- **Royalties:** A royalty fee of 2.5% on revenue will be paid to Oklahoma State University for their IP ownership.
- **Management and Operation Staff:** In the first three years, Momen will serve as the technical manager, Austin as a business manager, and Yasmine as an Operational engineer. Starting from year 3 we will start hiring more engineers reaching 10 in year six.
- **Management Salaries:** No salaries will be paid to Multivate team in year 1. Momen and Yasmine will work full time on Multivate development as part of their PhD thesis work, while Austin will be helping in setting up legal documents and partner agreements and he will

start working fulltime in year 2. Starting from year 2, the three founders will earn \$75,000 annually that will gradually increase as the company grows.

- **Marketing:** We budgeted \$5,000 per every on-site trial. Assuming every salesperson makes 8 onsite trials/year, we budgeted \$40,000 for marketing/salesperson + \$40,000 annually for trade shows and conferences.
- **Depreciation:** We assumed a 15-year life span for our bioreactor control units.
- **Taxes and Benefits:** We estimated 30% of our employees' salaries.
- **Equipment for Demos:** Control units will be dedicated to sales persons for demos and customer trials. We dedicated 2 equipment/salesperson.
- **Travel:** Travel assumptions are based on heavy traveling sales force, as well as an accompanying engineer for the demos. We budgeted \$25,000/salesperson/year
- **Office expense:** Initially, office space will be in Riata OSU incubator for startups at Stillwater, OK. Lab space will be in the chemical engineering department at OSU since Multivate product development is part of our founders PhD thesis work. In year 2 we will need to rent a lab space for the R&D work and a small office space that will need to expand in year 5.
- **Insurance and legal expenses:** We estimate a budget of 2% of COGS for insurance and 3% for general counsel and legal expenses
- **Miscellaneous expenses:** We estimated 3% of the gross profit on sales.

CHAPTER VI

CONCLUSIONS

Mammalian cell cultures are the dominant platform to produce biopharmaceutical drugs. Recombinant mammalian cells are grown in bioreactor vessels under controlled conditions to produce the pharmaceutical drug of interest. A high cell density in a large culture volume is required to produce a sufficient amount of the pharmaceutical drug of interest to make the production process economically efficient. The process of scaling-up mammalian cell culture from a few milliliters to thousands of liters at the production scale, however, is expensive, time consuming, and labor intensive.

In this work, a single-use bioreactor for mammalian cell culture with an innovative design was presented. The multi-chamber single-use bioreactor offers several advantages over the current solutions available on market. The new bioreactor design offers a reduction in capital costs, associated with the purchase and maintenance of multiple pieces of equipment, factory footprint, variable costs, and risks of microbial contamination. The first proof-of-concept prototype demonstrated comparative engineering characteristics to the commercially available bioreactors of similar volume. A convenient method for manufacturing the multi-chamber bioreactor with air-tight seals and FDA approved materials was proposed for a second generation, customer presentable prototype.

The engineering characterization of first prototype led to the identification of some areas

for potential improvements in the design. Computational fluid dynamics was recruited to study the effect of different hardware configuration on the performance of the bioreactor. Ring spargers were shown to be more efficient in terms of oxygen mass transfer than pipe spargers, with an optimum diameter that is 0.8 times the diameter of the bioreactor impeller. Larger impellers were also shown to be more efficient than smaller ones. The presented work combined both CFD and design of experiment approaches to correlate k_{LA} in a stirred-tank reactor to both its geometrical parameters and operating conditions. The resulting correlation can be used to predict k_{LA} in a bioreactor and to optimize its design, geometry, and operating conditions. All existing literature assumed a constant bioreactor geometry while correlating k_{LA} to the bioreactor operating conditions. This assumption limited the use of such correlations to optimizing an existing bioreactor, while they were not helpful in the process of designing a new bioreactor with a novel geometry and selecting the proper hardware.

To validate the value of the proposed invention, customer discovery interviews were conducted to understand the current industry problems and to bridge the gap between lab research and industrial needs. The interviews showed a wide acceptance from industry experts to the proposed multi-chamber bioreactor as a solution to current pains in the industry practices. A full business plan was presented in this work that proved the financial feasibility and economic attractiveness of further developing the invention to a market ready product. The extended business plan established the basis to developing a profitable business from the proposed technology on condition that the required investment is secured.

Testing the cell culture behavior is the next milestone on the road of developing the multi-chamber single-use bioreactor. The extensive engineering characterizations and CFD simulations that were carried out in this work are particularly valuable to minimize the risk of unsuccessful cell culture processes inside the proposed design. Actual cell culture runs with different cell lines and a wide variety of products is yet essential to completely validate the

concept. While this process is foreseen to be substantially expensive, establishing the right partnerships with biopharmaceutical manufacturers is a key to success. Testing the products of potential customers in our prototypes and providing sufficient data to compare the performance of our prototypes with the current systems is crucial to build the trust in our product, and it will also help to identify the areas for potential improvements in the bioreactor design.

Delivering a market ready product and accomplishing the full commercialization plan is an interdisciplinary effort that requires the cooperation of teams with different backgrounds and areas of expertise. Taking advantages of the many technical and financial resources at Oklahoma State University is another key for success. The New Product Development Center (NPDC) at Oklahoma State University is stocked with expert mechanical and design engineers that would provide a great help to establish an in-house bag manufacturing process for multi-chamber bioreactors to cover the whole production scale spectrum. Cowboy Technologies is a source of capital investment that aims to identify and work with the university generated technologies which have a promising commercialization potential. Working closely with Cowboy Technologies will provide a good opportunity to secure funds required to develop and test the next generation prototypes and to provide the project with the industry leads needed to establish the early customers network.

REFERENCES

- [1] Kern, S., et al. Model-based strategy for cell culture seed train layout verified at lab scale. BMC proceedings. Vol. 9. BioMed Central, 2015.
- [2] Heidemann, R., et al., A new seed-train expansion method for recombinant mammalian cell lines. Cytotechnology, 2002. 38(1-3): p. 99-108.
- [3] Li, F., et al., Current therapeutic antibody production and process optimization. BioProcessing Journal, 2007. 5(4): p. 16.
- [4] Tao, Y., et al., Development and implementation of a perfusion-based high cell density cell banking process. Biotechnology Progress, 2011. 27(3): p. 824-829.
- [5] Kleman, M.I., K. Oellers, and E. Lullau, Optimal conditions for freezing CHO-S and HEK293-EBNA cell lines: Influence of Me2SO, freeze density, and PEI-mediated transfection on revitalization and growth of cells, and expression of recombinant protein. Biotechnology and Bioengineering, 2008. 100(5): p. 911-922.
- [6] Voisard, D., et al., Potential of cell retention techniques for large-scale high-density perfusion culture of suspended mammalian cells. Biotechnology and Bioengineering, 2003. 82(7): p. 751-765.
- [7] Wright, B., et al., A novel seed-train process. Bioprocess International, 2015. 13: p. 16-25.
- [8] Kloth, C., et al., Inoculum expansion methods, animal cell lines. Upstream Industrial Biotechnology, 2013. 1: p. 297-310.
- [9] Pohlscheidt, M., et al., Optimizing capacity utilization by large scale 3000 L perfusion in seed train bioreactors. Biotechnology Progress, 2013. 29(1): p. 222-229.
- [10] Padawer, I., W.L.W. Ling, and Y. Bai, Case Study: An accelerated 8-day monoclonal antibody production process based on high seeding densities. Biotechnology Progress, 2013. 29(3): p. 829-832.

- [11] Madsen, B., J. Hurd, and C. Brau, *Simplify upstream process development and scale-up: single-use 5: 1 turndown-ratio bioreactor technology*. Bioprocess International, 2017. **15**(11).
- [12] Smith, M.T., et al., *Single-use bioreactors: performance and usability considerations part 2: performance and usability considerations*. BioProcess International, 2018. **16**(9).
- [13] Smith, M.T., B. Madsen, and T.W. Hsiao, *Single-use bioreactors: performance and usability considerations part 1: performance for process control*. BioProcess International, 2018. **16**(6).
- [14] Pollard, D., et al., *Standardized economic cost modeling for next-generation MAb production*. BioProcess International, 2016. **14**(8).
- [15] Singh, V., *Disposable bioreactor for cell culture using wave-induced agitation*. Cytotechnology, 1999. **30**(1): p. 149-158.
- [16] Brecht, R., *Disposable bioreactors: maturation into pharmaceutical glycoprotein manufacturing*, in *Disposable Bioreactors*. 2009, Springer. p. 1-31.
- [17] FDA, *Equipment cleaning and maintenance*. 2004.
- [18] FDA, *Guide to inspections validation of cleaning process*. 2006.
- [19] De Wilde, D., et al., *Superior scalability of single-use bioreactors*. Innovations in Cell Culture, 2014: p. 14.
- [20] Easwaran, S.S., *The pros and cons of single-use bioreactors*. <http://www.pharmtech.com>, 2010.
- [21] Markarian, J., *Sustainability in disposal of single-use systems*. BioPharm International, 2019. **32**(2): p. 19.
- [22] Gottschalk, U., *Disposables in downstream processing*, in *Disposable Bioreactors*. 2009, Springer. p. 171-183.
- [23] País-Chanfrau, J.M., K. Zorrilla, and E. Chico, *The impact of disposables on project economics in a new antibody plant: a case study*. BioPharm International, 2009. **22**(12).
- [24] Levine, H.L., et al., *Single-use technology and modular construction*. BioProcess International, 2013. **11**: p. 40-45.
- [25] Martin, J., *Bio-process systems alliance component quality test matrices*. BioProcess International, 2007. **4**: p. 1-12.

- [26] Lopes, A.G., *Single-use in the biopharmaceutical industry: A review of current technology impact, challenges and limitations*. Food and Bioproducts Processing, 2015. **93**: p. 98-114.
- [27] Barnoon, B.I. and B. Bader, *Lifecycle cost analysis for single-use systems*. BioPharm International, Issue 7, 2008.
- [28] Anicetti, V., *Biopharmaceutical processes: a glance into the 21st century*. BioProcess International, 2009. **7**(4): p. S4-S11.
- [29] Hammond, M., et al., *A cytotoxic leachable compound from single-use bioprocess equipment that causes poor cell growth performance*. Biotechnology Progress, 2014. **30**(2): p. 332-337.
- [30] Altaras, G.M., et al., *Quantitation of interaction of lipids with polymer surfaces in cell culture*. Biotechnology and Bioengineering, 2007. **96**(5): p. 999-1007.
- [31] Okonkowski, J., et al., *Cholesterol delivery to NS0 cells: challenges and solutions in disposable linear low-density polyethylene-based bioreactors*. Journal of Bioscience and Bioengineering, 2007. **103**(1): p. 50-59.
- [32] BPSA, *Guide to irradiation and sterilization validation of single-use bioprocess systems. Chapter 2*. BioProcess International Supplements 2008. May 2008: p. 10-22.
- [33] BPSA, *Recommendations for extractables and leachables testing, part 2: executing a program*. BioProcess International, 2008. **6**(1): p. 44.
- [34] Shukla, A.A. and U. Gottschalk, *Single-use disposable technologies for biopharmaceutical manufacturing*. Trends in Biotechnology, 2013. **31**(3): p. 147-154.
- [35] Challener, C.A., *Single-use bioreactors have reached the big time*. BioPharm International, 2017. **30**(3): p. 18-23.
- [36] Sinclair, A., et al., *The environmental impact of disposable technologies*. BioPharm International, 2008. **21**(11): p. S4-S15.
- [37] Healthcare, G., *Single-use technology and sustainability: quantifying the environmental impact in biologic manufacturing*. <https://www.gelifesciences.com/ko/kr/solutions/bioprocessing/knowledge-center/single-use-and-sustainability>, 2017. accessed Feb. 21, 2019.
- [38] Dreher, T., et al., *Microbial high cell density fermentations in a stirred single-use bioreactor*, in *Disposable Bioreactors II*. 2013, Springer. p. 127-147.
- [39] Galliher, P.M., et al., *Single-use bioreactor platform for microbial fermentation*. Single-Use Technology in Biopharmaceutical Manufacture, 2011: p. 241-250.

- [40] FDA, *Guidance for Industry: PAT—a framework for innovative pharmaceutical development, manufacturing, and quality assurance*. Rockville, MD, 2004.
- [41] Hinz, D.C., *Process analytical technologies in the pharmaceutical industry: the FDA's PAT initiative*. Analytical and Bioanalytical Chemistry, 2006. **384**(5): p. 1036-1042.
- [42] Lawrence, X.Y., *Pharmaceutical quality by design: product and process development, understanding, and control*. Pharmaceutical Research, 2008. **25**(4): p. 781-791.
- [43] Pordal, H., C. Matice, and T. Fry, *Computational fluid dynamics in the pharmaceutical industry*. Pharmaceutical Technology, 2002. **26**(2): p. 72-79.
- [44] Kremer, D. and B. Hancock, *Process simulation in the pharmaceutical industry: a review of some basic physical models*. Journal of Pharmaceutical Sciences, 2006. **95**(3): p. 517-529.
- [45] Wassgren, C. and J.S. Curtis, *The application of computational modeling to pharmaceutical materials science*. MRS bulletin, 2006. **31**(11): p. 900-904.
- [46] Harvey, P. and M. Greaves, *Turbulent flow in an agitated vessel. Part I: A predictive model*. Chemical Engineering Research and Design, 1982. **60**: p. 195-200.
- [47] Harvey, P. and M. Greaves, *Turbulent flow in an agitated vessel, Part II: Numerical solution and model predictions*. Chemical Engineering Research and Design, 1982. **60**: p. 201-210.
- [48] Pericleous, K.A. and M. Patel, *The modelling of tangential and axial agitators in chemical reactors*. Physicochemical Hydrodynamics, 1987. **8**(2): p. 105-123.
- [49] Placek, J., et al., *Turbulent flow in stirred tanks. Part II: A two-scale model of turbulence*. AIChE Journal, 1986. **32**(11): p. 1771-1786.
- [50] Joshi, J., A. Sahu, and P. Kumar, *LDA measurements and CFD simulations of flow generated by impellers in mechanically agitated reactors*. Sadhana, 1998. **23**(5-6): p. 505.
- [51] Murthy, B. and J. Joshi, *Assessment of standard $k-\epsilon$, RSM and LES turbulence models in a baffled stirred vessel agitated by various impeller designs*. Chemical Engineering Science, 2008. **63**(22): p. 5468-5495.
- [52] Torr , J.-P., et al., *Single and multiphase CFD approaches for modelling partially baffled stirred vessels: Comparison of experimental data with numerical predictions*. Chemical Engineering Science, 2007. **62**(22): p. 6246-6262.
- [53] Harris, C., et al., *Computational fluid dynamics for chemical reactor engineering*. Chemical Engineering Science, 1996. **51**(10): p. 1569-1594.

- [54] Aubin, J., D.F. Fletcher, and C. Xuereb, *Modeling turbulent flow in stirred tanks with CFD: the influence of the modeling approach, turbulence model and numerical scheme*. Experimental thermal and fluid science, 2004. **28**(5): p. 431-445.
- [55] Li, M., et al., *LDA measurements and CFD modeling of a stirred vessel with a retreat curve impeller*. Industrial & engineering chemistry research, 2004. **43**(20): p. 6534-6547.
- [56] Barrue, H., et al., *Eulerian simulation of dense solid-liquid suspension in multi-stage stirred vessel*. Journal of chemical engineering of Japan, 2001. **34**(5): p. 585-594.
- [57] Eggels, J.G., *Direct and large-eddy simulation of turbulent fluid flow using the lattice-Boltzmann scheme*. International journal of heat and fluid flow, 1996. **17**(3): p. 307-323.
- [58] Derksen, J. and H.E. Van den Akker, *Large eddy simulations on the flow driven by a Rushton turbine*. AIChE Journal, 1999. **45**(2): p. 209-221.
- [59] Revstedt, J. and L. Fuchs, *Large eddy simulation of flow in stirred vessels*. Chemical engineering & technology, 2002. **25**(4): p. 443-446.
- [60] Yeoh, S., G. Papadakis, and M. Yianneskis, *Numerical simulation of turbulent flow characteristics in a stirred vessel using the LES and RANS approaches with the sliding/deforming mesh methodology*. Chemical Engineering Research and Design, 2004. **82**(7): p. 834-848.
- [61] Delafosse, A., et al., *LES and URANS simulations of hydrodynamics in mixing tank: comparison to PIV experiments*. Chemical Engineering Research and Design, 2008. **86**(12): p. 1322-1330.
- [62] Gimbun, J., C.D. Rielly, and Z.K. Nagy, *Modelling of mass transfer in gas-liquid stirred tanks agitated by Rushton turbine and CD-6 impeller: A scale-up study*. Chemical Engineering Research and Design, 2009. **87**(4): p. 437-451.
- [63] Laakkonen, M., et al., *Modelling local bubble size distributions in agitated vessels*. Chemical Engineering Science, 2007. **62**(3): p. 721-740.
- [64] Laakkonen, M., et al., *Modelling local gas-liquid mass transfer in agitated vessels*. Chemical Engineering Research and Design, 2007. **85**(5): p. 665-675.
- [65] Oshinowo, L.M. and A. Bakker. *CFD modeling of solids suspensions in stirred tanks*. in *Symposium on Computational Modelling of Metals, Minerals and Materials, TMS Annual Meeting*. Seattle, WA. 2002.
- [66] Wang, F., et al., *Measurement of phase holdups in liquid-liquid-solid three-phase stirred tanks and CFD simulation*. Chemical Engineering Science, 2006. **61**(22): p. 7535-7550.

- [67] Qi, N., et al., *CFD simulation of particle suspension in a stirred tank*. Particuology, 2013. **11**(3): p. 317-326.
- [68] Dhanasekharan, K.M., et al., *A generalized approach to model oxygen transfer in bioreactors using population balances and computational fluid dynamics*. Chemical Engineering Science, 2005. **60**(1): p. 213-218.
- [69] Kumar, S. and D. Ramkrishna, *On the solution of population balance equations by discretization—III. Nucleation, growth and aggregation of particles*. Chemical Engineering Science, 1997. **52**(24): p. 4659-4679.
- [70] Marchisio, D.L., R.D. Vigil, and R.O. Fox, *Implementation of the quadrature method of moments in CFD codes for aggregation–breakage problems*. Chemical Engineering Science, 2003. **58**(15): p. 3337-3351.
- [71] Cheung, S.C., G. Yeoh, and J. Tu, *On the modelling of population balance in isothermal vertical bubbly flows—average bubble number density approach*. Chemical Engineering and Processing: Process Intensification, 2007. **46**(8): p. 742-756.
- [72] Fang, Z.D., *Applying computational fluid dynamics technology in bioprocesses-part 2*. BioPharm International, 2010. **23**(5).
- [73] Chisti, Y., *Hydrodynamic damage to animal cells*. Critical Reviews in Biotechnology, 2001. **21**(2): p. 67-110.
- [74] Elias, C.B., et al., *Turbulent shear stress—effect on mammalian cell culture and measurement using laser Doppler anemometer*. Chemical Engineering Science, 1995. **50**(15): p. 2431-2440.
- [75] Miller, J., M. Rogowski, and W. Kelly, *Using a CFD model to understand the fluid dynamics promoting E. coli breakage in a high-pressure homogenizer*. Biotechnology Progress, 2002. **18**(5): p. 1060-1067.
- [76] Derksen, J., *Numerical simulation of solids suspension in a stirred tank*. AIChE Journal, 2003. **49**(11): p. 2700-2714.
- [77] Decker, S. and M. Sommerfeld. *Calculation of particle suspension in agitated vessels with the Euler-Lagrange approach*. in *Institution of Chemical Engineers Symposium Series*. 1996. HEMISPHERE PUBLISHING CORPORATION.
- [78] Crowe, C., M. Sommerfeld, and Y. Tsuji, *Fundamentals of gas-particle and gas-droplet flows*. 1998, CRC Press, Boca Raton, USA.
- [79] Bakker, A., J.B. Fasano, and K.J. Myers. *Effects of flow pattern on the solids distribution in a stirred tank*. in *Institution of Chemical Engineers Symposium Series*. 1994. HEMISPHERE PUBLISHING CORPORATION.

- [80] Micale, G., et al., *CFD simulation of particle distribution in stirred vessels*. Chemical Engineering Research and Design, 2000. **78**(3): p. 435-444.
- [81] Ljungqvist, M. and A. Rasmuson, *Numerical simulation of the two-phase flow in an axially stirred vessel*. Chemical Engineering Research and Design, 2001. **79**(5): p. 533-546.
- [82] Montante, G., et al., *Experiments and CFD predictions of solid particle distribution in a vessel agitated with four pitched blade turbines*. Chemical Engineering Research and Design, 2001. **79**(8): p. 1005-1010.
- [83] ANSYS Fluent, *17.1-Theory Guide*, Pittsburgh, ANSYS Inc (2016).
- [84] Löffelholz, C., et al., *CFD as a tool to characterize single-use bioreactors*. Single-Use Technology in Biopharmaceutical Manufacture, 2010: p. 263-279.
- [85] Kazemzadeh, A., et al., *Hydrodynamic performance of a single-use aerated stirred bioreactor in animal cell culture: applications of tomography, dynamic gas disengagement (DGD), and CFD*. Bioprocess and Biosystems Engineering, 2018. **41**(5): p. 679-695.
- [86] Odeleye, A., et al., *On the fluid dynamics of a laboratory scale single-use stirred bioreactor*. Chemical Engineering Science, 2014. **111**: p. 299-312.
- [87] Kaiser, S., et al., *Fluid flow and cell proliferation of mesenchymal adipose-derived stem cells in small-scale, stirred, single-use bioreactors*. Chemie Ingenieur Technik, 2013. **85**(1-2): p. 95-102.
- [88] Schirmaier, C., et al., *Scale-up of adipose tissue-derived mesenchymal stem cell production in stirred single-use bioreactors under low-serum conditions*. Engineering in Life Sciences, 2014. **14**(3): p. 292-303.
- [89] Forgione, P. and M. Van Trier, *The End for Stainless Steel?* BioProcess International, 2006.
- [90] Morrow, K., *Disposable bioreactors gaining favor: New components and systems improve process reliability and reduce cost*. Genetic Engineering News, 2006: p. 26-12.
- [91] Oosterhuis, N., *The new age in bioprocessing: single-use bioreactors*. Journal of Biotechnology, 2010. **150**: p. 344.
- [92] Levine, H.L., et al., *Efficient, flexible facilities for the 21st century*. BioProcess International, 2012. **10**(11): p. 20-30.

- [93] Kaiser, S.C., R. Eibl, and D. Eibl, *Engineering characteristics of a single-use stirred bioreactor at bench-scale: The Mobius CellReady 3L bioreactor as a case study*. Engineering in Life Sciences, 2011. **11**(4): p. 359-368.
- [94] Dekarski, J., *Scalability of the Mobius CellReady Single-use Bioreactor Systems*. BioPharm International, 2013. **26**(4): p. s11-s17.
- [95] Löffelholz, C., *CFD als Instrument zur bioverfahrenstechnischen Charakterisierung von single-use Bioreaktoren und zum Scale-up für Prozesse zur Etablierung und Produktion von Biotherapeutika*. 2013, Universitätsbibliothek der BTU Cottbus.
- [96] Löffelholz, C., et al., *Dynamic single-use bioreactors used in modern liter-and m³-scale biotechnological processes: engineering characteristics and scaling up*, in *Disposable Bioreactors II*. 2013, Springer. p. 1-44.
- [97] Platas Barradas, O., et al., *Evaluation of criteria for bioreactor comparison and operation standardization for mammalian cell culture*. Engineering in Life Sciences, 2012. **12**(5): p. 518-528.
- [98] Nienow, A., *Gas dispersion performance in fermenter operation*. Chemical Engineering Progress, 1990. **86**(2): p. 61-71.
- [99] Ruszkowski, S. *A rational method for measuring blending performance, and comparison of different impeller types*. in *Institution of chemical engineers symposium series*. 1994. HEMSPHERE PUBLISHING CORPORATION.
- [100] Cooke, M., J. Middleton, and J. Bush. *Mixing and mass transfer in filamentous fermentations*. in *Proceedings of the 2nd International Conference on Bioreactor Fluid Dynamics*. 1988. Elsevier Applied Science Publishers: Amsterdam.
- [101] Nienow, A.W., *Stirring and stirred-tank reactors*. Chemie Ingenieur Technik, 2014. **86**(12): p. 2063-2074.
- [102] Couper, J.R., et al., *10 - Mixing and agitation*, in *Chemical Process Equipment (Third Edition)*. 2012, Butterworth-Heinemann: Boston. p. 277-327.
- [103] Lullau, E. and C. Fenge, *Cell culture bioreactors*, in *Cell Culture Technology for Pharmaceutical and Cell-Based Therapies*. 2005, CRC Press. p. 155-224.
- [104] Nyberg, G., et al., *Modeling of biopharmaceutical processes. Part 1: Microbial and mammalian unit operations*. Biopharm international, 2008. **21**(6).
- [105] Ma, N., J.J. Chalmers, and M. Mollet, *Aeration, mixing and hydrodynamics in bioreactors*, in *Cell culture technology for pharmaceutical and cell-based therapies*. 2005, CRC Press. p. 225-248.

- [106] Kane, J., *Measuring k_{LA} for better bioreactor performance*. BioProcess International, 2012. **10**(3).
- [107] Noack, U., et al., *Single-use stirred tank reactor BIOSTAT CultiBag STR: characterization and applications*. Single-Use Technology in Biopharmaceutical Manufacture, 2011: p. 225-240.
- [108] Rewatkar, V., et al., *Gas hold-up behavior of mechanically agitated gas-liquid reactors using pitched blade downflow turbines*. The Canadian Journal of Chemical Engineering, 1993. **71**(2): p. 226-237.
- [109] Yawalkar, A.A., et al., *Gas—liquid mass transfer coefficient in stirred tank reactors*. The Canadian Journal of Chemical Engineering, 2002. **80**(5): p. 840-848.
- [110] Gabelle, J.C., et al., *Effect of tank size on k_{La} and mixing time in aerated stirred reactors with non-newtonian fluids*. The Canadian Journal of Chemical Engineering, 2011. **89**(5): p. 1139-1153.
- [111] Smith, J., *Simple performance correlations for agitated vessels*, in *Fluid Mechanics of Mixing*. 1992, Springer. p. 55-63.
- [112] Amer, M., Y. Feng, and J.D. Ramsey, *Using CFD simulations and statistical analysis to correlate oxygen mass transfer coefficient to both geometrical parameters and operating conditions in a stirred-tank bioreactor*. Biotechnology Progress, 2019: p. e2785.
- [113] Eibl, R., C. Löffelholz, and D. Eibl, *Single-use bioreactors—an overview*. Single-Use Technology in Biopharmaceutical Manufacture, 2010: p. 33-51.
- [114] Noack, U., et al., *Single-use stirred tank reactor BIOSTAT CultiBag STR: Characterization and Applications*. Single-Use Technology in Biopharmaceutical Manufacture, 2010: p. 225-240.
- [115] Amer, M. and J.D. Ramsey, *Multi-chamber single-use bioreactor—A proof of concept prototype*. Biochemical Engineering Journal, 2018. **130**: p. 113-120.
- [116] Rathore, A., C. Sharma, and Persad, *Use of computational fluid dynamics as a tool for establishing process design space for mixing in a bioreactor*. Biotechnology Progress, 2012. **28**(2): p. 382-391.
- [117] Sarkar, J., et al., *CFD of mixing of multi-phase flow in a bioreactor using population balance model*. Biotechnology Progress, 2016. **32**(3): p. 613-628.
- [118] Villiger, T.K., et al., *Experimental and CFD physical characterization of animal cell bioreactors: From micro-to production scale*. Biochemical Engineering Journal, 2018. **131**: p. 84-94.

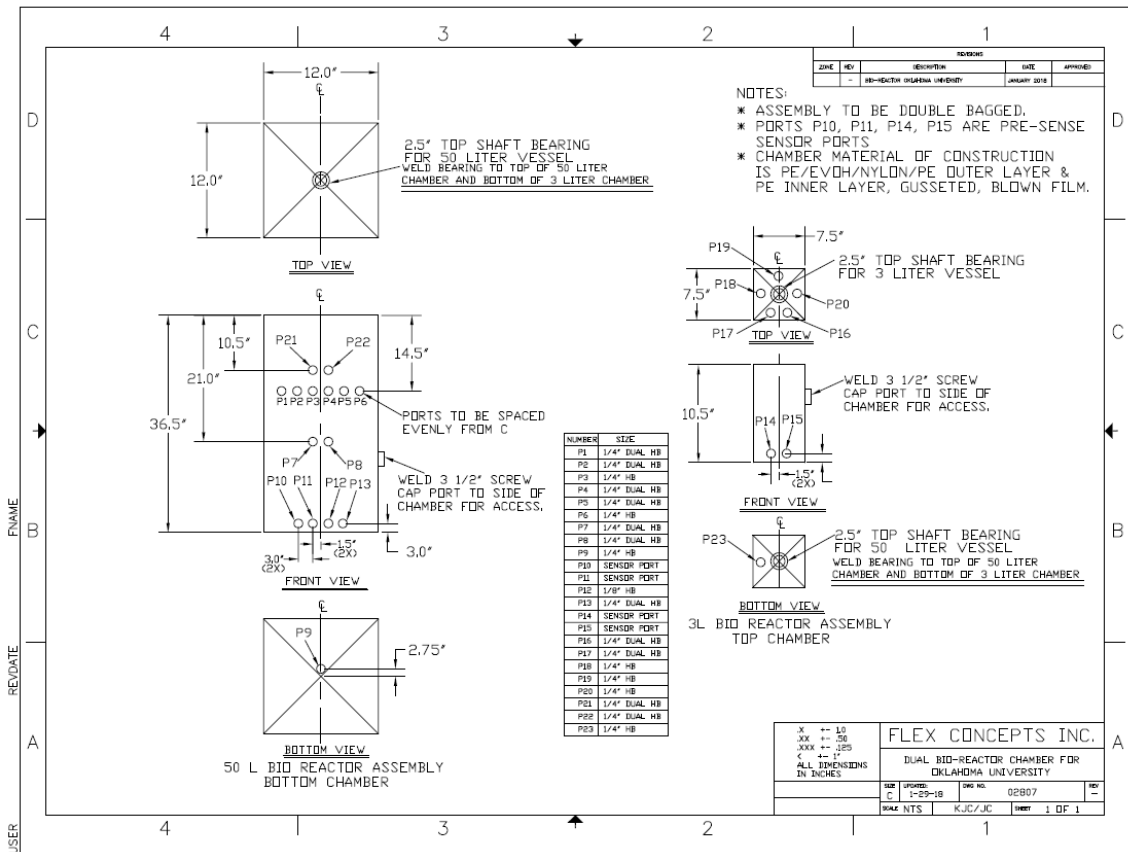
- [119] Markopoulos, J., C. Christofi, and I. Katsinaris, *Mass transfer coefficients in mechanically agitated gas-liquid contactors*. Chemical Engineering & Technology: Industrial Chemistry-Plant Equipment-Process Engineering-Biotechnology, 2007. **30**(7): p. 829-834.
- [120] ANSYS Fluent., *Fluent user's manual*. Software release, 2006. **13**.
- [121] Schiller, L., *A drag coefficient correlation*. Zeit. Ver. Deutsch. Ing., 1933. **77**: p. 318-320.
- [122] Kaiser, S.C., *Characterization and optimization of single-use bioreactors and biopharmaceutical production processes using computational fluid dynamic*, Doctoral Thesis, Technische Universität Berlin, 2015.
- [123] Bakker, A. and H. Van den Akker, *A computational model for the gas-liquid flow in stirred reactors*. Chemical Engineering Research and Design, 1994. **72**(A4): p. 594-606.
- [124] Khopkar, A., et al., *Gas-liquid flow generated by a Rushton turbine in stirred vessel: CARPT/CT measurements and CFD simulations*. Chemical Engineering Science, 2005. **60**(8-9): p. 2215-2229.
- [125] Deen, N.G., T. Solberg, and B.H. Hjertager, *Flow generated by an aerated Rushton impeller: two-phase PIV experiments and numerical simulations*. The Canadian Journal of Chemical Engineering, 2002. **80**(4): p. 1-15.
- [126] Rizk, M. and S. Elghobashi, *A two-equation turbulence model for dispersed dilute confined two-phase flows*. International Journal of Multiphase Flow, 1989. **15**(1): p. 119-133.
- [127] Zhang, H., K. Zhang, and S. Fan, *CFD simulation coupled with population balance equations for aerated stirred bioreactors*. Engineering in Life Sciences, 2009. **9**(6): p. 421-430.
- [128] Venneker, B.C., J.J. Derksen, and H.E. Van den Akker, *Population balance modeling of aerated stirred vessels based on CFD*. AIChE Journal, 2002. **48**(4): p. 673-685.
- [129] ANSYS Fluent, *Population Balance Module Manual*. 2011, SAS IP, Inc.
- [130] Sanyal, J., et al., *On the comparison between population balance models for CFD simulation of bubble columns*. Industrial & Engineering Chemistry Research, 2005. **44**(14): p. 5063-5072.
- [131] Kálal, Z., M. Jahoda, and I. Fořt, *Modelling of the bubble size distribution in an aerated stirred tank: theoretical and numerical comparison of different breakup models*. Chemical and Process Engineering, 2014. **35**(3): p. 331-348.

- [132] Chen, P., J. Sanyal, and M. Duduković, *Numerical simulation of bubble columns flows: effect of different breakup and coalescence closures*. Chemical Engineering Science, 2005. **60**(4): p. 1085-1101.
- [133] Bordel, S., R. Mato, and S. Villaverde, *Modeling of the evolution with length of bubble size distributions in bubble columns*. Chemical Engineering Science, 2006. **61**(11): p. 3663-3673.
- [134] Podila, K., et al., *CFD simulation of gas–liquid contacting in tubular reactors*. Chemical Engineering Science, 2007. **62**(24): p. 7151-7162.
- [135] Prince, M.J. and H.W. Blanch, *Bubble coalescence and break-up in air-sparged bubble columns*. AIChE journal, 1990. **36**(10): p. 1485-1499.
- [136] Luo, H. and H.F. Svendsen, *Theoretical model for drop and bubble breakup in turbulent dispersions*. AIChE Journal, 1996. **42**(5): p. 1225-1233.
- [137] Luo, H., *Coalescence, breakup and liquid circulation in bubble column reactors*. Dr. Ing. 1993, Thesis, Department of Chemical Engineering, The Norwegian Institute of Technology, Trondheim, Norway.
- [138] Chesters, A.K., *Modelling of coalescence processes in fluid-liquid dispersions: a review of current understanding*. Chemical Engineering Research and Design, 1991. **69**(A4): p. 259-270.
- [139] MARTÍNEZ-BAZÁN, C., J. Montanes, and J.C. Lasheras, *On the breakup of an air bubble injected into a fully developed turbulent flow. Part I. Breakup frequency*. Journal of Fluid Mechanics, 1999. **401**: p. 157-182.
- [140] Alopaeus, V., et al., *Simulation of the population balances for liquid–liquid systems in a nonideal stirred tank. Part 2—parameter fitting and the use of the multiblock model for dense dispersions*. Chemical Engineering Science, 2002. **57**(10): p. 1815-1825.
- [141] Lehr, F., M. Millies, and D. Mewes, *Bubble-size distributions and flow fields in bubble columns*. AIChE Journal, 2002. **48**(11): p. 2426-2443.
- [142] Higbie, R., *The rate of absorption of a pure gas into a still liquid during short periods of exposure*. Transactions of the AIChE, 1935. **31**: p. 365-389.
- [143] Panneerselvam, R., S. Savithri, and G.D. Surender, *CFD modeling of gas–liquid–solid mechanically agitated contactor*. Chemical Engineering Research and Design, 2008. **86**(12): p. 1331-1344.
- [144] Kaiser, S.C., et al., *CFD for characterizing standard and single-use stirred cell culture bioreactors*, in *Computational Fluid Dynamics Technologies and Applications*. 2011, InTech.

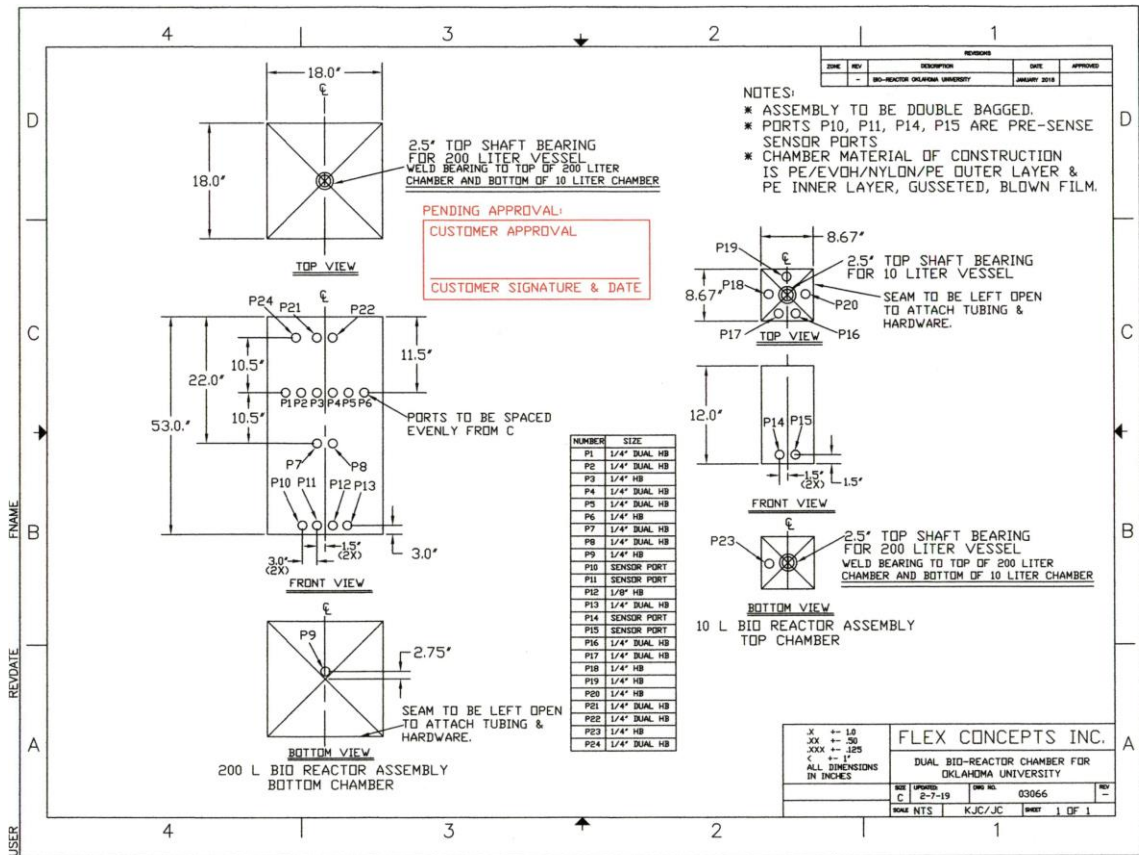
- [145] McFarlane, C.M., X.M. Zhao, and A.W. Nienow, *studies of high solidity ratio hydrofoil impellers for aerated bioreactors. 2. air—water studies*. Biotechnology Progress, 1995. **11**(6): p. 608-618.
- [146] Birch, D. and N. Ahmed, *The influence of sparger design and location on gas dispersion in stirred vessels*. Chemical Engineering Research and Design, 1997. **75**(5): p. 487-496.
- [147] García-Cortés, D., et al., *Effect of Dual Impeller-Sparger Geometry on the Hydrodynamics and Mass Transfer in Stirred Vessels*. Chemical Engineering & Technology: Industrial Chemistry-Plant Equipment-Process Engineering-Biotechnology, 2004. **27**(9): p. 988-999.
- [148] Langlois, C., M. Hogreve, and J.M. Cappia, *point-of-use leak testing of single-use bag assemblies*. Biopharm International, 2017. **30**(1): p. 26-30.
- [149] Markets and Markets, *Single-use bioreactors market worth 2,685.1 million USD by 2022*. Press Release, November 2017.
- [150] Grand View Research, Inc., *Cell line development market size, share & trends analysis report by product, by source (mammalian, non-mammalian), by type of cells, by application, by technology, and segment forecasts, 2012 - 2022*. Industry Report, February, 2018.
- [151] Generics and Biosimilar Initiative, *US \$67 billion worth of biosimilar patents expiring before 2020*. Retrieved online on March 2012. **4**: p. 2015.
- [152] Rader, R.A. and E. Langer, *Future manufacturing strategies for biosimilars*. BioProcess International, 2016. **14**(5).
- [153] Langer, E., *Year in review: Key outsourcing trends in biopharmaceutical manufacturing*. 2014, ADVANSTAR Communication Inc.

APPENDICES

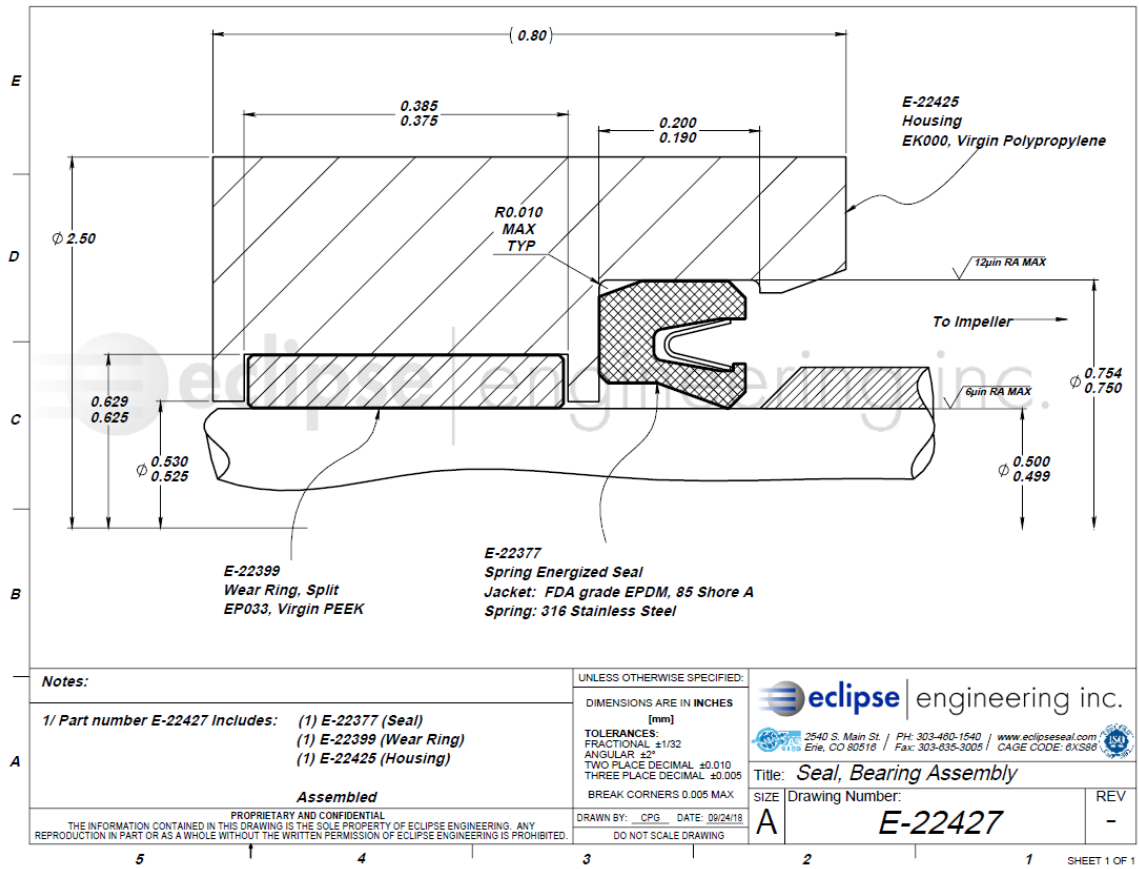
A.1. Technical drawing of the two chambers of the 50 L bioreactor prototype



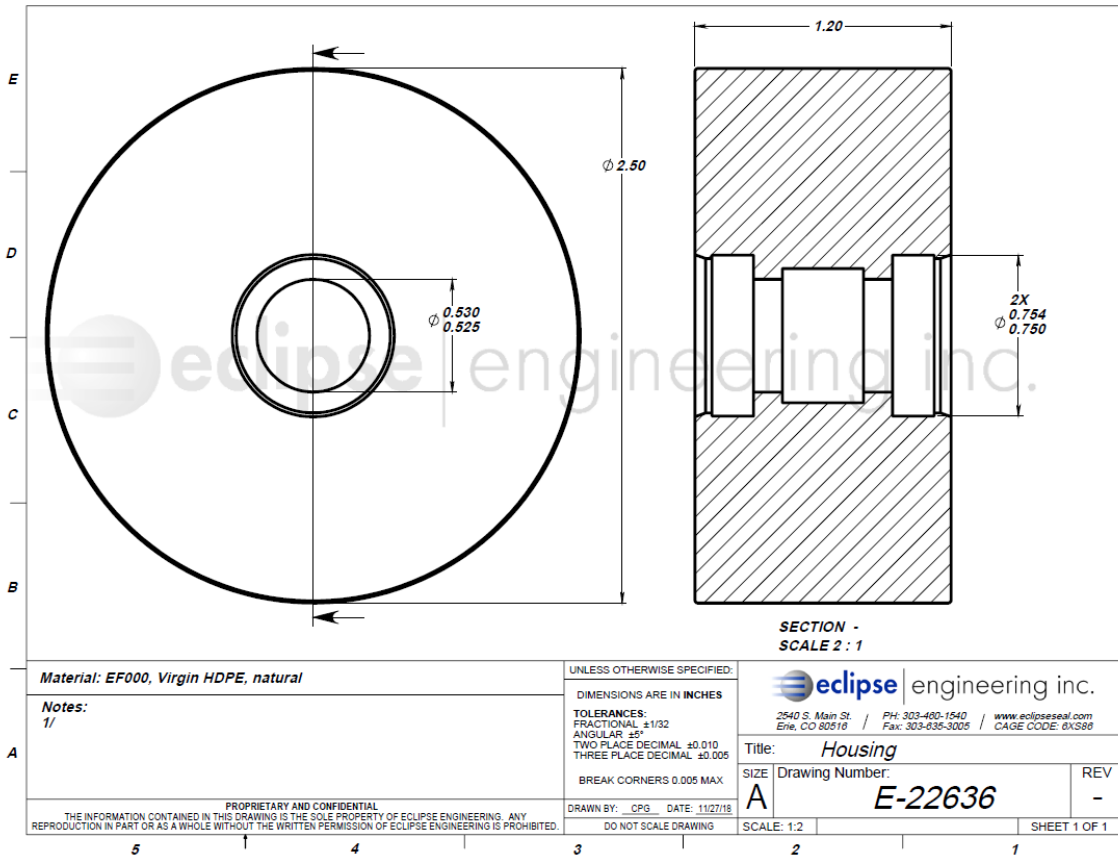
A.2. Technical drawing of the two chambers of the 200 L bioreactor prototype



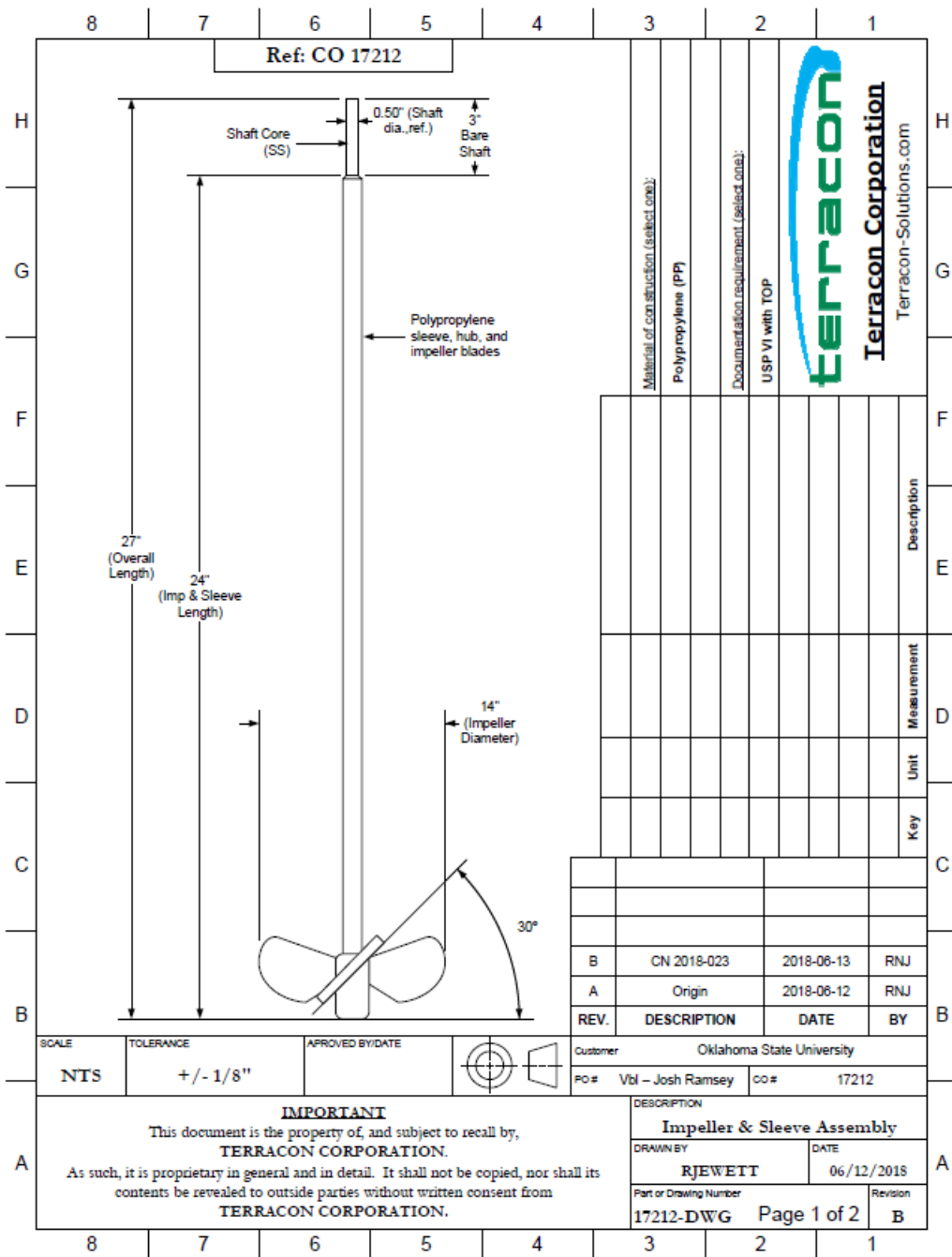
A.3. Technical drawing of the impeller seal and bearing



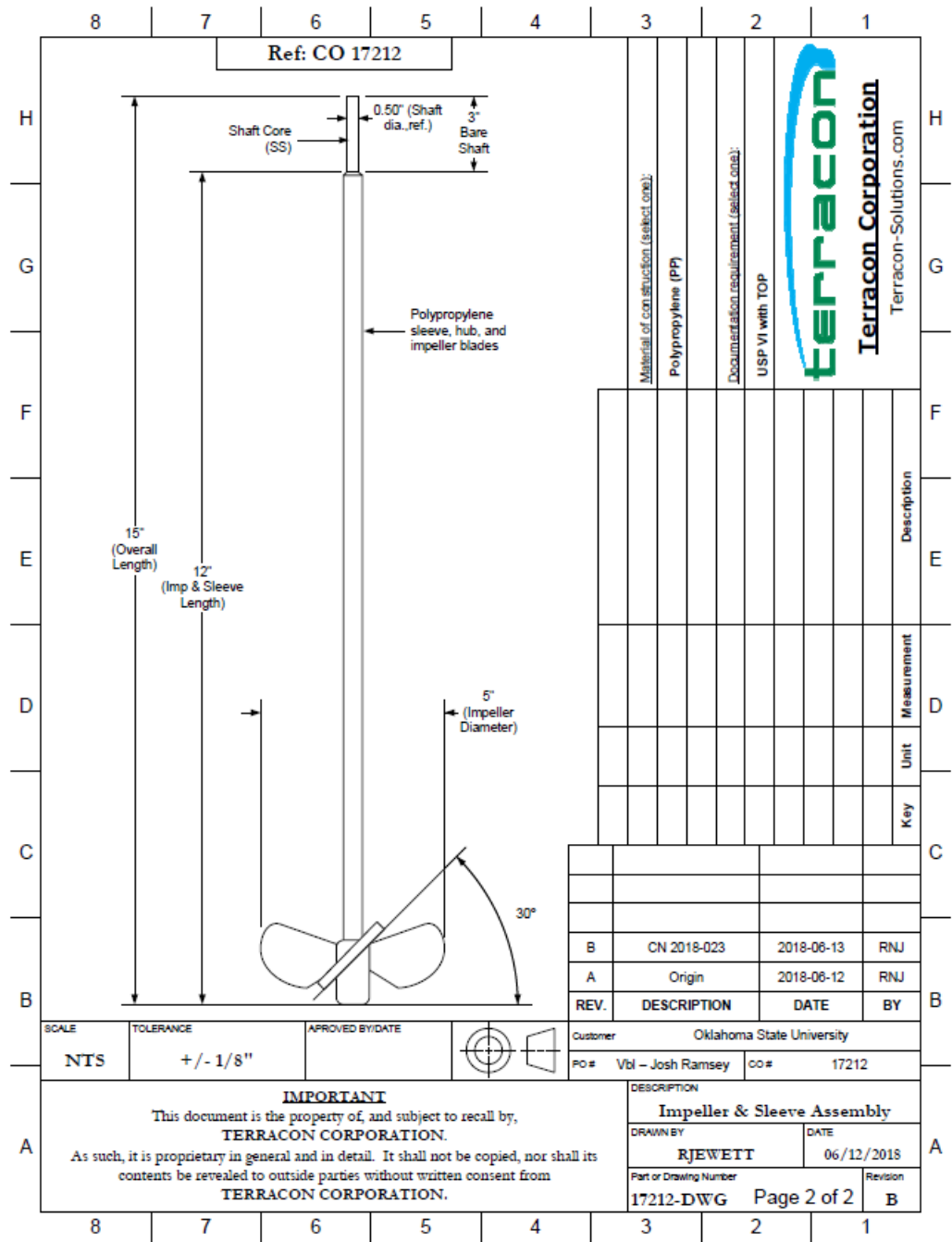
A.4. Technical drawing of the polyethylene housing for the impeller seal and bearing



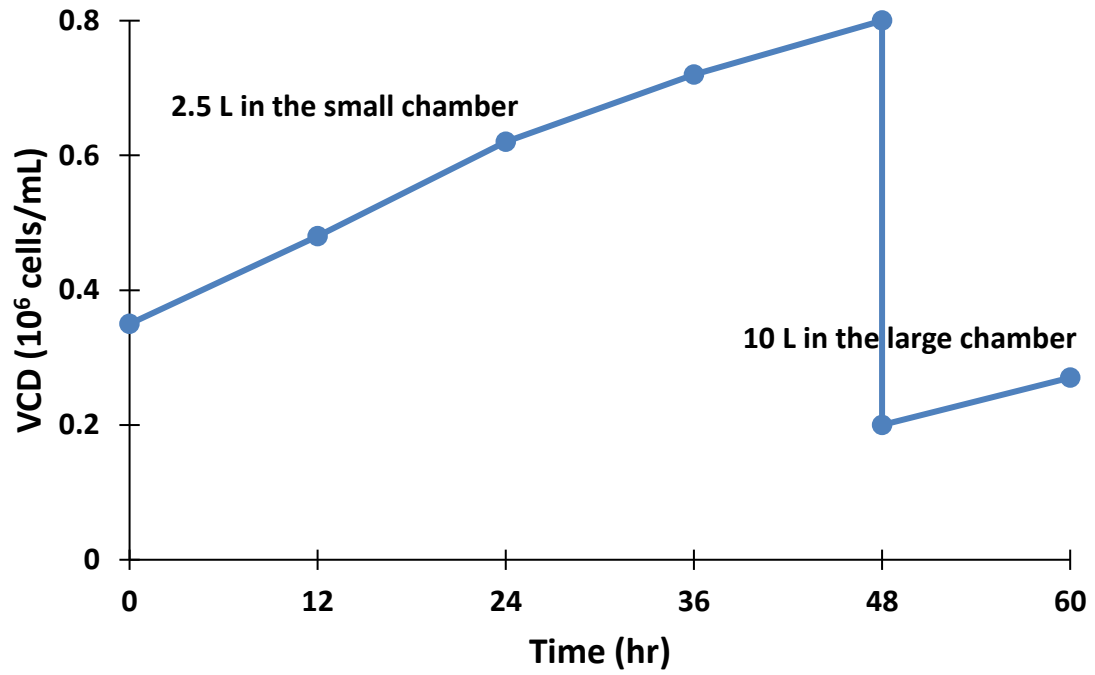
A.5. Technical drawing of the impeller in the 200 L chamber of the 200 L prototype



A.6. Technical drawing of the impeller in the 10 L chamber of the 200 L prototype



A.7. Viable cell density (VCD) of CHO cells in the two-chamber bioreactor prototype.



VITA

Momen Amer

Candidate for the Degree of

Doctor of Philosophy

Dissertation: DEVELOPMENT, CHARACTERIZATION, AND OPTIMIZATION OF
A MULTI-CHAMBER, SINGLE-USE BIOREACTOR

Major Field: Chemical Engineering

Biographical:

Education:

Completed the requirements for the Doctor of Philosophy in Chemical Engineering at Oklahoma State University, Stillwater, Oklahoma in May, 2019.

Completed the requirements for the Master of Science in Biotechnology at The American University in Cairo, Cairo, Egypt in May, 2014.

Completed the requirements for the Bachelor of Science in Pharmacy at Ain Shams University, Cairo, Egypt in 2006.

Experience:

Graduate Teaching and Research Assistant at the School of Chemical Engineering, Oklahoma State University, Stillwater, Oklahoma from August, 2014 through May 2019.

Scientific Researcher, Upstream Processing, at Rhein Minapharm Biogenetics, Egypt, from July 2011 through July 2014.